COORDINATED INTEGRATION OF BATTERY ELECTRIC VEHICLES TO A POWER SYSTEM AND ITS EFFECT ON THE LOAD CURVE

by

Arnaldo L. Nazario-Mattei

A Thesis Submitted in Partial Fulfillment of the Requirements for the Degree of

MASTER OF SCIENCE

In

ELECTRICAL ENGINEERING

University of Puerto Rico
Mayagüez Campus

2019

Approved by:

Erick Aponte Bezares, Dr. Engineering Member, Graduate Committee	Date
Lionel R. Orama Exclusa, Dr. Engineering Member, Graduate Committee	Date
José R. Cedeño Maldonado, Ph.D. President, Graduate Committee	Date
Evi De La Rosa Ricciardi, Ph.D. Representative of Graduate Studies	Date
Isidoro Couvertier Reyes, Ph.D. Chairperson of the Department	Date

Abstract

The proliferation of electric vehicles poses new challenges to the safe and economic operation of electric power systems. If electric vehicles are integrated without proper control strategies, load demand peaks will increase, and the grid may be overloaded. Coordinated methods are expected to introduce potential solutions to mitigate these negative impacts. To that end, this thesis presents a conceptual framework to effectively integrate plug-in electric vehicles into the grid. The proposed method is based on a two-stage optimization process that aims to reduce the overall load variance considering a discrete charge/discharge rate, which is largely unexplored. The first stage consists on solving a quadratic programming (QP) optimization problem, while the second stage aims at solving a mixed-integer quadratic programming (MIQP) optimization problem that uses binary variables to schedule the on/off states of the charging/discharging process. With this formulation, two approaches, vehicle-to-grid (V2G) and charging methods, were considered to evaluate the impact on the demand curve and generating costs due to the integration of electric vehicles within the system.

Case studies for a typical islanded power system and the Institute of Electrical and Electronics Engineers (IEEE) 10-unit system were conducted to demonstrate that the proposed algorithms perform as expected. Traditional unit commitment problem was used to address the variations of generating costs with and without the addition of plug-in electric vehicles. Numerical results reported for the different case studies and scenarios showed that V2G and charging operations can help flatten the overall load curves and

reduce generating costs by performing appropriate schedules of the charge and discharge process of electric vehicles.

Resumen

La proliferación de vehículos eléctricos presenta nuevos desafíos para la operación segura y económica de los sistemas de potencia eléctrica. Si los vehículos eléctricos se integran sin las estrategias de control adecuadas, los picos en la curva de carga aumentarán y la red se sobrecargará. Se espera que la utilización de métodos coordinados introduzca soluciones potenciales para mitigar estos impactos negativos. Con ese fin, esta tesis presenta una estrategia conceptual para integrar efectivamente los vehículos eléctricos con la red. El método propuesto está basado en un proceso de optimización de dos etapas que tiene como objetivo reducir la variación de la curva global de carga, considerando una razón de carga/descarga discreta, lo que ha sido investigado muy poco. La primera etapa consiste en resolver un problema de programación cuadrática, mientras que la segunda etapa tiene como objetivo resolver un problema de programación cuadrática entera-mixta que utiliza variables binarias para definir los estados de encendido/apagado del proceso de carga y descarga. Con esta formulación, se consideraron dos métodos, vehículo a red (“V2G”) y carga, para evaluar el impacto en la curva de demanda y los costos de generación debido a la integración de los vehículos eléctricos con el sistema.

Para demostrar que los algoritmos propuestos funcionan según esperado se realizaron estudios utilizando un típico sistema de potencia tipo isla y el sistema de 10 unidades del Instituto de Ingenieros Eléctricos y Electrónicos (IEEE por sus siglas en inglés). El problema tradicional de comisión de unidades se utilizó para evaluar la variación de los costos de generación con y sin la adición de los vehículos eléctricos. Los

resultados numéricos obtenidos para los diferentes casos de estudio y escenarios mostraron que las operaciones de “V2G” y carga de los vehículos pueden ayudar a nivelar las curvas globales de consumo y reducir los costos de generación mediante la implementación adecuadamente de los procesos de carga y descarga de los vehículos eléctricos.

Dedication

To my grandparents,

specially “Papa Hircio”, who always showed great interest in power systems

Acknowledgement

I would like to express earnest gratitude to my advisor, Prof. José R. Cedeño Maldonado, for his invaluable guidance, support, and patience during the time I spent through graduate studies, particularly during the development of this work. A pleasure to have been your student.

Likewise, I want to thank my committee members, Prof. Lionel Orama Exclusa and Prof. Erick Aponte Bezares for their support during my graduate school experience.

Sandy, our academic counselor, I am sincerely thankful. Your kindly motivation and tips during the journey were really appreciated.

Last but not the least, I would like to thank God for giving me the health, courage, and determination along the way.

Table of Contents

List of Figures

Chapter 2

Chapter 3

Chapter 4

Chapter 5

Appendix A

List of Tables

Chapter 5

List of Symbols

Chapter 3

C_T	total operating cost of all the scheduled units
i	index of generating unit
j	index of hour
P_i	real power supplied by unit i
P_{ij}	real power supplied by unit i at hour j
$F_i(P_i)$	fuel cost function of unit i in terms of P_i
N_G	number of generation units
N_{OG}	number of off-line generation units
T	number of time intervals
P_D	real power system demand
$P_L(P_i)$	transmission system losses in terms of P_i
P_i^{Min}	lower bound on real power generation at unit i
P_i^{Max}	upper bound on real power generation at unit i
a_i	cost coefficient of the generation unit i in $(\$/MWhr^2)$
b_i	cost coefficient of the generation unit i in $(\$/MWhr)$
c_i	cost coefficient of the generation unit i in $(\$/hr)$
$\hat{\mathbf{P}}$	vector of P_i's, $i = 1,...,N_G$
B_{ij}	ij^{th} element of the B coefficient square matrix B
B_{i0}	i^{th} element of the B coefficient vector B_0

B_{00}	*B* coefficient constant B_{00}
$\mathcal{L}$	*Lagrange function*
λ	*Lagrange multiplier*
U_{ij}	binary variable {0,1} for the on/off status of the unit *i* at hour *j*
SUC_{ij}	start-up cost of the unit *i* at hour *j*
SDC_{ij}	shut-down cost of the unit *i* at hour *j*
$H-SUC_{ij}$	hot start-up cost of unit *i* at hour *j*
$C-SUC_{ij}$	cold start-up cost of unit *i* at hour *j*
X_{ij-1}^{off}	down time of unit *i* up to hour *j-1*
CSH_i	number of hours it takes for the boiler of unit *i* to cool down
SR_j	spinning reserve requirement at hour *j*
Sup_j	supplemental reserve requirement at hour *j*
X_{ij-1}^{ON}	up-time of unit *i* up to hour $j-1$
X_{ij-1}^{OFF}	down-time of unit *i* up to hour $j-1$
T_i^{ON}	minimum up-time requirement of unit *i*
T_i^{OFF}	minimum down-time requirement of unit *i*
RUR_i	ramp-up rate limit
RDR_i	ramp-down rate limit

Chapter 4

t	index of the time slots (interval of times)
n	index of the PEVs

a	index of the aggregators
T	total number of time slots
N(a)	total number of PEVs at aggregator a
A	total number of aggregators
$OF_{1st\ Stage}$	objective function of the first optimization stage
$OF_{2nd\ Stage}$	objective function of the second optimization stage
Δt	length of the time slots
$P_{Base\ t}$	forecast load in time slot *t* (PEV load not included)
$P_{a,t}$	working power of aggregator *a* in time slot *t*, (decision variables in the first optimization stage)
$P_{Max\ Gen\ t}$	maximum real power generation capacity on time slot *t*
$P_{Rate\ n}^{a}$	charging/discharging rate of power inside the battery of PEV *n* at aggregator *a*
$P_{Max\ Rate\ n}^{a}$	maximum charging/discharging rate of power inside the battery of PEV *n* at aggregator *a*
η_{DH}	discharging efficiency
η_{CH}	charging efficiency
$\delta_n^a(t)$	binary variable for PEV *n* at aggregator *a* that indicates if the vehicle is plug-in (1) or not plug-in (0) during time slot *t*
$t_{start\ 1\ n}^{a}$	beginning of the next time interval of the first connection time for PEV *n* at aggregator *a*
$t_{start\ 2\ n}^{a}$	beginning of the next time interval of the second connection time for PEV *n* at aggregator *a*

$t_{end\,1\,n}^{a}$	beginning of the time interval of first leave time for PEV *n* at aggregator *a*
$t_{end\,2\,n}^{a}$	beginning of the time interval of second leave time for PEV *n* at aggregator *a*
$E_a(t)$	accumulated energy quantity from the first to the t-th time slot of all the PEVs at aggregator *a* as a whole
$E_a(t)_{LOWER}$	lower bound value of the accumulated energy quantity up to the time slot *t* of all the PEVs at aggregator *a* as a whole
$E_a(t)_{UPPER}$	upper bound value of the accumulated energy quantity up to the time slot *t* of all the PEVs at aggregator *a* as a whole
$E_{PEV\,n}^{a}(t)$	accumulated energy quantity from the first to the *t-th* time slot of the PEV *n* at aggregator *a* (on the grid side)
$E_{PEV\,n}^{a}(t)_{LOWER}$	lower bound value of the accumulated energy quantity up to time slot *t* of each individual PEV *n* at aggregator *a* (on grid side)
$E_{PEV\,n}^{a}(t)_{UPPER}$	upper bound value of the accumulated energy quantity up to time slot *t* of each individual PEV *n* at aggregator *a* (on grid side)
$SOC_{Lower\ n}^{a}$	minimum allowed state of charge value for the PEV *n* of the aggregator *a*
$SOC_{Upper\ n}^{a}$	maximum allowed state of charge value for the PEV *n* of the aggregator *a*
$SOC_{Desired\ n}^{a}$	minimum desired state of charge value for the PEV *n* of the aggregator *a* when leaving on the second connection period
$SOC_{1st\,Con\ n}^{a}$	state of charge value for the PEV *n* of aggregator *a* when plugged-

	in during the first connection period
$SOC_{Discrete\,1\,n}^{a}$	minimum state of charge value that the PEV *n* of aggregator *a* can achieve during the first connection period (algorithm limit)
$SOC_{Discrete\,2\,n}^{a}$	minimum state of charge value that the PEV *n* of aggregator *a* can achieve during the second connection period (algorithm limit)
$SOC_{Discrete\,3\,n}^{a}$	maximum state of charge value that the PEV *n* of aggregator *a* can achieve during the first connection period (algorithm limit)
$SOC_{Discrete\,4\,n}^{a}$	maximum state of charge value that the PEV *n* of aggregator *a* can achieve during the second connection period (algorithm limit)
$SOC(t)_{n}^{a}$	state of charge value at time slot *t* for PEV *n* of aggregator *a*
$SOC_{n}^{a}(t)\,\|\,Lower$	state of charge lower limit value at time slot *t* of PEV *n* of aggregator *a*
$SOC_{n}^{a}(t)\,\|\,Upper$	state of charge upper limit value at time slot *t* of PEV *n* of aggregator *a*
$Bat\ Cap_{n}^{a}$	battery capacity in kWh for the PEV *n* at the aggregator *a*
$Trip_{2\,n}^{a}$	energy consumed on the battery of PEV *n* of aggregator *a* due to the driving operation of the second trip (no units, value in terms of the SOC)
$TD_{2\,n}^{a}$	travel distance in miles (mi) for the second trip of PEV *n* of aggregator *a*
DC_{n}^{a}	driving consumption (kWh/mi) of the PEV *n* of aggregator *a*
$t_{critic\,1\,n}^{a}$	time slot where SOC lower limit value of PEV *n* of aggregator *a* begin to increase in the first connection period

$t_{critic\,2\,n}^{a}$ time slot where SOC lower limit value of PEV *n* of aggregator *a* begin to increase in the second connection period

$t_{critic\,3\,n}^{a}$ time slot where SOC upper limit value of PEV *n* of aggregator *a* stops increasing in the first connection period

$t_{critic\,4\,n}^{a}$ time slot where SOC upper limit value of PEV *n* of aggregator *a* stops increasing in the second connection period

$k_{1\,n}^{a}$ number of time slots needed to change the SOC lower limit value of PEV *n* of aggregator *a* from $SOC_{1st\,Con\,n}^{a}$ to $SOC_{Discrete\,1\,n}^{a}$

$k_{2\,n}^{a}$ number of time slots needed to change the SOC lower limit value of PEV *n* of aggregator *a* from $SOC_{Discrete\,1\,n}^{a}$ to the minimum allowed SOC when leaving the first period

$k_{3\,n}^{a}$ number of time slots needed to change the SOC lower limit value of PEV *n* of aggregator *a* from $SOC_{Discrete\,2\,n}^{a}$ to $SOC_{Desired\,n}^{a}$

$k_{4\,n}^{a}$ number of time slots needed to change the SOC upper limit value of PEV *n* of aggregator *a* from $SOC_{1st\,Con\,n}^{a}$ to $SOC_{Discrete\,3\,n}^{a}$

$k_{5\,n}^{a}$ number of time slots needed to change the SOC upper limit value of PEV *n* of aggregator *a* from the maximum allowed SOC when connecting on the second period to $SOC_{Discrete\,4\,n}^{a}$

$E_{Step\,1\,n}^{a}$ energy (grid side) associated to power losses of V2G between $(t_{critic\,3\,n}^{a}+1)$ and $(t_{end\,1\,n}^{a}-1)$ for PEV *n* of aggregator *a*

$E_{Step\,2\,n}^{a}$ energy (grid side) associated to power losses of V2G between $(t_{critic\,4\,n}^{a}+1)$ and $(t_{end\,2\,n}^{a}-1)$ for PEV *n* of aggregator *a*

$s_{1\,n}^{\,a}$	maximum number of intervals $E_{Step\,1\,n}^{\,a}$ can be activated from $(t_{critic\,3\,n}^{\,a}+1)$ to $(t_{end\,1\,n}^{\,a}-1)$ during the first connection period for PEV *n* of aggregator *a*
$s_{2\,n}^{\,a}$	number of intervals $E_{Step\,2\,n}^{\,a}$ is activated from $(t_{critic\,4\,n}^{\,a}+1)$ to $(t_{end\,2\,n}^{\,a}-1)$ during the second connection period for PEV *n* of aggregator *a*
$P_{CH\,n}^{\,a}$	charging rate of power (inside the battery, not in the grid) for the PEV *n* of aggregator *a*
$P_{DH\,n}^{\,a}$	discharging rate of power (inside the battery, not in the grid) for the PEV *n* of aggregator *a*
$U_{CH\,n,t}^{\,a}$	binary variable for PEV *n* at aggregator *a* that indicates if the vehicle is charging (1) or not charging (0) during time slot *t* (decision variable in second optimization stage)
$U_{DH\,n,t}^{\,a}$	binary variable for PEV *n* at aggregator *a* that indicates if the vehicle is discharging charging (1) or not discharging charging (0) during time slot *t* (decision variable in second optimization stage)
$SF_{CH}(t)_{n}^{\,a}$	switching frequency from charge-to-discharge-to-charge beginning at the time slot *t* for the PEV *n* at aggregator *a*
$SF_{DH}(t)_{n}^{\,a}$	switching frequency from discharge-to-charge-to-discharge beginning at the time slot *t* for the PEV *n* at aggregator *a*
$P_{Base-Aggregator}^{a}$	ideal base load curve that each aggregator *a* must follows on the second optimization stage to manage their PEVs
$PEV_{Status\,n}^{\,a}$	operating schedule for PEV *n* of aggregator *a*

List of Acronyms

A/S	Ancillary Services
ACE	Area Control Error
AGC	Automatic Generation Control
BESS	Battery Energy Storage System
BEV	Battery Electric Vehicle
CAESS	Compressed Air Energy Storage System
CCC	Central Control Center
DESS	Distributed Energy Storage System
DOD	Depth-of-Discharge
DSM	Demand Side Management
ED	Economic Dispatch
EDV	Electric Drive Vehicle
ESS	Energy Storage Systems
EV	Electric Vehicle
EVSE	Electric Vehicle Supply Equipment
FCV	Fuel Cell Vehicle
FESS	Fly-wheels Energy Storage System
GEV	Grid Enable Vehicle
HEV	Hybrid Electric Vehicle
ICE	Internal Combustion Engine

IEEE	Institute of Electrical and Electronics Engineers
kW	Kilowatt
kWh	Kilowatt Hour
LCO	Lithium Cobalt Oxide
LIP	Lithium Iron Phosphate
LMO	Lithium Manganese Oxide
LNMCO	Lithium Nickel-Manganese-Cobalt Oxide
MA	Master or Main Aggregator
MIQP	Mixed-Integer Quadratic Programming
MW	Megawatt
PEV	Plug-in Electric Vehicle
PHEV	Plug-in Hybrid Electric Vehicle
PHSS	Pumped Hydroelectric Storage System
QP	Quadratic Programming
SAE	Society of Automotive Engineers
SMESS	Super Magnetic Energy Storage System
SOC	State of Charge
TOU	Time-of-Use
UC	Unit Commitment
V2B	Vehicle-to-Building
V2G	Vehicle-to-Grid

Chapter 1

1 Introduction

The anticipation of large-scale penetration of electric vehicles has introduced new challenges in power system operations. This work emerges from the growing necessity to establish a sustainable integration of the electrical and transportation systems. The justification is addressed in section 1.1 of this chapter. Then, section 1.2 provides the main objectives of this work. A brief outline of the remainder of this thesis is presented in section 1.3.

1.1 Justification

Electric utilities ponder new means to maintain a secure, stable, and reliable network that can adapt and respond to increases in electricity demand due to population growth. The ability to supply this increase in demand has forced utilities to figure out alternative and innovative energy solutions to improve management and operation of their already aged systems. Therefore, one of the most recently promising alternatives is electrifying the transportation sector. Great interest has been given to vehicles, specifically electric vehicles, since they are used nearly 4% to 5% of the time for transportation purposes, making them available for utility functions the rest of the time [1]. This transition is expected to reduce fossil fuel consumption and consequently tailpipe gas emissions of

traditional automobiles, as well as integrate the transportation system to the power system [2], [3].

The idea of electric vehicles (EV) has been studied during the past years. Particular attention has been placed specifically on battery electric vehicles (BEV), since the natural storage capacity makes them a prominent choice if their batteries can be used without affecting the ability to power the vehicle for running operation. Several studies conducted by researchers and engineers have proved that if bi-directional power transfer can be adequately implemented, BEVs can provide potential benefits to the grid as a secondary function while they are parked and plugged in [4], [5]. They can provide ancillary services (A/S) like spinning reserve and frequency regulation, peak shaving, valley filling, and demand side management (DSM) [1], [5], [6]. In addition, they can be used to support large scale renewable resources since intermittency makes utilities unable to integrate these resources unless some means of storage is implemented [6]. This new concept to provide grid-side benefits from a vehicle to the power grid is termed vehicle-to-grid (V2G). Under the V2G concept, BEVs will play an important role, either as an electric load (charging) or as a generation source (discharging) to provide the grid services. As a result, utilities will be able to improve stability, reliability, and overall system efficiency, considering that BEVs will behave as a distributed energy storage system (DESS) to the power grid.

It has been stated that with the V2G concept, BEVs can participate actively on grid operations. If just a few vehicles are involved, the impact on the grid will be negligible because each individual battery has a small capacity when compared to the system. For this technique to be successful and provide the services mentioned above, there must be

a large amount of BEVs aggregated to the grid. Adding all these electric vehicles to the grid will create a new significant load to the system and even without doing V2G operations with the system, the effect of charging them will certainly stress power networks [7], [8], [9]. This in turn, can increase the complexity of power system operation, and if not well handled, it may result in serious problems of security, stability, and reliability. Moreover, if the large penetration of these BEVs is not accurately managed, it can make the system susceptible to experience outages due to the lack of generation. Therefore, to overcome this new electrical load, infrastructure has to be changed or new charging techniques have to be developed. Modifying existing infrastructure is a very costly and complex process. Hence, the solution is to develop charging methods that allow integration of BEVs to provide potential benefits to the grid without affecting current system operation.

This work is focused on developing a method that allows the integration of battery electric vehicles to the power system. These vehicles, given their natural characteristics, must be plugged in to charge their batteries. If restrictions are not applied to vehicle owners or if their accommodations are not properly met, this additional load could result in a nuisance rather than contribution. To manage this situation, it has been proposed to charge the batteries of BEVs during off-peak periods and then, if they have extra energy stored, release it back to the grid during peak periods to provide capacity and energy services. Through a smart technique, known as peak shaving and valley filling, utilities will not only be able to control these BEVs, but will also obtain huge benefits by flattening their load curves. This effect of reducing large swings on daily consumption reduces the

use of small expensive units, which result in a decrease of operational costs since base load generation can be maximized.

1.2 Objectives

The main objective of this work is to investigate an optimal way in which massive penetration of electric vehicles (EV), particularly battery electric vehicles, can be effectively integrated to the power system. The main goal is to obtain a coordinated day-ahead schedule pattern that, during an extended period of time, provides a net load curve with the least possible variation. Optimal strategies will be developed considering a two-stage approach for the V2G and charging operations using peak shaving and valley filling techniques. The effects of PEVs addition to the system will be evaluated on the resulting demand curve and its economic operation will be analyzed from the perspective of a traditional unit commitment.

The following specific goals will be fulfilled during the development of this research work:

- Identify an original power system net load curve to which a new electric vehicle charging load will be added and its effects will be evaluated.
- Determine a coordinated charging strategy for EV integration to the grid, considering the vehicle requirements, load demands, and charging/V2G constraints.
- Formulate the problem to effectively integrate the EVs to the power system, focused on leveling the load consumption curve.

- Develop a mathematical model that schedules the charge and discharge operations of the aggregated EVs during specific intervals.
- Use the results of the proposed methods to describe the benefits obtained by the coordinated charging and V2G strategies on flattening the load curve and show how EV penetrations reduce the cycling effects on generation utilities.
- Measure the EV impact on the load curve with and without coordinated methods.
- Evaluate the economic advantages that EV fleets bring to the power system when scheduled in coordination.

1.3 Work Outline

This chapter introduces the motivation of this research and highlight the specific objectives and contributions. The rest of the work is organized as described below:

Chapter 2 reviews the fundamental aspects of electric vehicles and their relationship with the power grid. In general, this chapter introduces the different electric vehicle types, energy storage systems (focusing on the batteries available in the electric vehicles), and the vehicle-to-grid (V2G) concept applications.

Chapter 3 provides a concise explanation regarding power system operations and discusses, along with their mathematical formulation, two of the main problems (economic dispatch and unit commitment) encountered in the power system engineering field. Understanding the concepts presented in this chapter is essential for the development of this work, because they provide the necessary tools used to assess the economic operation impacts of the system when the electric vehicles are added to the network load.

Chapter 4 presents a complete description of the proposed intelligent method to effectively integrate PEVs to the grid. Specifically, the chapter is dedicated to formulate and explain the mathematical model of the coordinated charging/discharging algorithms by means of a two-stage optimization problem that aims to flatten the load demand profile subject to the vehicle and power system constraints under the V2G concept. In addition, this chapter reviews the corresponding modifications to the V2G proposed algorithm that result on the charging-only optimization problem.

Chapter 5 presents the numerical results of the simulations and cases studies evaluated to prove the effectiveness of the V2G and charging algorithms. Also, the economic operation of the system between the base cases and the other simulated cases is tested by means the unit commitment problem. Concluding statements regarding the results between the different scenarios considered are presented in the final remarks section.

Finally, Chapter 6 provides the contributions and summarizes the general conclusions obtained throughout this work. A list of recommendations points out directions for future work.

Chapter 2

2 Background Theory

This chapter reviews the fundamental aspects of the main topics in this work. First, electric drive vehicles and their types are described. Then, a brief explanation on energy storage systems and their relationship with grid-enabled vehicles is presented. Furthermore, the concept of vehicle-to-grid is formally introduced and discussed with all its applications.

2.1 Electric Drive Vehicles

2.1.1 Introduction

Electric drive vehicles have begun to gain wider acceptance in the transportation sector due to the increasing price of gasoline. In addition, the generation and storage capacity of these vehicles have been a strong appeal for the V2G implementation on power systems. Automotive industries have understood the opportunity that electric drive vehicles (EDV) represent and have responded with the manufacture of different types. The EDV contribution to the network depends essentially on the vehicle type. Grid-enabled vehicles (GEV) are the heart of the concept but there are other EDVs without grid connection that can also help the system by providing grid services.

2.1.2 Electric Drive Vehicle Types

Three different types of electric drive vehicles are appropriate for the V2G integration. These are battery, hybrid, and fuel cell vehicles [1]. As their name implies, they use an electric motor to provide all or part of the power needed for drive operation, but have different principles of operation. A brief description of each type of EDV is discussed below according to the literature mentioned in [1], [10], [11], [12]. For a complete and exhaustive explanation with regards to the theory, fundamentals, and design methodologies of the electric vehicle types, the reader is referred to [13].

The battery electric vehicle depends on an electric motor for its operation. This motor runs with energy from a battery that is charged from an external source by plugging it into an electrical socket. In this sense, BEVs should be plugged in to fill up the battery and unplugged for drive operation. The distance the vehicle can travel is, between many factors, function of the amount of energy the battery can store and if the battery is depleted, the vehicle can no longer operate since it is the only way to feed the motor. The value of BEVs for the V2G concept is based on absorbing energy to charge the battery and releasing it back to the grid if it will not be used for running operation. They will behave as a distributed generation/storage energy device whenever they are parked and plugged in to the grid.

Hybrid electric vehicles (HEV) operate somewhat differently than pure electric vehicles or as priorly mentioned BEVs. These vehicles use either, an electric motor or a traditional internal combustion engine (ICE), to run, but can also operate with both simultaneously. The ICE runs with fuel like traditional vehicles, but the electric motor runs with energy from a battery. This battery is charged by the on-board internal

combustion engine or by regenerative braking. However, plug-in hybrid electric vehicles (PHEV) work similar to contemporary hybrid vehicles with the main difference that they possess an electrical connection to charge their batteries. This advantage makes PHEVs better than HEVs since they usually have large capacity batteries making their running operation longer.

Similar to BEVs that can provide vehicle-to-grid services, HEVs and PHEVs can also be used to support the grid. Hybrids, in particular, can provide the V2G either as a battery vehicle or as a generator vehicle (using fuel while parked to generate). In the special case of plug-in hybrid vehicles, they have within them grid connection for transportation purposes, making them suitable for V2G applications. Conversely, HEVs have no grid connection. Figure 2.1 below shows the electric vehicles discussed up to this point with their main differences.

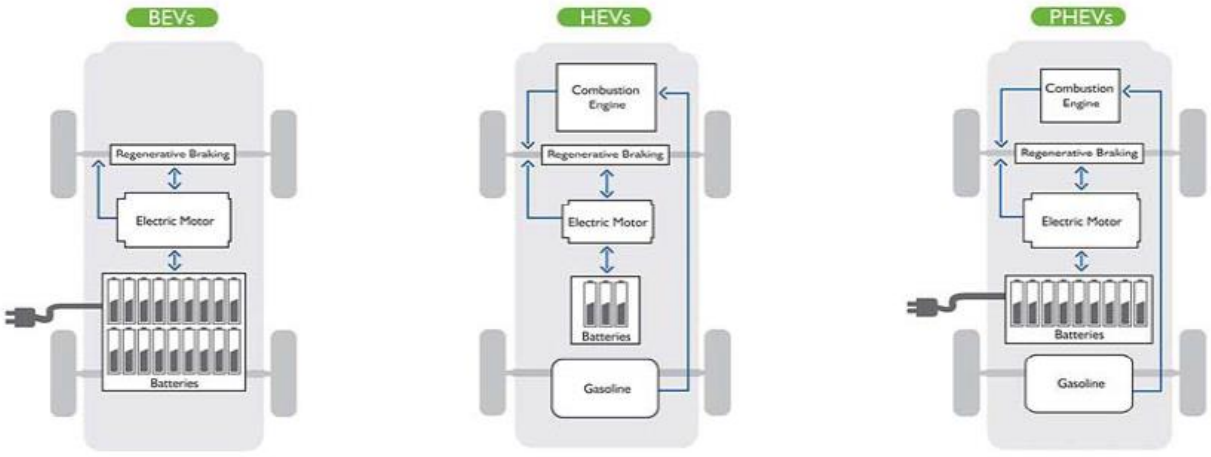

Figure 2.1 Battery, hybrid, and plug-in hybrid electric vehicles [14]

The less commonly used type of EDV is the fuel cell vehicle (FCV). Basically, these vehicles run its electric motor with electricity produced by a fuel cell. This cell converts hydrogen gas stored in the vehicle tank in combination with atmospheric oxygen to generate electricity and feed the on-board electric motor. As can be seen, the fuel cell vehicles' value for V2G is limited to generation, since they can produce electricity in the fuel cell. However, these vehicles have no connection to the grid, so the cost associated to plug in these vehicles to use them as distributed generation devices do not respond to transportation system and electric grid integration.

In general, battery electric vehicles (BEV) and plug-in hybrid electric vehicles (PHEV) can contribute to V2G by providing electric storage capacity, while hybrid electric vehicles (HEV) and fuel cell vehicles (FCV) can contribute by providing generation capacity [15]. Throughout this work, particular attention has been placed on BEVs in order to use their storage capacity as an energy storage system when a significant amount of these vehicles is aggregated.

2.2 Energy Storage Systems

2.2.1 Introduction

Global dependence on electric energy is rapidly evolving during recent years. This has made energy storage systems (ESS) an essential component of electrical power grids. The ability to store electricity when excess is produced and then release it when demand is high has allowed for greater flexibility in system operation. Also, energy storage devices offer a new strategic business tool that can be crucial to improve power network stability and reliability.

Electric energy does not have the characteristic to be stored directly as electricity. Therefore, it has to be converted to another form of energy. Then, the stored energy is converted back to electrical energy when needed. This process of energy conversion is done by the ESS. Energy can be converted into many forms, but the most common include mechanical, chemical, electrochemical, thermochemical, thermal, and electrical energy [16]. Different types of energy storage system technologies exist, the most popular being battery energy storage systems (BESS), compressed air energy stored systems (CAESS), fly-wheels energy storage systems (FESS), pumped hydroelectric storage systems (PHSS), and superconducting magnetic energy storage systems (SMESS).

Energy storage systems can be used to meet technical power systems requirements regarding generation, distribution or even end-user consumers. They play an important role in energy management, power system quality, and power system protection based on the nature of each ESS characteristics. In report [17], R. Carnegie *et al.* state that ESS are able to: (1) deal with the increase in peak demands while satisfying the system constraints, (2) integrate renewable energy resources, and (3) provide ancillary services to the grid. Nevertheless, a more detailed list of ESS applications has been described by X. Luo *et al.* in [16], including ramping and load following, time shifting, peak shaving and load leveling, transmission and distribution stabilization, voltage regulation and control, transportation applications, spinning and standing reserve, among others.

Integration of battery electric vehicles to the electrical network is the focus of this work. As previously mentioned, the contribution of these vehicles to the grid is based

on the storage capacity of their on-board batteries. Consequently, battery energy storage systems will be the only storage system technology considered among all others mentioned and will be further discussed in Section 2.2.2.

2.2.2 Battery Energy Storage Systems (BESS)

A battery energy storage system technology is used to store electrical energy as chemical energy to serve the electrical loads. Its main component is the battery, which consists of a single or multiple electrochemical stack cells connected in series or parallel to produce electricity at a specific system voltage and current level from an electrochemical reaction. Each cell contains an anode, a cathode, and an electrolyte and is responsible to bi-directionally convert electrical and chemical energy. During discharge, the electrons move from anode to cathode in a reduction-oxidation reaction. In contrast, during charging, the reverse reaction takes place and the battery is recharged by placing potential difference at their terminals [16], [17], [18]. A visual representation of the charge and discharge process inside the battery is illustrated on Figure 2.2.

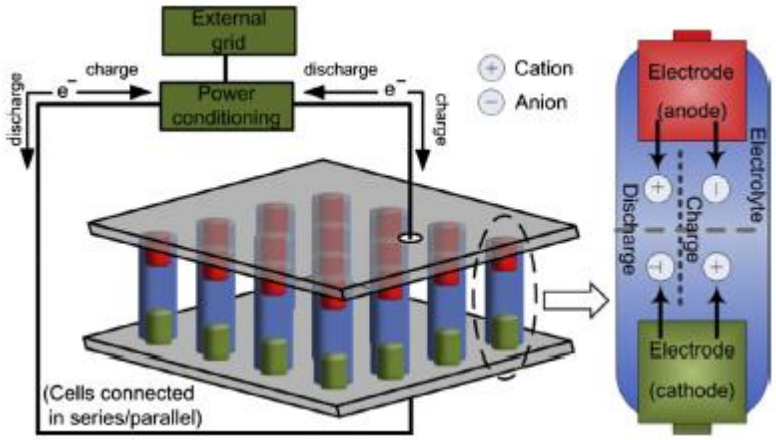

Figure 2.2 Battery energy storage system (BESS) schematic diagram [16]

Currently, many different types of batteries have been developed. Great efforts are being conducted regarding the progress and technology of batteries. Among all kinds of batteries, lead-acid are the most used since they are the oldest and most developed. In contrast, sodium-sulphur (NaS), nickel-cadmium (NiCd), and lithium-ion (Li-ion) appear to be the last incoming technology with the latter having the greatest potential for future development [18]. Li-ion batteries have high density and cycle efficiencies, low self-discharge loss, and no meaningful memory effect [19], but can be expensive and their cycles can create negative effects on battery life. Different from traditional batteries, Li-ion are composed of four major components, which include anode, cathode, electrolyte, and separator. The lithium ions, rather than electrons, move to the cathode when the battery discharges and leave the cathode when charges. As mentioned in [20], the electrolyte allows the movement of the lithium ions between anode and cathode, and the separator, which is a micro-porous membrane,

prevents short circuits from anode to cathode by allowing only lithium ions to pass through the pores.

Batteries have been very attractive for electrical applications since they have the advantage to respond quickly (on the order of milliseconds) to load changes. However, the frequent switching of the state of charge (SOC), which is a measure of the energy stored in the battery to the battery capacity, depth of discharge (DOD), and operating temperature cause battery degradation. In theory, batteries should be operated above certain tolerance level and under a temperature range to achieve optimum benefits. Other important features of batteries are efficiency, energy density, and self-discharge.

2.2.3 Electric Vehicle Batteries

Electric vehicles, either pure, hybrid or plug-in hybrid, own a direct relation with a power source for their operations. However, significant issues relative to the energy storage systems used by EVs involve challenges related to costs, reliability, capacity, cycles, among others.

Recently, different battery technologies have been linked to these vehicles such as lead acid, nickel metal hydride, nickel cadmium, and lithium-ion. One of the most widely used coincides with Li-ion batteries for its advantages on high energy density, high voltage, low self-discharge rate, long cycle life, and high charge/discharge rate capability compared with other technologies [21]. Typical values for energy-to-weight and power-to-weight ratios are 180 Wh/kg and 1500 W/kg, respectively [22]. The types

of Li-ion batteries used with EVs are Lithium Cobalt Oxide (LCO), Lithium Manganese Oxide (LMO), Lithium Iron Phosphate (LFP), and Lithium Nickel–Manganese– Cobalt Oxide (NMC). Table 2 on [21] illustrates the different characteristics between these types of batteries, while Table 1 on [23] shows the different Li-ion battery pack manufacturers and the EVs models in which the batteries are used. In addition, [24] also reviews more characteristics of the different types of rechargeable batteries discussed in this section.

Additional to the Li-ion batteries described, researchers are investigating other energy storage systems that provide greater performance characteristics for EVs. According to [23], the Li-S battery offers outstanding advantages over traditional lithium-ion batteries. Although they are capable of higher energy densities, wider operating temperature ranges, and lower costs with greater safety, this technology has not been extensively marketed because of technical drawbacks.

2.2.4 EVs as Energy Storage Devices under the V2G Concept

At the end of Section 2.1.2, it was mentioned that BEVs, particularly, can behave as distributed energy storage systems. This is technically possible with the premise that these vehicles are parked most of the time and can be plugged in to exchange energy with the grid to bring positive effects during idle time. For example, in [7], optimal scenarios consider BEVs to withdraw energy during off-peak or low demand periods and then feedback the energy to the grid during periods when utility needs it. The exchange of this energy should certainly guarantee that BEVs have enough

charge for transportation purposes for at least the next trip or the next grid connection. This task will be carried out through the V2G concept (explained later in Section 2.3) by optimizing the charging/discharging schedules of each vehicle to provide grid services while at the same time adequately fulfill the vehicle's owner requirements. The basic idea is to encourage BEV's owners to enter this market of managing and regulating their consumption and charging profiles by using financial incentives, electricity pricing such as time-of-use (TOU) tariffs, and subsidies.

BEVs batteries are only used for running operation. Given that the vehicles can travel daily distances without consuming all their stored energy, electric companies have seen these batteries as an opportunity for storage with little investment. Therefore, it is the on-board battery in next-generation BEVs that appears most likely to be used as energy storage devices to provide power system electrical network support. However, the high cost and the low lifetime of batteries are the biggest challenges with electric vehicle development. Further improvements in batteries to reduce cost and avoid fast degradation will increase the interest and broaden the application of EVs as distributed energy storage devices.

2.3 Vehicle-to-Grid (V2G) Concept

2.3.1 Approach

Electric drive vehicles have the potential to benefit utilities as generation/storage devices. The on-board battery in every individual BEV or PHEV, represents the initial step toward the V2G implementation of aggregated vehicles as fleets. Typical storage capability of these batteries is in the 1-60 kWh range [25], depending on the type of

battery and vehicle being used. In spite of their small capability, since vehicles are idle and parked most of the time, not all the stored energy is consumed during normal daily distances traveled. Even though each battery can contribute with remaining energy, it is too small to significantly impact the grid. To deal with this problem, many vehicles must be grouped so that the aggregation forms an appropriate size capacity that can impact the network on a mega-watt (MW) order. This task is performed by an aggregator, whose role is to effectively collect individual vehicles into a single entity to provide the energy and capacity for grid services.

The aggregator introduces a crucial piece into implementation of the V2G concept. It is responsible for determining the optimal selection of vehicles to join and accurately manage to ensure controllability. Such control allows load fluctuation leveling which results in simplified system operations by avoiding or delaying start-up of cycling and peaking units. For that reason, if aggregators can certainly sell their services with enough precision, power system operators may opt to do transactions with them since dispatching a flat load curve is much easier than a varying and fluctuating load curve [7]. However, these power transfers must be balanced with the vehicle to reduce inefficiency and battery life impacts. The vehicle contribution depends mainly on the state of charge of each individual battery, but the aggregator should always consider the frequency of fluctuations and the depth of discharge when optimizing their schedule because both lead to battery degradation [26].

2.3.2 Assumptions

The V2G concept is mainly based on the opportunity that EDVs send power back to the grid. However, V2G is in the conceptual stages and for it to be technically feasible, some key assumptions must be considered. According to [27], these preeminent assumptions are:

- The batteries of electric cars are underutilized. This implies that electric vehicles do not use all the stored energy in their batteries to perform daily operation. Thus, with the remaining energy in each individual battery, EVs can be aggregated to act as a significant storage device and provide a second function to the power system.
- EVs are idle and parked most of the time during a 24-hour period. Vehicles, in general, are used to drive to work in the morning and to return home in the afternoon, allowing them to be connected to the grid while not being used for transportation purposes. In fact, according to their patterns of use, most of EVs parked times coincide with the periods where the utilities would need to use them. EVs can be connected overnight to charge when the demand is low and provide grid services during the day when demand is high.
- EVs batteries do not represent a cost for electric utilities. Therefore, utilities will benefit from having available an energy storage system without having invested on it.
- The V2G transactions can be predicted with much certainty, as possible. It has been stated that for V2G to have some impact on the network, many vehicles should participate. Therefore, because many electric cars are considered

within the concept, consistent patterns can be obtained regardless of the variability of each vehicle. The aggregator will be responsible for encouraging vehicle's users to keep their vehicles plugged in whenever possible in order to achieve accurate V2G transactions. Once this strategy is achieved, the aggregator can suitably integrate EVs to the grid.

2.3.3 Key Elements for Interconnection

In order to provide the V2G services, every vehicle must comply with several required elements to send and receive electric power adequately. These fundamental elements are:

- Grid connection – Individual vehicles should be plugged in to make electrical energy flow between the electric vehicle and the power system.
- Communication system – When electric vehicles are grouped to provide vehicle-to-grid services, they must be able to communicate effectively with the aggregator. Each vehicle should send and receive relevant information like availability, location, power and energy capacity, dispatch commands, driving needs, expected usage, and other data.
- Metering – Since vehicle-to-grid services involve energy transfer, every vehicle must include a metering device (on-board or off-board) capable of measuring energy flow between the vehicle and the grid.

2.3.4 Vehicle-to-Grid (V2G) Services

Electric vehicles participating on V2G can provide several grid services. Most of these services, depending on jurisdiction and power system, are carried out through different power markets by system operators in real time. Some vehicles might be appropriate for one service but might not necessarily be well suited for other services. Thus, vehicles and power markets should be matched in order to be profitable. Basically, power markets differ in their applications, terminologies, control methods, response times, power dispatch durations, contract terms, and prices. This section describes some of the EV services found in the literature. The most important are:

- Base Load Generation

  This is the principal source of electricity generation of all power systems. It runs continuously and is typically provided by low cost kWh generating units like nuclear, coal-fired, natural gas, and hydroelectric [28]. Up until now, no EDV has showed to provide bulk generation at competitive price because of limited energy storage, short lifetimes, and high kWh energy price [1]. In addition, most EDVs do not produce electricity; they store it in their batteries. Fuel cell vehicle generating capability is negligible for this type of service or market.

- Ancillary Services (A/S)

  All power systems, besides bulk generation, use ancillary services to support the transmission of electricity from generation to ultimate consumers. Some utilities have them along with their systems. Others buy those services through an energy market. Regardless of the way, these services are

responsible for balancing the supply and demand fluctuation in real time and maintain the reliable operation of the system. Different tasks are comprised as ancillary services, but spinning reserve and regulation are the most suitable to be implemented with EDVs.

Spinning reserve refers to the additional generation capacity that is running and synchronized to the grid. It is used when unpredictable events occur like the loss of a generator or equipment failure. Operating reserves are rarely used, but must be ready to respond quickly during any contingency when called by the system operator. As mentioned in [28], EDVs with storage capability are favorable to perform this task because they: (1) can be brought online fast to serve the load without the need to have been spinning and (2) do not affect battery life since it is rarely brought into operation.

Regulation is another form of A/S. It is used to maintain a steady frequency and voltage on the grid by continuously matching supply (generation) with demand (load). Typically, this is carried out by rapid start gas fired plants or by hydroelectric plants with the capacity to vary their power output fast. These units have to be equipped with automatic generation control (AGC) and may be capable of adjusting (ramp up/down) their output accordingly to real time signals (almost every 2 – 4 seconds) and operator requests. Two different signals can be received by the generation units. If the load exceeds generation, the frequency and voltage drop and the received signal calls for regulation up. In contrast, if the load is less than generation, it requests regulation down.

Similar to spinning reserve, regulation has to be available 24 hours a day, every day, but unlike spinning reserve, it can be called for operation hundreds of times per day. EDVs are appropriate to provide regulation because: (1) vehicle batteries have fast response capabilities and (2) the vehicles, due to their nature, can participate in this market even if back-feed of power is disabled within the grid; in this sense, vehicles will only provide regulation down through charging [25]. In addition, regulation involves patterns of low depth of discharge which minimizes battery degradation.

Among all electric vehicles, BEVs and PHEVs satisfy the basic requirements to participate on spinning reserve and regulation power markets. In spinning reserve, higher state of charge is preferred in order to have enough energy available if activated. However, the SOC for regulation cannot be 100%. Batteries on these vehicles perform regulation down while charging and regulation up when sending power back to the system. Thus, batteries should have an adequate SOC capable to respond to either of the regulation signals.

Spinning reserve and regulation, both power market prices, are divided in two components, capacity (kW) and energy (kWh) price. The former is paid for the amount of power that is available and ready during a specific time and the latter is paid for the energy delivered in real time when the unit is called. This means that electric vehicles providing A/S through V2G will be paid for capacity price even if they are not sending or receiving power to/from the grid, making it an attractive market for vehicle owners.

- Peak Power and Peak Shaving/Valley Filling

Utilities purchase peak power when a high demand is expected, due to the daily load fluctuations. Typically, peak power is provided with high-cost, fast-response units, such as gas generators that can be turned on and off for periods of 3 – 5 hours per day. With respect to electric vehicles, they are attractive because batteries do not have a startup cost or a shutdown cost. However, the low storage capacity of the on-board battery is the biggest limitation. Also, as discussed in [29], it is evident that EVs would only replace traditional peaking units if the payment to vehicle owners is less than what utilities actually invest on that service.

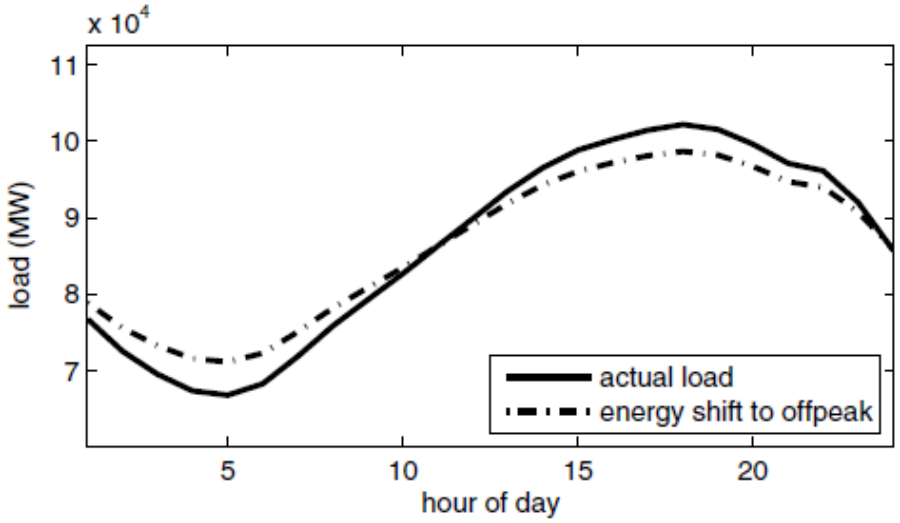

Figure 2.3 Peak shaving and valley filling demonstration [30]

Another EV service is to store electricity during surplus (off-peak or low demand) and release it back to the grid during high demand periods. This

technique is known as peak shaving/valley filling and the goal is to smooth the load curve to simplify power system daily operations. Figure 2.3 depicts this behavior by shifting energy from peak to off-peak period. Electrical utilities incur in significant costs associated to the underutilized capacity of their generation units. In addition, the large variation on the load curve requires small units to start up and shut down at considerable cost to satisfy the balance constraints. The combination of these problems often results in the operation below design point of the running generators.

EVs, even without performing V2G operations, must charge their batteries for running operation. With appropriate charging schedules during off-peak periods, these vehicles can contribute to valley filling by substantially leveling the load curve. If the remaining energy left on the batteries can optimally be sent back to the grid for peak shaving, system operators will be fortunately since dispatching a flat curve is less complex than dispatching a varying curve. As a result, underutilized baseload generation costs along with capacity requirements for peak demand and cycling costs can be drastically reduced. Overall, the ability to schedule both charging and discharging of BEVs or PHEVs could increase power system utilization in a significant manner. The problem arises with the large depth of discharge involved in this application, which can seriously affect battery life.

- Renewable Integration

Renewable energy has turned out to be a significant challenge for utilities. Regions where there is no water for hydroelectric plants, constant wind patterns

for wind farms, or uninterruptible periods of solar light for PV arrays are, but not limited to, some of the leading issues regarding renewable sources integration. Therefore, one of the most attractive applications of EVs is to support large scale of renewable resources [6]. As it is well known, these resources are intermittent, and their value entirely depends on environmental conditions. Hence, on-board electric batteries of EVs offer storage capacity absorbing energy during surplus and delivering it back during shortage. This way, renewable resources can be adequately implemented since fluctuating renewable supply can be matched with the already changing load.

2.3.5 Aggregator

Electric vehicle batteries have low kWh storage capability. Consequently, hundreds of vehicles should be grouped to create a meaningful impact on the system scale. In addition, grid services usually call for power on a MW basis, making the aggregation apparent. The main idea of aggregation is to join as much vehicles as possible to create an appropriate size of batteries that can support the grid in an efficient and reliable manner. Once these vehicles are aggregated, they are able to provide different services to the system [31].

Those grid services are mostly scheduled and contracted through a power market with the system operator. To complete the agreements, the system operator does not want to deal with individual vehicles; instead he will directly deal with an intermediary called the aggregator, which is a control interface between both the vehicles and the

system operator. The aggregator can be a sub-system operator on the distribution level or a private owner such as a parking lot manager.

The aggregators' role, as indicated in [25] and [27], is to effectively collect the EVs into a single entity to provide energy and capacity grid services. It is the aggregators' responsibility to determine which vehicles to select to join the aggregation and accurately monitor, control and manage them according to their needs. In addition, he should accurately regulate the charge and discharge operations of each vehicle through a strategic method considering that the primary goal of plugging in the vehicle is charging the battery to serve the next drive. His business corresponds to selling the energy and capacity services to the vehicle owners and then providing them to the system operator. As an advantage for vehicle owners, transactions undertaken by means of the aggregator, will considerably result in lower costs than would be incurred by individual vehicles.

Figure 2.4 illustrates what the aggregators role should be by means of an uncoordinated versus coordinated charging schedule of a plugged-in vehicle. From the illustration below, it is evident that a PEV does not have to begin its charging process exactly when it is plugged in. Simply, the aggregator should find the appropriate time, based on an optimal system condition, to charge the vehicle as long as he guarantees the PEV gets the desired SOC value at departure time. This task of controlling the charging schedules of PEVs while considering owner requirements is what an aggregator is expected to realize in order to control large-scale penetrations of battery electric vehicles.

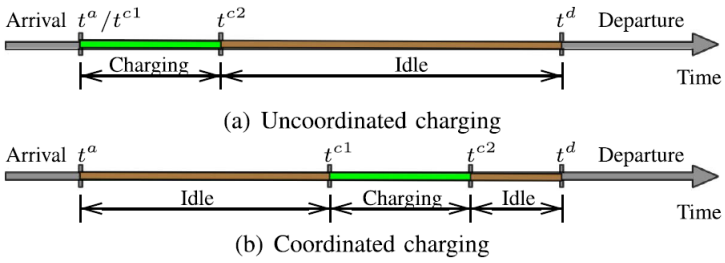

Figure 2.4 Uncoordinated versus coordinated charging scheme [32]

BVs aggregations or fleets can be utilized to perform two main functions. They can act either as controllable loads or as generation storage devices [25]. As a controllable load, the aggregator can manipulate the charging process of the vehicles allowing the power system to reduce the load fluctuations or level the load curve shape. In contrast, as a generation/storage device, they can help the system by supplying both energy and capacity services. Depending on the state of charge, the batteries can either absorb or discharge energy performing regulation down or regulation up. Also, they can supply power back to the grid to lower peak periods and be available as reserve capacity. Since most of the operations of electric vehicles under the control of the aggregator require continuous charge and discharge, battery degradation is the highest concern of vehicles owners. Therefore, the aggregator should pay enough attention to this delicate matter.

2.3.6 Regions and/or Systems Expected to Adopt the V2G Concept

Several applications, benefits, and advantages of the V2G concept have been highlighted. Strategies for implementation and key elements for interconnection have also been described. However, it has not been pointed out which power systems or regions are well suited to adopt the V2G concept. W. Kempton and J. Tomić consider this aspect in [6], arguing about diverse characteristics of jurisdictions that would consider earlier implementation. Below, a simple list of power system characteristics that might facilitate V2G adoption are presented:

- Power systems that want to improve their network providing more reliability and stability without having large investment on new infrastructure associated to generation.
- Regions that have grid isolation. Typically, this occurs on small islands where its own system receives no support from another system because of the lack of electrical connection.
- Power systems where the cost for ancillary services are high, or regions where there is no source of hydropower.
- Countries that have adopted new policies and goal targets for new technology investment, high penetration of renewable energy resources, such as wind and solar, and reductions on power plant emissions.
- Places where the price of gasoline is high compared to the price of electricity, so that people can be motivated to move from traditional vehicles to electric vehicles.

Chapter 3

3 Power System Operation

The purpose of this chapter is to present a brief explanation regarding power system operations. In addition to the general description provided in Section 3.1, this chapter focuses on the economic operation of available generation units, particularly, thermal units. Section 3.2 and 3.3 explore the fundamental concepts and mathematical formulation of the two main problems encountered in power system operations: economic dispatch and unit commitment. The material illustrated throughout these sections is supported by journal articles [30], [33], [34] and a thesis work by R. Pérez [35]. For a complete description and examples of the economic dispatch and unit commitment problems, the reader is referred to the following textbooks [36], [37].

3.1 System Overview

An electric power system, or electric grid, is a network of electrical components capable of supplying, transferring and using electric power. Four major physical elements comprise the grid: generation, transmission, distribution, and load. Generation corresponds to all the plants electrically connected to the grid that supply the power. Transmission is the essential component that ties the generation plants with the load centers through high voltage lines. Distribution links, by means of low voltage lines, the

load centers with the industries, business, or homes that are the load of the system. The load is the final element where electrical energy should be effectively delivered to be utilized by end consumers.

Achieving balance among all the grid elements is the fundamental challenge of utilities. As it is well known, demand is not constant, and its uncertainty makes the engineering, planning, and operation of the overall system a difficult task. Since electric utilities cannot predict the load with certainty, they use historical data and forecast algorithms for planning purposes. Operationally, supply and demand must be dynamically balanced. Since load is not directly under the control of system operators, utilities must change generators' output to satisfy this grid constraint.

Utilities project or forecast the electric demand and carry out several processes to deal with the load fluctuations at different time frames. Unit commitment (UC) and economic dispatch (ED) are these two main processes. Unit commitment establishes the generator operating schedules in advance of operating time; in other words, it determines which generators will be needed to satisfy the load forecast for the next day. Typically, UC includes large thermal units that take a long time to start up and reach operating conditions. In contrast, economic dispatch is the process of choosing the generators' output level of the committed units, which results in the minimum cost to meet the demand. Usually, ED can be done relatively close to operating time, hours or even minutes before dispatching the units. In addition, three other mechanisms are used to overcome the small fluctuations between UC forecast and actual demand. These mechanisms are out of the economic margin but provide the flexibility to inject power to the grid in short time scales. The first method that aids for this control is the opposition to

load changes by means of the addition or extraction of kinetic energy from the rotating inertia of the generators spinning on the system. If this method does not compensate, then the second method is to activate the droop characteristic of the generators. Generators, by means of a governor, can instantaneously change their output according to frequency deviation once it strays beyond a set point. The third mechanism, automatic generation control (AGC), is the most commonly used by utilities. It provides a feedback signal from the system's frequency issuing an increase or decrease on the output level of the generators. The resulting signal is known as the area control error (ACE) and the goal of the AGC is to minimize it requesting the desire changes.

Another issue regarding system operation occurs when there is a sudden loss of power on the grid. System operators need to ensure that there is additional generation capacity available to the previously scheduled to attend unforeseen events. This generation capacity above scheduled demand is known as spinning reserve and has a significant cost for being idle waiting for a contingency to occur.

Despite their attempts, the fundamental process to produce electricity and deliver it to end user remains the same. The lack of storage capacity forces generation (supply) and load (demand) to be balanced at all times. In general, the continuously varying load along with the large swing on daily consumption requires the system operator to constantly maintain and control the flow of electricity at the dispatch center to satisfy the balance constraints. Therefore, successful planning and dispatch of generation units is crucial in power systems operations.

3.2 Economic Dispatch Problem

Undoubtedly, the economic dispatch (ED) is an essential problem on power system engineering. It is, in essence, a unit commitment optimization sub problem that seeks to allocate the real power output of each scheduled unit so that the overall generation fuel costs are minimized and a set of technical constraints are satisfied. The problem is stated just for a specific load level and for simplicity, the constraints considered are the forecast load demand, the systems losses, and the generator output operating limits. Modelling this behavior is critical on the system operation because it guarantees optimal economic states in all their online units already connected to the grid. Mathematically, the ED optimization problem can be formulated as:

$$\min C_T = \sum_{i=1}^{N_G} F_i(P_i) \qquad (3.\ 1)$$

subject to:

$$\sum_{i=1}^{N_G} P_i = P_D + P_L(P_i) \qquad (3.\ 2)$$

$$P_i^{Min} \le P_i \le P_i^{Max}, \forall\ i \in [1, N_G] \qquad (3.\ 3)$$

where C_T is the total operating cost of all the scheduled units, P_i the real power supplied by unit i, $F_i(P_i)$ the fuel cost function of the i^{th} unit in terms of P_i, N_G the number of scheduled units, P_D the real power system demand, $P_L(P_i)$ the transmission system losses in terms of P_i, and P_i^{Min}, P_i^{Max} are the lower and upper operational limits of the i^{th}

unit, respectively. The constraint of equation 3.2 establishes the power system equilibrium which is met when generation equals demand plus system losses, and equation 3.3 enforces the units to operate under their design capacities.

The fuel cost function, in $/hr, relates the cost of the fuel used in terms of the real power output of a generation unit. Usually, a quadratic equation is used to model that input-output relationship and is given by:

$$F_i(P_i) = a_i P_i^2 + b_i P_i + c_i \ \ (\$/hr) \qquad (3.4)$$

where a_i, b_i, and c_i are the cost coefficients of the generation unit i, with units of $/MWhr^2, $/MWhr, and $/hr, respectively. Figure 3.1 illustrates a traditional representation of a fuel cost function in terms of power output.

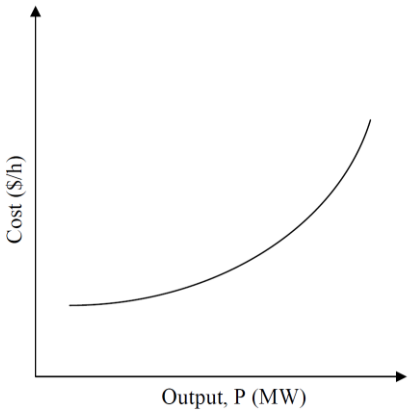

Figure 3.1 Typical fuel cost function of a thermal generation unit [35]

The corresponding predefined system condition under the ED problem is the system demand load (P_D) and generally is assumed that has been previously estimated from any particular forecast algorithm.

A common practice is to approximate the transmission losses in terms of the power output of the plants by the Kron's loss formula method. Its value can be obtained by means of the B matrix loss formula expressed as:

$$P_L(P_i) = \hat{\mathbf{P}}^T [B] \hat{\mathbf{P}} + B_0^T \hat{\mathbf{P}} + B_{00} \qquad (3.5)$$

or formally as:

$$P_L(P_i) = \sum_{i=1}^{N_G} \sum_{j=1}^{N_G} P_i B_{ij} P_j + \sum_{i=1}^{N_G} B_{i0} P_i + B_{00} \qquad (3.6)$$

where B_{ij}, B_{i0}, and B_{00} are the *B* coefficients.

From equations 3.1 – 3.3, the ED problem is a constrained optimization problem that consist of an objective function, an equality constraint and inequality constraints. Therefore, the problem can optimally be solved by the following *Lagrange function*:

$$\mathcal{L} = C_T + \lambda (P_D + P_L(P_i) - \sum_{i=1}^{N_G} P_i) \qquad (3.7)$$

where $\mathcal{L}$ is the *Lagrange function* and λ the *Lagrange multiplier* associated to the constraint of equation 3.2. Taking the first derivative of equation 3.7 with respect to the N_G power output variables and λ, and then equating to zero results in the below coordination equations:

$$\frac{\partial \mathcal{L}}{\partial \lambda} = P_D + P_L(P_i) - \sum_{i=1}^{N_G} P_i = 0 \qquad (3.\ 8)$$

$$\frac{\partial \mathcal{L}}{\partial P_i} = \frac{dF_i(P_i)}{dP_i} + \lambda\left(\frac{\partial P_L(P_i)}{\partial P_i} - 1\right) = 0, \forall\, i \in [1, N_G] \qquad (3.\ 9)$$

Observe from equation 3.8 that the solution merely returns the constraint equation, so from equation 3.9, the value of λ can be re-arranged as:

$$\lambda = \frac{dF_i(P_i)}{dP_i} \times \left(1 - \frac{\partial P_L(P_i)}{\partial P_i}\right)^{-1} \qquad (3.\ 10)$$

where the term $\frac{dF_i(P_i)}{dP_i}$ is the incremental cost and $\left(1 - \frac{\partial P_L(P_i)}{\partial P_i}\right)^{-1}$ is called the penalty factor, both for the i^{th} generation unit.

Finally, it can be observed that the minimal cost occurs when the product of the incremental cost and the penalty factor is the same for all the units at some value of λ. Indeed, we must verify that the sum of all power outputs satisfies the demand and the losses, and in addition guarantee the feasibility of the solution by enforcing the lower and upper generator limits of equation 3.3.

3.3 Unit Commitment Problem

Another crucial task on power system engineering is how to economically handle the load fluctuations and cycles throughout the different days, weeks, and even seasons. Therefore, electric utilities must decide in advance when and for how long the generators

should be turned on and off to reduce the production costs. This is done by means of a computational process called unit commitment (UC) which according to reference [38] is defined as:

> *"a critical combinatorial optimization problem for daily economic planning and operation of the modern power systems which collectively performs suitable on/off decision of generating units and distributes generated power among the committed units to achieve minimum generation cost while satisfying power demand, reserve, and other basic constraints over a scheduled time horizon".*

From the above definition, recognize that UC is different from the ED problem because it involves finding the minimum cost using the optimal mix of the different available units of the whole system and not just allocating the output power of the online generators. Therefore, the objective function of the UC problem can be stated as the minimization of the total running cost, mainly including fuel costs, startup costs, and shut down costs of the units. Mathematically, for N_G thermal power units over a scheduled time period T, it is given by:

$$\min C_T = \sum_{j=1}^{T}\sum_{i=1}^{N_G}\left\{F_i\left(P_{ij}\right)\times U_{ij} + SUC_{ij}\times U_{ij}\times\left[1-U_{ij-1}\right] + SDC_{ij}\times U_{ij-1}\times\left[1-U_{ij}\right]\right\} \qquad (3.\ 11)$$

where C_T is the total cost (\$), $F_i\left(P_{ij}\right)$ the fuel cost function of the unit i (\$/hr), P_{ij} the real power output of the thermal unit i at hour j (MW), U_{ij} the binary variable {0,1} for the on/off status of the unit i at hour j, SUC_{ij} the startup cost of the unit i at hour j (\$/hr), SDC_{ij} the

shut-down cost of the unit *i* at hour *j* ($/hr), *T* the number of time intervals under the study (hr), and N_G the number of power thermal units.

The fuel cost function $F_i\left(P_{ij}\right)$ is the same as $F_i\left(P_i\right)$ from equation 3.4 but in terms of real power of unit *i* at hour *j*. The shutdown cost is assumed to be constant and independent of the length of time the unit has been running before shutting down. A common practice is to assign a value of zero in the study [34]. On the other hand, the start-up cost is associated to restarting a decommitted unit and is related to the temperature of the boiler or the number of hours the unit has been down. If the unit is cold (shut-down for a long time), it requires more fuel and energy to achieve the corresponding boiler temperature than if the unit is hot or recently shutdown (removed from service not long ago). A simple way to represent the start-up cost of the units is with the step function given by:

$$SUC_{ij} = \begin{cases} H - SUC_{ij}, & X_{ij-1}^{off} \le CSH_i \\ C - SUC_{ij}, & otherwise \end{cases} \qquad (3.12)$$

where $H - SUC_{ij}$ is the hot start-up cost of unit *i* at hour *j*, $C - SUC_{ij}$ the cold start-up cost of unit *i* at hour *j*, X_{ij-1}^{off} the down time of unit *i* up to hour *j-1*, and CSH_i the number of hours it takes for the boiler of unit *i* to cool down.

The unit commitment problem from equation 3.11 involves a set of physical and operational constraints that must be satisfied. Each individual power system imposes their own rules, and hence the constraints, depending on their procedures and standards. The

most typical constraints are related to system and unit requirements, and can be defined as follows:

- Power Balance

  The generated power from all the committed units must satisfy the forecasted demand and the losses of the system over the scheduled horizon. This is:

$$\sum_{i=1}^{N_G} P_i \times U_{ij} = P_D - P_L(P_i), \forall\ j \in [1,T] \qquad \textit{(3. 13)}$$

- Spinning and Supplemental Reserves

  Unforeseen load changes and forced outages of generating units are the reason for reserve requirements. The stable and reliable operation of power systems rely on maintaining the sum of the maximum generating capacities of the online units above an acceptable value that includes the power balance plus the reserve requirement. Formally, spinning reserve can be defined as the unused capacities of the committed units that are unloaded but ready to respond on the event of disturbances, in addition to what is needed to serve the actual demand (including losses). These capacities should be provided by units that are already synchronized to the network. In contrast, supplemental reserve includes the generation capacities of off-line units that can be available within minutes (usually 10 minutes). Unlike spinning reserve, they are not synchronized to the grid and normally come on-line once the spinning reserve are depleted.

  Some of the common rules used to determine the reserve requirements are: (1) a given percentage of the load or even the peak demand, (2) the amount of power equal to bring on the largest committed unit, and (3) other regulations that

may vary according to jurisdictions. The equations of these reserve requirements are:

$$\sum_{i=1}^{N_G} P_i^{Max} \times U_{ij} \geq \sum_{i=1}^{N_G} P_i \times U_{ij} + SR_j, \forall\ j \in [1,T] \qquad (3.\ 14)$$

$$\sum_{i=1}^{N_G} (P_i^{Max} - P_{ij}) \times U_{ij} + \sum_{k=1}^{N_{OG}} P_i^{Max} \geq SR_j + Sup_j, \forall\ j \in [1,T] \qquad (3.\ 15)$$

where SR_j is the specified spinning reserve requirement at hour *j*, Sup_j the specified supplemental reserve requirement at hour *j*, and N_{OG} the number of off-line generating units. Equation 3.14 is for spinning reserve requirement, while equation 3.15 is for supplemental reserve requirement.

- Minimum Up/Down Times

Once a unit is committed or decommitted, there is a predefined minimum time before any change can occur. As a result, two thermal operating unit constraints may arise: minimum up-time and minimum down-time. The former is the minimum time the unit should be running prior to shutting it down once it is committed, and the latter is the minimum time the unit has to be shut-down before it can start up if it is decommitted. The minimum up-time and minimum down-time constraint equations are:

$$\left[X_{ij-1}^{ON} - T_i^{ON} \right] \times \left[U_{ij-1} - U_{ij} \right] \geq 0, \forall\ i \in [1,N_G], \forall\ j \in [1,T] \qquad (3.\ 16)$$

$$\left[X_{ij-1}^{OFF} - T_i^{OFF} \right] \times \left[U_{ij-1} - U_{ij} \right] \geq 0, \forall\ i \in [1,N_G], \forall\ j \in [1,T] \qquad (3.\ 17)$$

respectively, where X_{ij-1}^{ON} is the up-time of unit *i* up to hour $j-1$, T_i^{ON} the minimum up-time requirement of unit *i*, X_{ij-1}^{OFF} the down-time of unit *i* up to hour $j-1$, and T_i^{OFF} the minimum down-time requirement of unit *i*.

- Ramp Rates

  The output power difference from one hour to another is physical restricted for the thermal units. This implies that under a certain time interval, P_{ij} cannot exceed P_{ij-1} by more than a certain ramp-up value, nor may it be less than a certain ramp-down value. Hence, the rate of changes from previous to actual time intervals on each generator are controlled by specified ramp up/down constraints expressed as:

$$P_{ij} - P_{ij-1} \le RUR_i, \forall\, i \in [1, N_G], \forall\, j \in [1, T] \qquad (3.18)$$

$$P_{ij-1} - P_{ij} \le RDR_i, \forall\, i \in [1, N_G], \forall\, j \in [1, T] \qquad (3.19)$$

  where RUR_i is the ramp-up rate limit of unit *i* , and RDR_i is the ramp-down rate limit of the unit *i*.

- Unit Operating Range

  The committed units must generate power within their operational range. Upper and lower limits are given by:

$$P_i^{Min} \times U_{ij} \le P_{ij} \le P_i^{Max} \times U_{ij}, \forall\, i \in [1, N_G], \forall\, j \in [1, T] \qquad (3.20)$$

The unit commitment problem formulation explained so far consists of the objective function of equation 3.11 subject to the constraints of equations 3.13 - 3.20. Constraints from equations 3.13 - 3.15 are related to system requirements, while constraints from equations 3.16 - 3.20 correspond to the thermal units. Several techniques have been employed to solve the UC problem. Traditional optimization methods like priority list, dynamic programming, Lagrangian relaxation, and branch-and-bound are the most common. Also, various meta-heuristic methods recently applied to the UC solution are the evolutionary computation algorithms including differential evolution, genetic algorithm, particle swarm optimization, evolutionary programming, ant colony optimization, among others. Despite the technique utilized, UC is a very difficult problem to solve due to the large quantity of subsets (combinations) that can arise from the N_G units considered. In addition, its formulation involves integer and continuous decision variables, making evident the complexity of the problem.

Chapter 4

4 Plug-in Electric Vehicle Integration Algorithm

This chapter provides a complete overview of the proposed intelligent method to integrate PEVs to the grid. First, a brief introduction is presented in Section 4.1. Section 4.2 summarizes some of the previous works related to V2G and charging integration methods. Section 4.3 presents background information about the model used as reference in this work, while Section 4.4 describes the main features considered in our proposed model. Details associated to the shared data between vehicle owners and system operators are explained in Section 4.5. The two-stage mathematical formulations for V2G and charging optimization problems are discussed in Section 4.6 and 4.7, respectively. Finally, Section 4.8 offers the final remarks of the optimization algorithms suggested.

4.1 Introduction

Electric vehicles, due to their energy savings and low carbon emissions, have recently gained enough attention in many countries as the new emerging transportation technology option. However, from the point of view of electric utilities, as these vehicles get wider acceptance by the transportation sector, the charging process of large-scale penetration can seriously become a burden to the operations of existing power systems

if adequate coordination is not implemented. Therefore, the smart integration of EVs into the grid is, along with many other tasks, one of the most important problems that electric utilities will have to face.

During the past years, many studies have shown that intelligent V2G techniques are the fundamental key to achieve active participation of electric vehicles on the grid and improve the power system operations. Although there are numerous findings and contributions on these techniques, there is still space to further extend research on this topic since it is at its conceptual stages.

In this work, a coordinated charging/discharging implementation framework for V2G is proposed using a two-stage optimization algorithm. The model approach emphasizes on an effective strategy to handle a large penetration of PEVs while providing benefits to grid operations. This chapter is dedicated to formulate and explain the mathematical model of the optimization problem that aims to minimize the overall load and flatten the load profile subject to the vehicle and system constraints under the V2G concept.

4.2 Literature Review

Currently, large scale electric vehicle penetration threatens to destabilize current power system operations. With the urgency to avoid that harmful direction, different EVs integration methods have been presented in the literature. Many of them comprise optimization procedures to minimize or maximize a specific objective. Other methods are heuristic; whose main objective is to prevent the system from operating out of its limits. A wide range of objectives exist to implement intelligent charging strategies, but the most

common are costs minimization, profit maximization, or the improvement of a specific operational aspects of the system.

Given the low energy consumption at night and the underutilized power grid during that period, a typical PEV integration method is the passive strategy that use off-peak periods for charging the vehicles. However, if all PEVs start their recharging process at the same time (no coordination), this solution may result in several disadvantages. Hence, active strategies such as minimize load variance, maximize load factor, and load leveling are among other common objectives for coordinated charging/discharging methods. Z. Wang and S. Wang suggest in [39] a peak shaving and valley filling V2G algorithm through an objective function that aims to match a target load curve with a planned curve (forecast load plus EVs load). Authors in [40] present a similar approach in which they used the same objective function to implement their control strategy algorithm for demand side management. In article [7], the authors proposed a double-layer optimal charging strategy to minimize the overall load variance of a net load curve to deal with the computational complexity of large scale penetration optimization problem.

A multi-objective optimization problem was considered by [8] for the EVs charge and discharge. The first objective function evaluates the operational cost minimization, while the second objective function assess the difference between the minimum and maximum demand. This methodology aims to set the load factor equal to one, while operational costs are reduced. Particular attention should be placed on scheduling algorithms with multi-objective optimization problems because they can achieve optimal solutions considering multiple strategies. This is the case for the work performed on [9], which evaluated various aspects in the objective function from the customer interest to the

system operator objectives. Their approach presented the need for the system operator to reduce the peak load and that of the customer perspective, who is financially motivated, but concerned with the battery degradation as the V2G takes place.

The charging and discharging operation of PEVs can also be extended to demand side management on buildings. Instead of V2G, it is termed as vehicle-to-building (V2B). In [41], the authors considered the utilization of PHEVs smart processes to minimize the square Euclidean distance between instantaneous energy demand and the average demand of the building by controlling their schedules. Another work related to this topic [42], examines a mathematical model for peak shaving and valley filling on the load profile of a non-residential building under the presence of solar cells in order to flatten the power consumption curve. L. Jian *et al.* explored in [43] the possibility to smooth out the load variance in a household microgrid by controlling the charging patterns of PHEVs. In [44], K. Mets *et al.* presents quadratic programming algorithms to schedule PEVs where the objective function aims to minimize the square Euclidean distance between a target load profile and a real demand curve. In their approach, the real load profile corresponds to the household load profile in the local algorithm and to the load profile observed by the transformer to which the households are connected in the iterative global and global algorithms. Although these techniques have been developed for households or buildings, they can be applied in a similar way to the grid, since their objective to reduce peaks, fill valleys, and flatten an overall load profile are still the same.

In addition to minimizing load variance, maximizing load factor, or load leveling, PEVs can be optimally integrated with other goals. Some of the most common control methods found in the literature include decrease network losses, balance renewable energy

services, reduce emissions, minimize operational costs, and provide ancillary services. Despite the objective function goal, these control methods can be categorized under two architectures no matter if they are for charging only, or if they include charging and discharging. The architectures are commonly referred to as centralized and decentralized controls [45].

In the centralized or direct control, all instructions and decisions regarding the charge/discharge of each vehicle falls directly on an external entity, usually an aggregator. This entity is responsible for collecting all the necessary information from both, the plugged-in vehicles and the system operator. With this data, the corresponding optimal algorithms should be applied to achieve the proposed objectives while satisfying vehicle owner requirements. Finally, with the results obtained, the entity must instruct and manage all the vehicles under its governance.

Decentralized or indirect control architecture, in contrast, makes each vehicle acts as an independent decision-making agent rather than an external entity or an aggregator. Although every PEV decides the charge/discharge process by itself, the decision is influenced by a price or a control signal sent by the external entity which seeks to achieve a common objective between all users. Zhang *et al.* proposed in [46] a decentralized charging protocol where each vehicle determines its optimal charging schedule based on a cost signal sent by an aggregator. Then, every single PEV submits his schedule to the aggregator, so that the load curve and the cost signal can be updated when a certain number of vehicles are plugged in. However, in spite of the signal or factors used to influence the customers' decision in decentralized control algorithms, there is no guarantee of optimal results from the system operator's point of view [47].

The authors of [45] presented a review of different strategies and methods that many researchers on the topic have done to effectively integrate electric vehicles with the grid. Table 1 and Table 2 of this reference provide a summary of references regarding algorithms for the centralized and decentralized control, respectively. Both tables are organized by their main objectives, if the algorithm includes V2G, and the software, solver or tools employed to solve the problem.

Most optimal algorithms proposed in the literature evaluate the schedules of their PEVS by continuous charging/discharging rates, varying from zero to maximum power. Very few works investigate the coordination of electric vehicles based on discrete rate methods. The author's motivation in [48] to carry out its work concerning discrete rates is based on the fact that continuous charging rate is difficult to implement and chargers in current practice can only support several discrete charging levels.

4.3 V2G Model Background

An unlimited number of V2G algorithms that aim at flattening the load curve are defined as optimization problems. Usually, their mathematical formulation comprises an objective function whose decision variables rely on the charging/discharging rate of every PEV during each time slot. The basic constraints consist of maintaining the total load below maximum generation limits, ensuring charging/discharging rates are between lower and upper limits, and guaranteeing that minimum/maximum state of charges allowed are satisfied. Many other constraints can be added for controlling additional restrictions, but it will result on problem enlargement because the number of constraints

and the decision variables increase with the number of PEVs involved and with the number of time intervals considered. Evidently, this implies that with a large penetration of electric vehicles into the grid and with smaller time slots (more time intervals) evaluated, the computational complexity of the coordinated algorithms will become immensely high and a very difficult task for operators.

A previous work developed by L. Jian *et al.* in [7] proposed a double-layer optimal charging scenario in order to deal with this problem and to reduce the computational complexity associated with large scale PEV integration. These authors suggested to divide the problem in two optimization layers. In the first layer, a Central Control Center (CCC) determines the optimal schedule for each individual charging station as a whole, aiming to minimize the overall load variance of the base load and the aggregation of the PEVs. Next, in the second layer, every single charging station plans the charging/discharging schedule of each charging post, following the instructions ordered by the CCC in the first layer. Figure 4.1 depicts the schematic diagram of the double-layer optimization strategy from [7].

The problem division technique (two-layers) suggested in [7] provides great advantages to deal with large scale penetration of PEVs. Undoubtedly, it reduces the number of variables resulting from the optimization algorithm compared to the problem without the division. Particularly, the second layer avoids computing the schedule of each vehicle at once, reducing the number of variables and constraints significantly. Instead, the double-layer strategy allows to compute all the second layers simultaneously in a smaller scale between all aggregators, simplifying the computational complexity of the overall optimization problem.

An important fact is that the single model is not exactly equivalent to the double-layer optimal charging strategy. Although authors found a small difference on optimal results between the single model (no division) and the proposed model (two-layer division), the optimal strategy agrees very well with the design objective. Therefore, no disadvantage is associated with implementing this technique to effectively integrate PEVs.

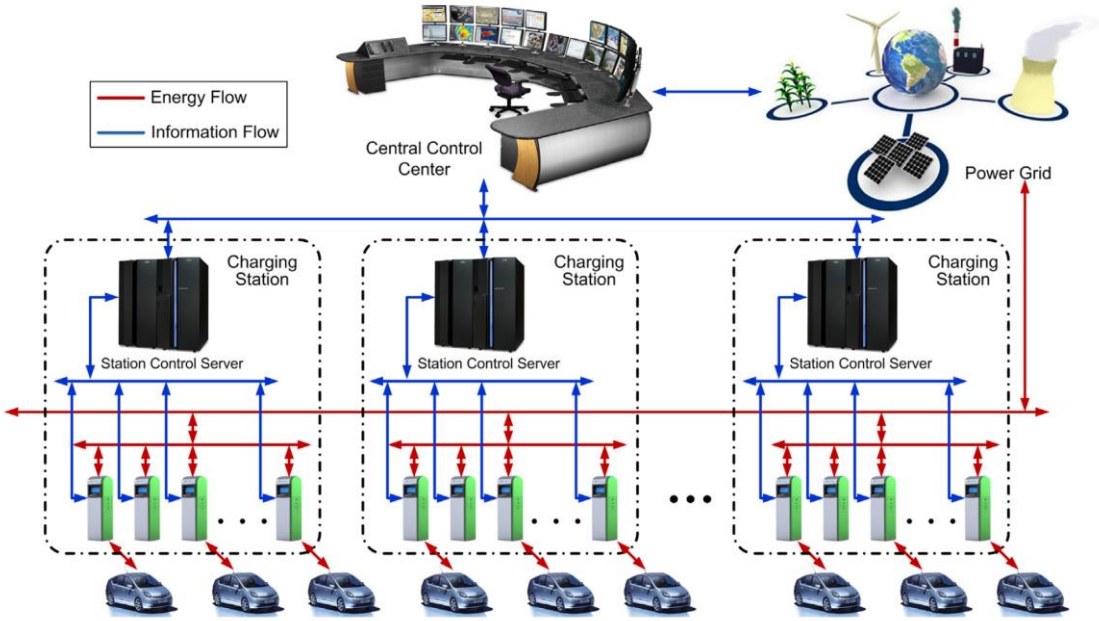

Figure 4.1 Energy and information flow of the double-layer optimization strategy [7]

4.4 V2G Model Description

Throughout this work, a coordinated V2G algorithm to effectively integrate PEVs into the grid is suggested based on the methodology of the double-layer optimization strategy proposed in [7]. Similar to the mentioned reference, our focus is to determine an improved optimal V2G schedule that results on peak shaving and valley filling by means of a two-

stage method approach. Besides utilizing the two-stage optimization strategy to decrease the computational complexity, the objective function has been simplified to reduce the overall load variance, while using the least possible amount of power. This change in objective function, allows the algorithm to evaluate larger PEVs penetrations and to compensate for the computational effort associated to the increase in variables.

Furthermore, our previous guideline reference [7] examined the optimal V2G schedule for daily services offered by the charging stations. However, the target is to include the charging/discharging optimal schedules in the periods that can take place during nights, in addition to those services that can be obtained through the charging stations during the day. PEV users may not live near a charging station and neither they will leave their PEVs at the charging stations during night. Therefore, the interaction between the vehicles with the grid should be controlled even if they are operating outside of a charging station. This way, it can be ensured that each vehicle will be controlled not only in the charging pole at work, or any other parking lot station, but also while at home. Specifically, we center the analysis on two periods during the coming one-day cycle to coordinate the day ahead optimal PEV schedules. The first period coincides with the arrival and departure time of work, while the second corresponds to the arrival back home until the next day. Figure 4.2 shows the time intervals over a complete cycle.

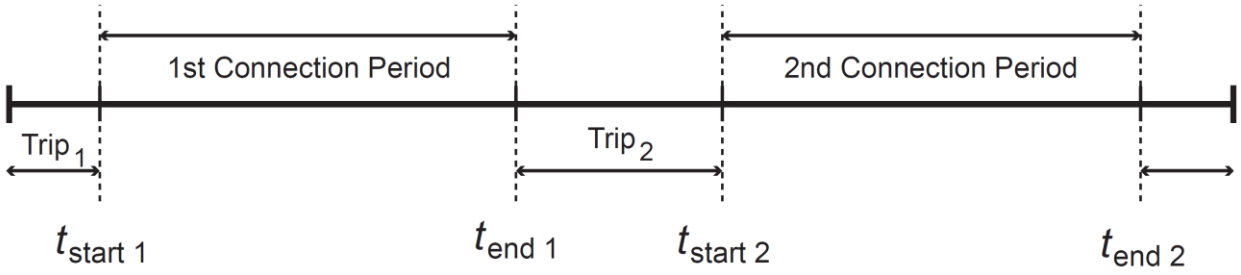

Figure 4.2 Time interval over a complete cycle

In addition, as an effort to look at a more realistic scenario, charging and discharging efficiencies have been included in the algorithm. The energy transfer between the network and the PEVs is not ideal, and neglecting these losses is not practical. Both efficiencies should be considered to account for the energy transfer losses between the battery pack of PEVs and the system, which may impact the overall load curve if their value is not high enough. Also, since battery degradation is one of the greatest drawbacks of the V2G concept, a discrete and constant rate of charge and discharge for the PEVs have been evaluated within the proposed algorithm. Although continuous methods are promising in the future, in this work it is believed that discrete rates will also impact the upcoming research and will co-exist in the long run. Furthermore, as pointed out in [49], the majority of electric vehicle supply equipment (EVSE) and standards just enable discrete rates. These rates depend on the charging level type contemplated in the vehicle design. In North America, according to the Society of Automotive Engineers, the standard SAE J1772 defines several types of charging levels. The most common are AC Level 1 for charges on 120 V outlets and AC Level 2 for 240 V plugs. Table 1 in [50] summarized the different charging power levels and their characteristics for the SAE and IEC Standards.

Along with the fixed rate, constraints are introduced in the algorithm to prevent fast deterioration of the vehicle batteries by avoiding the frequency of switches between the charge and discharge modes. The restriction will limit the algorithm to schedule alternating modes (charge and discharge) between consecutive time slots. This means that the schedule for any period t to $t + 1$ to $t + 2$ will never change their states from charge to discharge to charge, and neither will change from discharge to charge to discharge.

This work goes beyond other PEVs integration algorithms. As revealed in [44], it is emphasized on adjusting the PEVs power consumption to support optimal operation of the network instead of adapting the power generation to their power demand. Here is where the big challenges exist on the new incoming technology about electrifying the transportation sector. Manipulating or controlling the lifestyle of PEV owners concerning their charging schedules, will be a much-complicated task if appropriate social implementation is not performed.

4.5 V2G Model Input Data

To properly operate a smart technique through a centralized algorithm, it is essential to have good communication between the electric vehicles, the network, and the operators. The flow of information among these parts is indispensable and can be effectively managed by means of an online software and a cell phone application able to establish direct communication with the EVSE used to managed the charge/discharge operation of every single PEV. First, data from every vehicle should be shared with the external entity during a registration process in order to actively participate in the proposed V2G centralized program. During the registration, vehicle owners should provide the

following information about their vehicles: model (PEV_{MODEL}), battery type ($PEV_{BAT\ TYPE}$), battery capacity ($PEV_{BAT\ CAP}$), and the energy consumed as consequence of the driving action or driving consumption (PEV_{DC}). Additionally, they must notify the aggregator to which they will belong ($Aggregator_{ID}$). Then, a unique identification number is assigned to the vehicle to distinguish between all other vehicles subscribed to the program. Once the vehicle is registered, it can join the V2G operations under the supervision of the selected aggregator. If for any reason, the information submitted in the registration has changed, it must be updated.

Aggregators must know in advance the vehicle owner's requirements prior to determine optimal schedules. Therefore, each vehicle who intends to join the operations during the coming one-day cycle is required to submit the data before a specific deadline time. With the PEV_{ID}, they need to send to the aggregators, at least, the indicated information in the following data string:

$$PEV_{ID} = [\ Date,\ LOC_{1st\ Period},\ Time_{1st\ Con},\ Time_{1st\ Leave},\ SOC_{1st\ Con},\ LOC_{2nd\ Period},$$
$$TD_{2nd\ Trip},\ Time_{2nd\ Con},\ Time_{2nd\ Leave},\ SOC_{Desired},\ SOC_{Lower},\ SOC_{Upper}]$$

where *Date* is the proposed date to which the PEV is willing to participate, $LOC_{1st\ Period}$ the location of the first plug-in period, $Time_{1st\ Con}$ the plug-in time of the first connection period, $Time_{1st\ Leave}$ the un-plug time of the first connection period, $SOC_{1st\ Con}$ the state of charge value when connected in the first period, $LOC_{2nd\ Period}$ the location of the second plug-in period, $TD_{2nd\ Trip}$ the travel distance for the second PEV trip of the day, i.e. the distance that the EV expects to travel between the first and second connection periods, $Time_{2nd\ Con}$ the plug-in time of the second connection period, $Time_{2nd\ Leave}$ the un-plug time of the second connection period, $SOC_{Desired}$ the minimum desired state of charge value

when leaving on the second connection period, SOC_{Lower} the allowed lower limit (minimum) value for the state of charge of the battery, and SOC_{Upper} the allowed upper limit (maximum) value for the state of charge of the battery.

These input data depend entirely on the behavior of each user, and clearly, will be provided at first by inference. However, as the PEV owners get more knowledge of their actions and experience from their vehicle, they will be able to provide more accurate estimates about their parameters.

4.6 V2G Model Mathematical Formulation

Our proposed mathematical model, as previously mentioned, follows the problem division of the double-layer optimization charging strategy used in [7]. Nevertheless, we have developed our own perspective about the two-stage formulation by expanding the second stage so that an aggregator can manage the V2G operations of PEVs on parking lots during the day as well as their homes during the night. Figure 4.3 shows our suggested schematic diagram representation for the two-stage V2G problem.

The main idea is that all PEVs submit their input data to the aggregators before a deadline time. Next, each of the aggregators must process this information and send it to the master or main aggregator (MA) as a total from all its PEVs. As soon as the MA receives the data reports from all the aggregators, he proceeds to calculate the optimal V2G schedule associated to each aggregator based on the vehicle needs. Once the results have been obtained, he imparts the instructions to each of the aggregators so they can manage all the PEVs under its domain independently of where they are located. The work performed by the master aggregator corresponds to the first optimization stage while

the work performed by the other aggregators is part of the second stage. Both stages will be explained in detail in Sections 4.6.1 and 4.6.2.

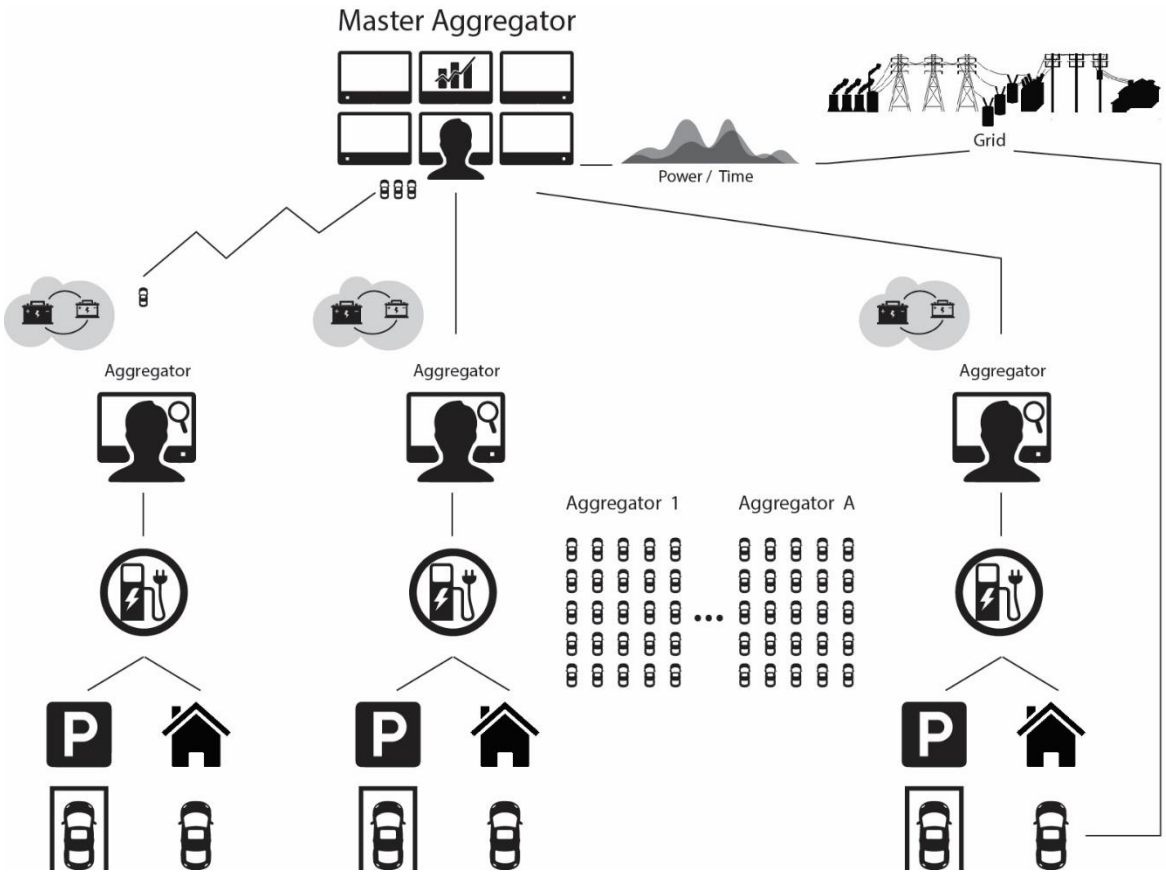

Figure 4.3 Two-stage schematic diagram

4.6.1 First Optimization Stage

In the first optimization stage, the master aggregator has the function to develop the optimal schedules for all the aggregators with the aim of minimizing the overall load variance using the least possible amount of power. The main goal of this stage is to allocate the operating power schedule during each time slot for every aggregator

over the entire period, which will be then used by the aggregators on the second optimization stage. Thus, the objective function can be defined as:

$$OF_{1st\ Stage} = \min \sum_{t=1}^{T} \left(P_{Base\ t} + P_{Aggregator\ t} \right)^2 \quad (4.\ 1)$$

$$P_{Aggregator\ t} = \sum_{a=1}^{A} P_{a,t}, \forall\ t \in [1,T] \quad (4.\ 2)$$

where T is the total number of time slots, A is the total number of aggregators, $P_{Base\ t}$ is the forecast load in *t-th* time slot and is assumed to be known, and $P_{a,t}$ is the operating power of the *a-th* aggregator in the *t-th* time slot. From the objective function described in equation 4.1 it can be seen that the decision variables are $P_{a,t}$, and there are $A \times T$ of them. Under this formulation, in general, the algorithm will assign the positive values of $P_{a,t}$ (PEV's charging their batteries) during the periods of low $P_{Base\ t}$ and the negative values (PEV's discharging their batteries) when $P_{Base\ t}$ is high, resulting on a new flattened load curve.

The minimization of the objective function is subject to a set of inequality constraints that take control of some of the system limitations and EV user preferences. The constraints included in the formulation are defined as:

- Maximum Generation Limit

$$P_{Base\ t} + P_{Aggregator\ t} \leq P_{Max\ Gen\ t}, \forall\ t \in [1,T] \quad (4.\ 3)$$

This constraint guarantees that the new load curve resulting from the addition of the PEVs will be maintained below the maximum generation limits

of the system during each time slot. Here, $P_{Max\,Gen\,t}$ is the maximum generation limit of the *t-th* time slot, and in total, there will be T constraints (one for each time slot) associated to the maximum generation limit. If the algorithm performs well in leveling the load curve with the addition of the PEVs, this constraint should have no problem because the peaks will decrease, and the valleys are the segments of the curve that will increase. However, if the aggregation of PEVs is large enough that the new load curve results in averages above the peaks, this constraint will activate its role in the algorithm.

- Lower and Upper Aggregator Operational Power Limits

The lower and upper limits of the charging/discharging rates of the aggregators during each time slot ($P_{a,t}$) depend on the quantity of PEVs and whether they are or not plugged in to the grid. The constraint is defined as:

$$-\sum_{n=1}^{N(a)}\left(\delta_n^a(t)\times P_{Max\,Rate\,n}^{\,a}\times\eta_{DH}\right)\le P_{a,t}\le\sum_{n=1}^{N(a)}\left(\delta_n^a(t)\times P_{Max\,Rate\,n}^{\,a}\times 1/\eta_{CH}\right), \quad \forall\, t\in[1,T],\ \forall\, a\in[1,A] \qquad (4.4)$$

where $P_{Max\,Rate\,n}^{\,a}$ is the maximum charging/discharging rate inside the battery for the *n-th* vehicle at the *a-th* aggregator, η_{DH} the discharging efficiency (between battery and grid), η_{CH} the charging efficiency (between grid and battery), and $\delta_n^a(t)$ is a binary variable for the *n-th* PEV at the *a-th* aggregator that is 0 if the PEV is not plugged-in and 1 if it is plugged-in. The mathematical representation is expressed in equation 4.5 as:

$$\delta_n^a(t) = \begin{cases} 0, \forall\ t \notin [t_{start\ 1\ n}^{\ a}, t_{end\ 1\ n}^{\ a} - 1], [t_{start\ 2\ n}^{\ a}, t_{end\ 2\ n}^{\ a} - 1] \\ 1, \forall\ t \in [t_{start\ 1\ n}^{\ a}, t_{end\ 1\ n}^{\ a} - 1], [t_{start\ 2\ n}^{\ a}, t_{end\ 2\ n}^{\ a} - 1] \end{cases} \quad (4.5)$$

$$\forall\ t \in [1, T], \forall\ n \in [1, N(a)], \forall\ a \in [1, A]$$

in which the value of $t_{start\ 1\ n}^{\ a}$ and $t_{start\ 2\ n}^{\ a}$ represent the beginning of the next time interval of $Time_{1st\ Con}$ and $Time_{2nd\ Con}$, respectively, for the *n-th* PEV in the *a-th* aggregator. In a similar way, the value of $t_{end\ 1\ n}^{\ a}$ and $t_{end\ 2\ n}^{\ a}$ denote the beginning of the time interval of $Time_{1st\ Leave}$ and $Time_{2nd\ Leave}$, respectively, for the *n-th* PEV at the *a-th* aggregator.

The nomenclature of the time intervals (time slots) in the algorithm is of outmost importance. Therefore, the following example have been developed for better understanding of the reader. Assumes that $\Delta t = 1$ hour, the study period has 24 time slots (T = 24), and the cycle starts up at 8:00 a.m. and ends at 8:00 a.m. the next day. Therefore, if for any particular PEV the $Time_{1st\ Con}$, $Time_{1st\ Leave}$, $Time_{2nd\ Con}$, and $Time_{2nd\ Leave}$ are 8:10 a.m., 4:55 p.m., 6:37 p.m., and 7:25 a.m., respectively, then, $t_{start\ 1}$ is 2, $t_{end\ 1}$ is 9, $t_{start\ 2}$ is 12, and $t_{end\ 2}$ is 24. Observe that t_{start} is the beginning of the time interval where the PEV will start its operation, but t_{end} is the end of the last time interval (or the beginning of the next time interval) where the PEV will stop its operation. For the example previously showed $t_{end\ 1}$ was 9, meaning that the last time interval where the PEV will be doing V2G transactions during the first period is the 8th, but is equivalent to say that end operations at the beginning of 9th interval. Using

these times (t_{start} and t_{end}) in the algorithm is a practical way to ensure that the PEVs initiate their V2G operations after being connected and cease before they leave the grid.

Both constraints (upper and lower) stated in equation 4.4, ensure that each aggregator maintains its operational V2G charging/discharging rate between the limits that can be achieved with the vehicles plugged in, even if they are at their maximum rates during each time slot. Since the problem has $A \times T$ decision variables, then, there will be $A \times T$ constraints (one for each time slot of every aggregator) associated to the upper and lower limits of the decision variables.

- Minimum and Maximum Aggregator Accumulated Energy

  Analogous to the state of charge of a battery, we can establish an accumulated energy limitation for every aggregator. At first, it might be thought that the aggregators should have no minimum or maximum limit with the amount of energy that they can handle, because the network is able to send and receive all the energy associated to these vehicles as long as the energy transfer between the vehicles and the grid comply with the equipment and operational limits. However, this is not a valid argument. Each aggregator has a minimum and maximum accumulated energy quantity that is directly linked with the number of PEVs connected to the grid and with the minimum and maximum state of charge paths that every single PEV can have during its plug-in period. Therefore, we define the accumulated energy quantity from the first time slot to the *t-th* time slot by the *a-th* aggregator as:

$$E_a(t) = \sum_{t=1}^{t} \left(\Delta t \times P_{a,t} \right), \forall\, a \in [1, A] \qquad (4.\ 6)$$

and the constraint as:

$$E_a(t)_{LOWER} \le E_a(t) \le E_a(t)_{UPPER}, \forall\, t \in [1, T], \forall\, a \in [1, A] \qquad (4.\ 7)$$

where Δt is the length of the time slots with units of hours. The terms $E_a(t)_{LOWER}$ and $E_a(t)_{UPPER}$ in equations 4.7 are the lower and upper boundaries of the accumulated energy quantity of the *a-th* aggregator, respectively. These two parameters can be summarized as the minimum and maximum amount of energy that can accumulate each aggregator to the t-th time slot. Mathematically they are expressed as:

$$E_a(t)_{LOWER} = \sum_{n=1}^{N(a)} {E_{PEV}}_n^a(t)_{LOWER}, \forall\, t \in [1, T], \forall\, a \in [1, A] \qquad (4.\ 8)$$

and

$$E_a(t)_{UPPER} = \sum_{n=1}^{N(a)} {E_{PEV}}_n^a(t)_{UPPER}, \forall\, t \in [1, T], \forall\, a \in [1, A] \qquad (4.\ 9)$$

where ${E_{PEV}}_n^a(t)_{LOWER}$ and ${E_{PEV}}_n^a(t)_{UPPER}$ are the lower and upper boundaries of the accumulated energy quantity of each individual PEV (i.e. *n*), respectively, in the *a-th* aggregator. Up to this point, it is important to recognize the difference between the upper and lower limits of $E_a(t)$ and ${E_{PEV}}_n^a(t)$. The first corresponds to the accumulated energy quantity limits from the first time slot to the *t-th* of the *a-th* aggregator as a whole, while the latter is the same but for each *n-th*

PEV of the *a-th* aggregator. The summation of the $E_{PEV\,n}^{\,a}(t)$ limits under each time slot forms equations 4.8 and 4.9. Another important fact about the accumulated energy to the *t-th* time slot is that both, $E_a(t)$ and $E_{n\,PEV}^{a}(t)$, are quantities of energy on the grid side and not on the PEV batteries.

The $E_{PEV\,n}^{\,a}(t)_{LOWER}$ and $E_{PEV\,n}^{\,a}(t)_{UPPER}$ values depend on the lower and upper limit paths that each PEV battery state of charge takes during the charging or discharging process. Figure 4.4 illustrates this behavior through a graphical route of the state of charge limits that a PEV can undergo while plugged in. The red lines represent the lower and upper limits of the state of charge using any charging/discharging rate (no discrete rate) while the blue lines show the lower and upper state of charge limits considering a discrete charging/discharging rate. Since the operational rate considered in the proposed algorithm is discrete, the blue route sets the minimum and maximum state of charge values of each PEV. It can be observed that as long as the state of charge values are maintained in the blue area, all the state of charge constraints will be satisfied. In addition, due to the discrete rate, you can see that the charging and discharging slopes are the same during all time slots but with different sign. Mathematically they are defined as $\frac{P_{Rate\,n}^{\,a} \times \Delta t}{Bat\,Cap_{\,n}^{\,a}}$ for charging and $\frac{-P_{Rate\,n}^{\,a} \times \Delta t}{Bat\,Cap_{\,n}^{\,a}}$ for discharging. For better understanding, in the middle of both periods, there is a charging and a discharging process during one time slot (i.e. from *t* to *t+1*).

Figure 4.4 is intended to show a graphical interpretation of the state of charge values during all time slots of a complete cycle. Therefore, we make the following clarifications:

- It is not drawn to scale.
- It provides the SOC limit paths for continuous rates (red), as well as for discrete rates (blue). The discrete representation is above the continuous.
- The $SOC_{Discrete\,1}$ value is not necessarily greater than $SOC_{Discrete\,2}$.
- Neither the $SOC_{Discrete\,4}$ value is greater than $SOC_{Discrete\,3}$.
- All these values depend on every single PEV value for $SOC_{1st\ Con}$, SOC_{Lower}, SOC_{Upper}, $SOC_{Desired}$, and $Trip_2$.
- The SOC quantity on the *y* axis is unitless, since it is a ratio (kWh/kWh).
- The *x* axis corresponds to time over a 24-hour period and is represented by *t* to define the time intervals (8:00 a.m. to 8:00 a.m.) or the time slots (1 – T). This quantity is also unitless.

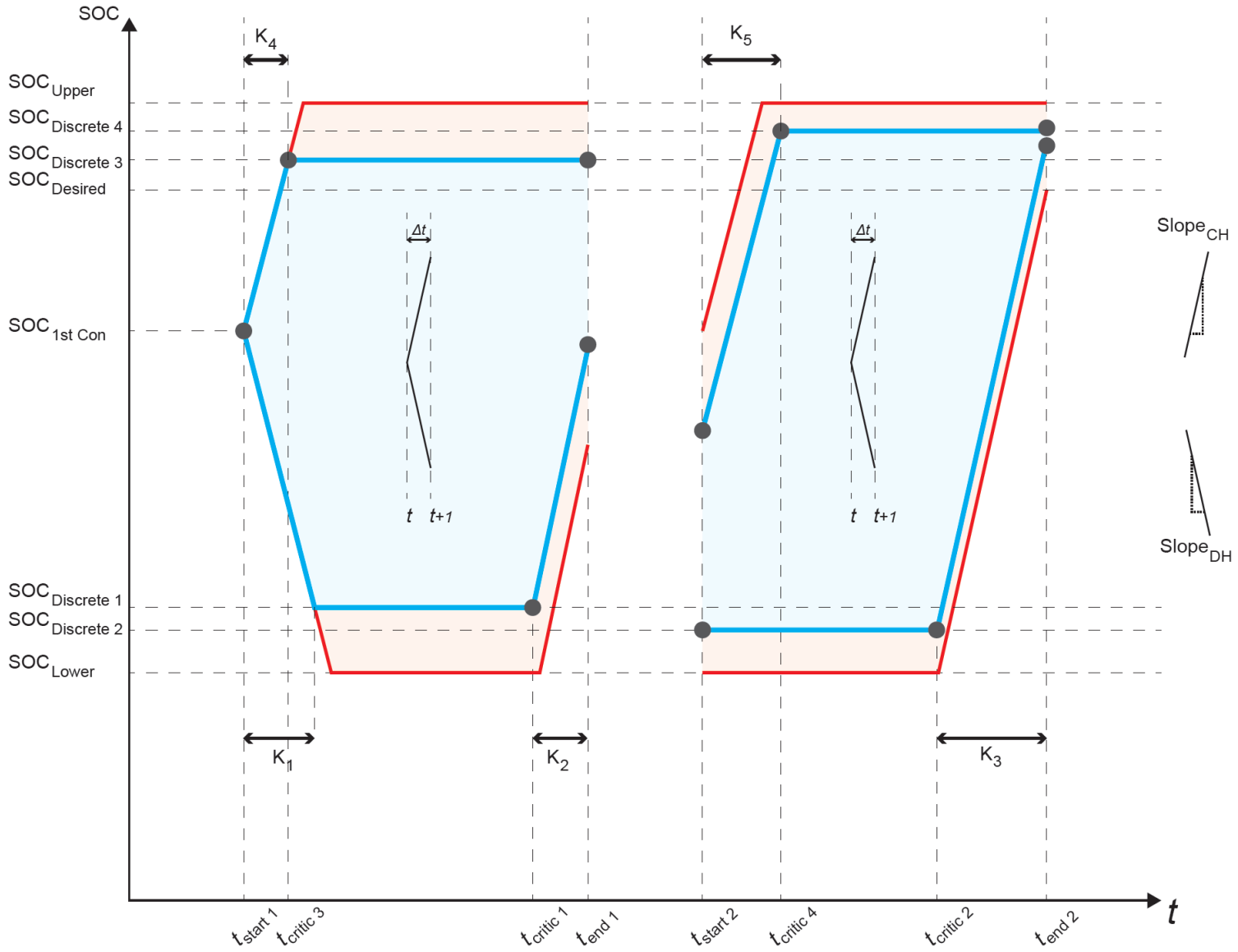

Figure 4.4 Minimum/maximum state of charge values during the V2G process

Hence, based on Figure 4.4, we can derive the following equations:

$$E_{PEV\ n}^{\ a}(t)_{LOWER} = \begin{cases} 0, & t < t_{start\ 1\ n}^{\ a} \\ \left(SOC_{\ n}^{\ a}(t) \mid Lower - SOC_{1st\ Con\ n}^{\ a}\right) \times Bat\ Cap_{\ n}^{\ a} \times \eta_{DH}, & t_{start\ 1\ n}^{\ a} \le t < t_{critic\ 1\ n}^{\ a} \\ E_{PEV\ n}^{\ a}(t-1)_{LOWER} + \left(SOC_{\ n}^{\ a}(t) \mid Lower - SOC_{\ n}^{\ a}(t-1) \mid Lower\right) \times Bat\ Cap_{\ n}^{\ a} \times (1/\eta_{CH}), & t_{critic\ 1\ n}^{\ a} \le t < t_{end\ 1\ n}^{\ a} \\ E_{PEV\ n}^{\ a}(t_{end\ 1\ n}^{\ a} - 1)_{LOWER}, & t_{end\ 1\ n}^{\ a} \le t < t_{start\ 2\ n}^{\ a} \\ E_{PEV\ n}^{\ a}(t_{end\ 1\ n}^{\ a} - 1)_{LOWER}, & t_{start\ 2\ n}^{\ a} \le t < t_{critic\ 2\ n}^{\ a} \\ E_{PEV\ n}^{\ a}(t-1)_{LOWER} + \left(SOC_{\ n}^{\ a}(t) \mid Lower - SOC_{\ n}^{\ a}(t-1) \mid Lower\right) \times Bat\ Cap_{\ n}^{\ a} \times (1/\eta_{CH}), & t_{critic\ 2\ n}^{\ a} \le t < t_{end\ 2\ n}^{\ a} \\ E_{PEV\ n}^{\ a}(t_{end\ 2\ n}^{\ a} - 1)_{LOWER}, & t_{end\ 2\ n}^{\ a} \le t \end{cases} \quad (4.\ 10)$$

$$\forall\ t \in [1,T],\ \forall\ n \in [1,N(a)],\ \forall\ a \in [1,A]$$

$$E_{PEV\ n}^{\ a}(t)_{UPPER} = \begin{cases} 0, & t < t_{start\ 1\ n}^{\ a} \\ \left(SOC_{\ n}^{\ a}(t) \mid Upper - SOC_{1st\ Con\ n}^{\ a}\right) \times Bat\ Cap_{\ n}^{\ a} \times (1/\eta_{CH}), & t_{start\ 1\ n}^{\ a} \le t < t_{critic\ 3\ n}^{\ a} \\ E_{PEV\ n}^{\ a}(t-1)_{UPPER} + E_{Step\ 1\ n}^{\ a}, & t_{critic\ 3\ n}^{\ a} \le t < t_{end\ 1\ n}^{\ a} \\ E_{PEV\ n}^{\ a}(t_{end\ 1\ n}^{\ a} - 1)_{UPPER}, & t_{end\ 1\ n}^{\ a} \le t < t_{start\ 2\ n}^{\ a} \\ E_{PEV\ n}^{\ a}(t_{end\ 1\ n}^{\ a} - 1)_{UPPER} + \left(SOC_{\ n}^{\ a}(t) \mid Upper - \left(SOC_{Discrete\ 3\ n}^{\ a} - Trip_{2\ n}^{\ a}\right)\right) \times Bat\ Cap_{\ n}^{\ a} \times (1/\eta_{CH}), & t_{start\ 2\ n}^{\ a} \le t < t_{critic\ 4\ n}^{\ a} \\ E_{PEV\ n}^{\ a}(t-1)_{UPPER} + E_{Step\ 2\ n}^{\ a}, & t_{critic\ 4\ n}^{\ a} \le t < t_{end\ 2\ n}^{\ a} \\ E_{PEV\ n}^{\ a}(t_{end\ 2\ n}^{\ a} - 1)_{UPPER}, & t_{end\ 2\ n}^{\ a} \le t \end{cases} \quad (4.\ 11)$$

$$\forall\ t \in [1,T],\ \forall\ n \in [1,N(a)],\ \forall\ a \in [1,A]$$

where

$$SOC_{n}^{a}(t)\,|\,Lower = \begin{cases} \max\begin{cases} SOC_{Discrete\,1\,n}^{a} \\ SOC_{1st\,Con\,n}^{a} - \dfrac{P_{Rate\,n}^{a} \times \Delta t \times (t - t_{start\,1\,n}^{a} + 1)}{Bat\,Cap_{n}^{a}} \\ SOC_{Discrete\,1\,n}^{a} + \dfrac{k_{2\,n}^{a} \times P_{Rate\,n}^{a} \times \Delta t}{Bat\,Cap_{n}^{a}} + \dfrac{P_{Rate\,n}^{a} \times \Delta t \times (t - (t_{end\,1\,n}^{a} - 1))}{Bat\,Cap_{n}^{a}} \end{cases} & t_{start\,1\,n}^{a} \le t < t_{end\,1\,n}^{a} \\ \max\begin{cases} SOC_{Discrete\,2\,n}^{a} \\ SOC_{Discrete\,2\,n}^{a} + \dfrac{k_{3\,n}^{a} \times P_{Rate\,n}^{a} \times \Delta t}{Bat\,Cap_{n}^{a}} + \dfrac{P_{Rate\,n}^{a} \times \Delta t \times (t - (t_{end\,2\,n}^{a} - 1))}{Bat\,Cap_{n}^{a}}, \end{cases} & t_{start\,2\,n}^{a} \le t < t_{end\,2\,n}^{a} \end{cases} \quad (4.\ 12)$$

$$\forall\, t \in [t_{start\,1\,n}^{a}, t_{end\,1\,n}^{a} - 1], [t_{start\,2\,n}^{a}, t_{end\,2\,n}^{a} - 1],\ \forall\, n \in [1, N(a)],\ \forall\, a \in [1, A]$$

$$SOC_{n}^{a}(t)\,|\,Upper = \begin{cases} \min\begin{cases} SOC_{Discrete\,3\,n}^{a} \\ SOC_{1st\,Con\,n}^{a} + \dfrac{P_{Rate\,n}^{a} \times \Delta t \times (t - t_{start\,1\,n}^{a} + 1)}{Bat\,Cap_{n}^{a}}, \end{cases} & t_{start\,1\,n}^{a} \le t < t_{end\,1\,n}^{a} \\ \min\begin{cases} SOC_{Discrete\,4\,n}^{a} \\ SOC_{Discrete\,3\,n}^{a} - Trip_{2\,n}^{a} + \dfrac{P_{Rate\,n}^{a} \times \Delta t \times (t - t_{start\,2\,n}^{a} + 1)}{Bat\,Cap_{n}^{a}}, \end{cases} & t_{start\,2\,n}^{a} \le t < t_{end\,2\,n}^{a} \end{cases} \quad (4.\ 13)$$

$$\forall\, t \in [t_{start\,1\,n}^{a}, t_{end\,1\,n}^{a} - 1], [t_{start\,2\,n}^{a}, t_{end\,2\,n}^{a} - 1],\ \forall\, n \in [1, N(a)],\ \forall\, a \in [1, A]$$

$$E_{Step\,1\,n}^{\ a}=\begin{cases}\begin{cases}P_{Rate\ n}^{\ a}\times\Delta t\times((1/\eta_{CH})-\eta_{DH}),\ t=t_{critic\,3\,n}^{\ a}+1:2:t_{critic\,3\,n}^{\ a}-1+2\times k_{1\,n}^{\ a} & k_{1\,n}^{\ a}>0\\ 0, \quad otherwise\end{cases}\\ 0, & k_{1\,n}^{\ a}=0\end{cases}$$

$$\forall\, t\in[t_{critic\,3\,n}^{\ a},t_{end\,1\,n}^{\ a}-1],\ \forall\, n\in[1,N(a)],\ \forall\, a\in[1,A]$$

(4. 14)

$$E_{Step\,2\,n}^{\ a}=\begin{cases}\begin{cases}P_{Rate\ n}^{\ a}\times\Delta t\times((1/\eta_{CH})-\eta_{DH}),\ t=t_{critic\,4\,n}^{\ a}+1:2:t_{critic\,4\,n}^{\ a}-1+2\times s_{2\,n}^{\ a} & s_{2\,n}^{\ a}>0\\ 0, \quad otherwise\end{cases}\\ 0, & s_{2\,n}^{\ a}=0\end{cases}$$

$$\forall\, t\in[t_{critic\,4\,n}^{\ a},t_{end\,2\,n}^{\ a}-1],\ \forall\, n\in[1,N(a)],\ \forall\, a\in[1,A]$$

(4. 15)

$$SOC_{Discrete\,1\,n}^{\ a}=SOC_{1st\,Con\ n}^{\ a}-\frac{k_{1\,n}^{\ a}\times P_{Rate\ n}^{\ a}\times\Delta t}{Bat\ Cap_{\ n}^{\ a}},\quad \forall\, n\in[1,N(a)],\ \forall\, a\in[1,A] \tag{4. 16}$$

$$SOC_{Discrete\,2\,n}^{\ a}=SOC_{Discrete\,1\,n}^{\ a}+\frac{k_{2\,n}^{\ a}\times P_{Rate\ n}^{\ a}\times\Delta t}{Bat\ Cap_{\ n}^{\ a}}-Trip_{2\ n}^{\ a},\quad \forall\, n\in[1,N(a)],\ \forall\, a\in[1,A] \tag{4. 17}$$

$$SOC_{Discrete\,3\,n}^{\ a}=SOC_{1st\,Con\ n}^{\ a}+\frac{k_{4\,n}^{\ a}\times P_{Rate\ n}^{\ a}\times\Delta t}{Bat\ Cap_{\ n}^{\ a}},\quad \forall\, n\in[1,N(a)],\ \forall\, a\in[1,A] \tag{4. 18}$$

$$SOC_{Discrete\,4\,n}^{\ a}=SOC_{Discrete\,3\,n}^{\ a}-Trip_{2\ n}^{\ a}+\frac{k_{5\,n}^{\ a}\times P_{Rate\ n}^{\ a}\times\Delta t}{Bat\ Cap_{\ n}^{\ a}},\quad \forall\, n\in[1,N(a)],\ \forall\, a\in[1,A] \tag{4. 19}$$

$$k_{1\,n}^{\,a} = floor\left(\frac{SOC_{1st\,Con\,n}^{\,a} - SOC_{Lower\,n}^{\,a}}{\frac{P_{Rate\,n}^{\,a} \times \Delta t}{Bat\,Cap_{n}^{\,a}}}\right), \quad \forall\, n \in [1, N(a)], \forall\, a \in [1, A] \qquad (4.\ 20)$$

$$k_{2\,n}^{\,a} = ceiling\left(\frac{SOC_{Lower\,n}^{\,a} + Trip_{2\,n}^{\,a} - SOC_{Discrete\,1\,n}^{\,a}}{\frac{P_{Rate\,n}^{\,a} \times \Delta t}{Bat\,Cap_{n}^{\,a}}}\right), \quad \forall\, n \in [1, N(a)], \forall\, a \in [1, A] \qquad (4.\ 21)$$

$$k_{3\,n}^{\,a} = ceiling\left(\frac{SOC_{Desired\,n}^{\,a} - SOC_{Discrete\,2\,n}^{\,a}}{\frac{P_{Rate\,n}^{\,a} \times \Delta t}{Bat\,Cap_{n}^{\,a}}}\right), \quad \forall\, n \in [1, N(a)], \forall\, a \in [1, A] \qquad (4.\ 22)$$

$$k_{4\,n}^{\,a} = floor\left(\frac{SOC_{Upper\,n}^{\,a} - SOC_{1st\,Con\,n}^{\,a}}{\frac{P_{Rate\,n}^{\,a} \times \Delta t}{Bat\,Cap_{n}^{\,a}}}\right), \quad \forall\, n \in [1, N(a)], \forall\, a \in [1, A] \qquad (4.\ 23)$$

$$k_{5\,n}^{\,a} = floor\left(\frac{SOC_{Upper\,n}^{\,a} - (SOC_{Discrete\,3\,n}^{\,a} - Trip_{2\,n}^{\,a})}{\frac{P_{Rate\,n}^{\,a} \times \Delta t}{Bat\,Cap_{n}^{\,a}}}\right), \quad \forall\, n \in [1, N(a)], \forall\, a \in [1, A] \qquad (4.\ 24)$$

$$t_{critic\,1\,n}^{\,a} = t_{end\,1\,n}^{\,a} - k_{2\,n}^{\,a}, \forall\, n \in [1, N(a)], \forall\, a \in [1, A] \qquad (4.\ 25)$$

$$t_{critic\,2\,n}^{\,a} = t_{end\,2\,n}^{\,a} - k_{3\,n}^{\,a}, \forall\, n \in [1, N(a)], \forall\, a \in [1, A] \quad (4.\,26)$$

$$t_{critic\,3\,n}^{\,a} = t_{start\,1\,n}^{\,a} + k_{4\,n}^{\,a}, \forall\, n \in [1, N(a)], \forall\, a \in [1, A] \quad (4.\,27)$$

$$t_{critic\,4\,n}^{\,a} = t_{start\,2\,n}^{\,a} + k_{5\,n}^{\,a}, \forall\, n \in [1, N(a)], \forall\, a \in [1, A] \quad (4.\,28)$$

$$s_{1\,n}^{\,a} = ceiling\left(\frac{t_{end\,1\,n}^{\,a} - (t_{critic\,3\,n}^{\,a} + 1)}{2}\right), \forall\, n \in [1, N(a)], \forall\, a \in [1, A] \quad (4.\,29)$$

$$s_{2\,n}^{\,a} = \max\begin{cases} k_{1\,n}^{\,a} - s_{1\,n}^{\,a} \\ 0, \end{cases}, \forall\, n \in [1, N(a)], \forall\, a \in [1, A] \quad (4.\,30)$$

$$Trip_{2\,n}^{\,a} = \frac{TD_{2\,n}^{\,a} \times DC_{n}^{\,a}}{Bat\,Cap_{n}^{\,a}}, \forall\, n \in [1, N(a)], \forall\, a \in [1, A] \quad (4.\,31)$$

where the *SOC* notation stands for state of charge value at the end of the *t-th* period, $SOC_{1st\,Con\,n}^{\,a}$ is the state of charge when plugged-in during the first connection period, $SOC_{Lower\,n}^{\,a}$ is the allowed lower limit (minimum) value for the state of charge of the battery, $SOC_{Upper\,n}^{\,a}$ is the allowed upper limit (maximum) value for the state of charge of the battery, $SOC_{Desired\,n}^{\,a}$ is the minimum desired state of charge value when leaving on the second connection period. The term $Bat\,Cap_{n}^{\,a}$ is the battery capacity, $Trip_{2\,n}^{\,a}$ is the energy consumed on the battery due to the driving operation of the second trip of the PEV, $TD_{2\,n}^{\,a}$ is travel distance for the second PEV trip of the day, $DC_{n}^{\,a}$ is the driving consumption of

the PEV, and $P_{Rate\,n}^{\,a}$ is the charging/discharging rate of power inside the battery, where *n* is for the *n-th* PEV and *a* is for the *a-th* aggregator.

The energy associated to the power losses of the V2G is considered in terms $E_{Step\,1\,n}^{\,a}$ and $E_{Step\,2\,n}^{\,a}$.They are used to correct the energy upper limits in equation $E_a(t)_{UPPER}$.The number of times these terms are used is determined by equations $k_{1\,n}^{\,a}$ in the first connection period and $s_{2\,n}^{\,a}$ for the second connection period. The rest of the terms are detailed in the list of symbols at the beginning of this document.

All equations from 4.10 - 4.31 have been obtained by analyzing and understanding Figure 4.4. They incorporate all the PEV owners' requirements and reflect the behavior of the SOC limits of each vehicle during its charging/discharging process in order to construct the accumulated energy limits ($E_a(t)_{LOWER}$ and $E_a(t)_{UPPER}$) of the constraint in equation 4.7.

The constraint in equation 4.7 is set to guarantee the minimum and maximum demanded energy quantities on each of the aggregators. Like the constraint of equation 4.4, in equation 4.7 there are $A \times T$ number of constraints associated to the accumulated energy limits from the first time slot to the *t-th* time slot of the *a-th* aggregator.

The first optimization stage concludes here. In summary, it consists on the objective function in equation 4.1 and the three constraints in equations 4.3, 4.4, and

4.7. Throughout this formulation, the master aggregator can achieve optimal results on the decision variables $P_{a,t}$. Once obtained, the MA must send the corresponding guideline to each of the aggregators separately. This instruction only includes the ideal base curve that each aggregator must follow on the second stage to manage their PEVs. We have named it aggregator instruction curve or mathematically as $P^{a}_{Base-Aggregator}$ for the *a-th* aggregator, and can be expressed in vector form as:

$$P^{a}_{Base-Aggregator} = \begin{bmatrix} P_{a,1} \\ P_{a,2} \\ P_{a,3} \\ \vdots \\ P_{a,T} \end{bmatrix}, \forall\, a \in [1, A] \qquad (4.\ 32)$$

4.6.2 Second Optimization Stage

The second optimization stage involves the aggregators and the PEVs. In this stage, the aggregators should coordinate the charging/discharging power for each of their PEVs following the instructions ordered by the master aggregator from the first optimization stage. They are responsible for determining during which time slots the PEVs should charge, discharge or remain idle while meeting the PEVs requirements. As a target, they dispatch all their scheduled vehicles using the reference signal $P^{a}_{Base-Aggregator}$, aiming to minimize the difference between both curves over each time slot. Hence, the second stage task can be formulated as:

$$OF_{2nd\ Stage} = \min \sum_{t=1}^{T} \left(\frac{1}{T} \left(P_{PEV}{}_{t}^{a} - P_{Base-Aggregator}{}_{t}^{a} \right)^2 \right), \forall\, a \in [1, A] \qquad (4.\ 33)$$

$$P_{PEV}{}_{t}^{a} = \sum_{n=1}^{N(a)} \left(\frac{U_{CH}{}_{n,t}^{a} \times P_{CH}{}_{n}^{a}}{\eta_{CH}} - \left(U_{DH}{}_{n,t}^{a} \times P_{DH}{}_{n}^{a} \times \eta_{DH} \right) \right), \quad \forall\, t \in [1, T], \forall\, a \in [1, A] \qquad (4.\ 34)$$

where $P_{CH}{}_{n}^{a}$ and $P_{DH}{}_{n}^{a}$ are the charging and discharging rates (inside the battery, not in the grid) for the *n-th* PEV at the *a-th* aggregator, respectively. Concerning these two parameters, it is important that $P_{CH}{}_{n}^{a}$ and $P_{DH}{}_{n}^{a}$ are equal to $P_{Rate}{}_{n}^{a}$ in order to match the first optimization stage with the second. If they are not equal, the algorithm loses compatibility between both stages. The formulation uses $U_{CH}{}_{n,t}^{a}$ and $U_{DH}{}_{n,t}^{a}$ as the decision variables of the problem. They are binary variables and indicate the charging/discharging status of the V2G operation during the *t-th* time slot of the *n-th* PEV at the *a-th* aggregator. Since there are two decision variables per time slot, a total of $2 \times N \times T$ variables are associated with equation 4.33.

The second stage objective function is subject to various equality and inequality constraints in order to satisfy the user preferences. These constraints are:

- Charging/Discharging Status

  The $U_{CH}{}_{n,t}^{a}$ and $U_{DH}{}_{n,t}^{a}$ are binary {0,1} variables that indicate whether the charging or discharging process are activated or not during a specific time slot. For example, $U_{CH}{}_{n,t}^{a} = 0$ means that during the *t-th* time slot, the *n-th* PEV at the *a-th* aggregator is not charging, while if $U_{CH}{}_{n,t}^{a} = 1$ it is charging. The same

occurs with $U_{DH\,n,t}^{\,a}$ but for discharging mode. Thus, associated to these operational statuses we can derive the following constraints:

$$U_{CH\,n,t}^{\,a} = 0, \forall\, t \notin [t_{start\,1\,n}^{\,a}, t_{end\,1\,n}^{\,a} - 1], [t_{start\,2\,n}^{\,a}, t_{end\,2\,n}^{\,a} - 1] \quad \forall\, n \in [1, N(a)], \forall\, a \in [1, A] \qquad \textit{(4. 35)}$$

$$U_{DH\,n,t}^{\,a} = 0, \forall\, t \notin [t_{start\,1\,n}^{\,a}, t_{end\,1\,n}^{\,a} - 1], [t_{start\,2\,n}^{\,a}, t_{end\,2\,n}^{\,a} - 1] \quad \forall\, n \in [1, N(a)], \forall\, a \in [1, A] \qquad \textit{(4. 36)}$$

$$U_{CH\,n,t}^{\,a} + U_{DH\,n,t}^{\,a} \leq 1, \forall\, t \in [1, T], \forall\, n \in [1, N(a)], \forall\, a \in [1, A] \qquad \textit{(4. 37)}$$

Equations 4.35 and 4.36 guarantee that there is no charging or discharging operation (no V2G) when the PEVs are not plugged in and equation 4.37 assures that any PEV cannot charge and discharge simultaneously in the same time slot. For the first two equations, the total number of constraints can be quantified as $\sum_{n=1}^{N(a)} \left((t_{start\,1\,n}^{\,a} - 1) + (t_{start\,2\,n}^{\,a} - t_{end\,1\,n}^{\,a}) + (T - t_{end\,2\,n}^{\,a} + 1) \right)$ on each aggregator, while the latter, Equation 4.37, has a total of $N \times T$ constraints on each aggregator too.

- Lower and Upper State of Charge

  The state of charge is a measure of how much energy is left on the PEV battery as a percent of its full capacity. In this algorithm, it is modeled as:

$$SOC(t)_n^a = \begin{cases} SOC_{1st\ Con\ n}^{\ a} + \sum_{t_{start\ 1\ n}^{\ a}}^{t} \left(\frac{U_{CH\ n,t}^{\ a} \times P_{CH\ n}^{\ a} \times \Delta t}{Bat\ Cap_n^a} - \frac{U_{DH\ n,t}^{\ a} \times P_{DH\ n}^{\ a} \times \Delta t}{Bat\ Cap_n^a} \right), & t_{start\ 1\ n}^{\ a} \le t < t_{end\ 1\ n}^{\ a} \\ SOC(t_{end\ 1\ n}^{\ a} - 1)_n^a - Trip_{2\ n}^{\ a} + \sum_{t_{start\ 2\ n}^{\ a}}^{t} \left(\frac{U_{CH\ n,t}^{\ a} \times P_{CH\ n}^{\ a} \times \Delta t}{Bat\ Cap_n^a} - \frac{U_{DH\ n,t}^{\ a} \times P_{DH\ n}^{\ a} \times \Delta t}{Bat\ Cap_n^a} \right), & t_{start\ 2\ n}^{\ a} \le t < t_{end\ 2\ n}^{\ a} \\ N/A \quad (Unknown), & otherwise \end{cases}$$

$$\forall\, t \in [1,T], \forall\, n \in [1,N(a)], \forall\, a \in [1,A] \qquad (4.\ 38)$$

where $SOC(t)_n^a$ is the state of charge value at the end of the *t-th* time slot of the *n-th* PEV at the *a-th* aggregator. However, to guarantee that the PEV batteries are neither overcharged nor deeply discharged during V2G operations, a constraint with upper and lower limits is established and defined as:

$$SOC_{Lower\ n}^{\ a} \le SOC(t)_n^a \le SOC_{Upper\ n}^{\ a},$$
$$\forall\, t \in [t_{start\ 1\ n}^{\ a}, t_{end\ 1\ n}^{\ a} - 1], [t_{start\ 2\ n}^{\ a}, t_{end\ 2\ n}^{\ a} - 1], \forall\, n \in [1,N(a)], \forall\, a \in [1,A] \qquad (4.\ 39)$$

where the lower and upper state of charge values are set by owner preferences before joining the grid. In total, equation 4.39 has $N \times T$ constraints for each limit at each aggregator.

- Minimum Desired State of Charge at Leave Time

$$SOC(t_{end\ 2\ n}^{\ a} - 1)_n^a \ge SOC_{Desired\ n}^{\ a}, \forall\, n \in [1,N(a)], \forall\, a \in [1,A] \qquad (4.\ 40)$$

where $SOC(t_{end\ 2\ n}^{\ a} - 1)_n^a$ is the state of charge value at the end of the last time interval of the second connection period of the *n-th* PEV at the *a-th* aggregator.

By means of this constraint, PEVs can leave their second connection period with a state of charge value above the minimum, as requested to the aggregator when they submitted their preferences. Equation 4.40 consists of *N* constraints on each aggregator.

- Switching Frequency Limitation

It is known that PEV battery degradation is directly proportional to the number of cycles given. Therefore, to reduce the battery degradation as a consequence of V2G operations, the frequency of switching between the charging and discharging modes in continuous time slots must be limited. Two constraints can formally be used to control this behavior, which can be stated as:

$$SF_{CH}(t)_n^a \leq 2, \quad \forall\, t \in [t_{start\,1\,n}^{\,a}, t_{end\,1\,n}^{\,a} - 3], [t_{start\,2\,n}^{\,a}, t_{end\,2\,n}^{\,a} - 3], \forall\, n \in [1, N(a)], \forall\, a \in [1, A] \qquad (4.41)$$

$$SF_{DH}(t)_n^a \leq 2, \quad \forall\, t \in [t_{start\,1\,n}^{\,a}, t_{end\,1\,n}^{\,a} - 3], [t_{start\,2\,n}^{\,a}, t_{end\,2\,n}^{\,a} - 3], \forall\, n \in [1, N(a)], \forall\, a \in [1, A] \qquad (4.42)$$

where $SF_{CH}(t)_n^a$ is the switching frequency from charge-to-discharge-to-charge and $SF_{DH}(t)_n^a$ is the switching frequency from discharge-to-charge-to-discharge beginning at the *t-th* time slot for the *n-th* vehicle at the *a-th* aggregator. Both equations consist of $N\,x\,(T-2)$ number of constraints on each aggregator. Equations 4.43 and 4.44 define $SF_{CH}(t)_n^a$ and $SF_{DH}(t)_n^a$, respectively.

$$SF_{CH}(t)_{n}^{a} = U_{CH\ n,t}^{\ a} + U_{DH\ n,(t+1)}^{\ a} + U_{CH\ n,(t+2)}^{\ a},$$
$$\forall\ t \in [t_{start\ 1\ n}^{\ a}, t_{end\ 1\ n}^{\ a} - 3], [t_{start\ 2\ n}^{\ a}, t_{end\ 2\ n}^{\ a} - 3],\ \forall\ n \in [1, N(a)],\ \forall\ a \in [1, A] \qquad \textit{(4. 43)}$$

$$SF_{DH}(t)_{n}^{a} = U_{DH\ n,t}^{\ a} + U_{CH\ n,(t+1)}^{\ a} + U_{DH\ n,(t+2)}^{\ a},$$
$$\forall\ t \in [t_{start\ 1\ n}^{\ a}, t_{end\ 1\ n}^{\ a} - 3], [t_{start\ 2\ n}^{\ a}, t_{end\ 2\ n}^{\ a} - 3],\ \forall\ n \in [1, N(a)],\ \forall\ a \in [1, A] \qquad \textit{(4. 44)}$$

This is the end of the second optimization stage. Recapping, the second stage comprises an objective function stated by equation 4.33 subject to the equality constraints of equations 4.35 and 4.36 and to the inequality constraints of equations 4.37, 4.39, 4.40, 4.41, and 4.42. The optimal results of this stage provide the operating charging/discharging schedule of each PEV by means of its operational status (charge, discharge, or idle) during each time slot. With this schedule, the aggregator must control and manage the V2G operation of every PEV under its domain by sending the $PEV_{Status\ n}^{\ a}$ signal to the charging/discharging device to which the PEV is plugged in. Below, an illustrative matrix of the PEV status is displayed.

$$PEV_{Status\ n}^{\ a} = \begin{bmatrix} U_{CH\ n,1}^{\ a} & U_{DH\ n,1}^{\ a} \\ U_{CH\ n,2}^{\ a} & U_{DH\ n,2}^{\ a} \\ U_{CH\ n,3}^{\ a} & U_{DH\ n,3}^{\ a} \\ \vdots & \vdots \\ U_{CH\ n,T}^{\ a} & U_{DH\ n,T}^{\ a} \end{bmatrix},\ \forall\ n \in [1, N(a)],\ \forall\ a \in [1, A] \qquad \textit{(4. 45)}$$

4.6.3 V2G Model Algorithm Assumptions

The V2G model presented in this chapter was developed based on the premise to evaluate the impact that PEVs can create on the load curve as a consequence of their interaction with the grid. Therefore, a set of reasonable assumptions have been considered concerning the power system, the PEVs capabilities, and the personal preferences of each PEV. These assumptions are:

- The power system has a reliable communication system that allows the flow of information between users, aggregators, and the charge/discharging devices.
- Transformers and lines capacities are never above operational limits in the parking lots nor in the homes. This implies that the utility grid has done the necessary upgrades to the system in order to adequately handle PEV charging or discharging processes. In contrast, it can also mean that the utility only allows V2G interactions on places where the system has the capacity to manage the PEVs without affecting actual grid operations.
- All parking lots charging stations or aggregators and charging/discharging devices at homes are equipped with the adequate outlets to manage the corresponding charging/discharging rate.
- The converter device used to charge and discharge the plug-in electric vehicle is modeled only by means of a charge and discharge efficiency.
- These efficiencies are to be equal for all the PEVs during the whole study. This assumption is valid because the charge and discharge rates used in the algorithm are constant.

- The PEV onboard batteries are thought of as ideal, where the transient performance of the charge/discharge process is not considered. In addition, any battery inefficiency such as self-discharge, loss of capacity, and poor operation due to temperature changes have been neglected.
- The battery capacity is fixed to a specific kWh value. The study period is one day (24 hours), so the battery capacity is not supposed to change in that short time.
- PEV owners have similar life styles and driving patterns. Their vehicle main purpose is commuting. That is, users just drive from home to work in the morning, and back home in the evening/night with just a minimal deviation for another task. This argument is not far from reality, since actual PEV batteries do not provide enough capacity to travel beyond commuting purposes.
- The energy consumed on the PEV corresponds to the distance traveled, and no other activity is realized other than driving. The PEV heaters, radios, lights, A/C units, between many other electrical devices consume energy and drains the battery. This effect is disregarded in the PEV batteries.
- In addition, the aspects considered in the algorithm are just some of the operational features of the V2G concept and in no way contemplates all the limitations of the system or other economic aspects.

4.7 Charging Model Mathematical Formulation

The two-stage V2G algorithm proposed in Section 4.6 to effectively integrate PEVs with the grid can be simplified a charging-only operation within the electric vehicles

instead of considering both charge and discharge. This section illustrates the changes that have to be done in the algorithm to avoid any kind of PEV discharge with the grid.

The changes in both stages are minimal and most of them associated to the lower limits. In the first optimization stage, major changes occur in equations 4.4, 4.10, 4.11, and 4.12. Also, equations 4.17 and 4.21 require adjustments. On the other hand, the second stage changes involve the elimination of the discharging status variables and remove their terms from all the corresponding equations. These changes are on equations 4.34, 4.37, 4.38, and 4.45, while equations 4.36 and 4.41 - 4.44 are eliminated. A detailed explanation regarding all modifications along with the new equations is shown for each stage.

4.7.1 First Stage Modifications

The first change corresponds to equation 4.4. If discharge is not allowed, PEVs are only able to charge. Thus, the aggregator rate limits equation should be modified to:

$$0 \le P_{a,t} \le \sum_{n=1}^{N(a)} \left(\delta_n^a(t) \times P_{Max\ Rate\ n}^{\ a} \times 1/\eta_{CH} \right), \quad \forall\, t \in [1,T], \forall\, a \in [1,A] \qquad (4.46)$$

where the difference is in the lower limit which is set to zero. Respect to equations 4.10, 4.11, and 4.12, Figure 4.5 allows an easier understanding on how to proceed with their modifications. Similar to the V2G process, this figure depicts the state of charge limit values of a particular PEV undergoing the charging-only process. From the figure, it can be observed that, since the PEV discharges at no time, the state of

charge is never below the value at which begins in the first and second connection periods. In order to correct the equations, it is also important to notice that the value of k_2 is set to any integer value greater than zero, but in practice, it can be equal to zero depending on the $SOC_{1st\ Con}$, SOC_{Lower}, and $Trip_2$. If it is zero, it means that $t_{critic\,1} = t_{end\,1}$ in the first connection period. Hence, considering all these statements, the resultant changes in the first optimization stage are:

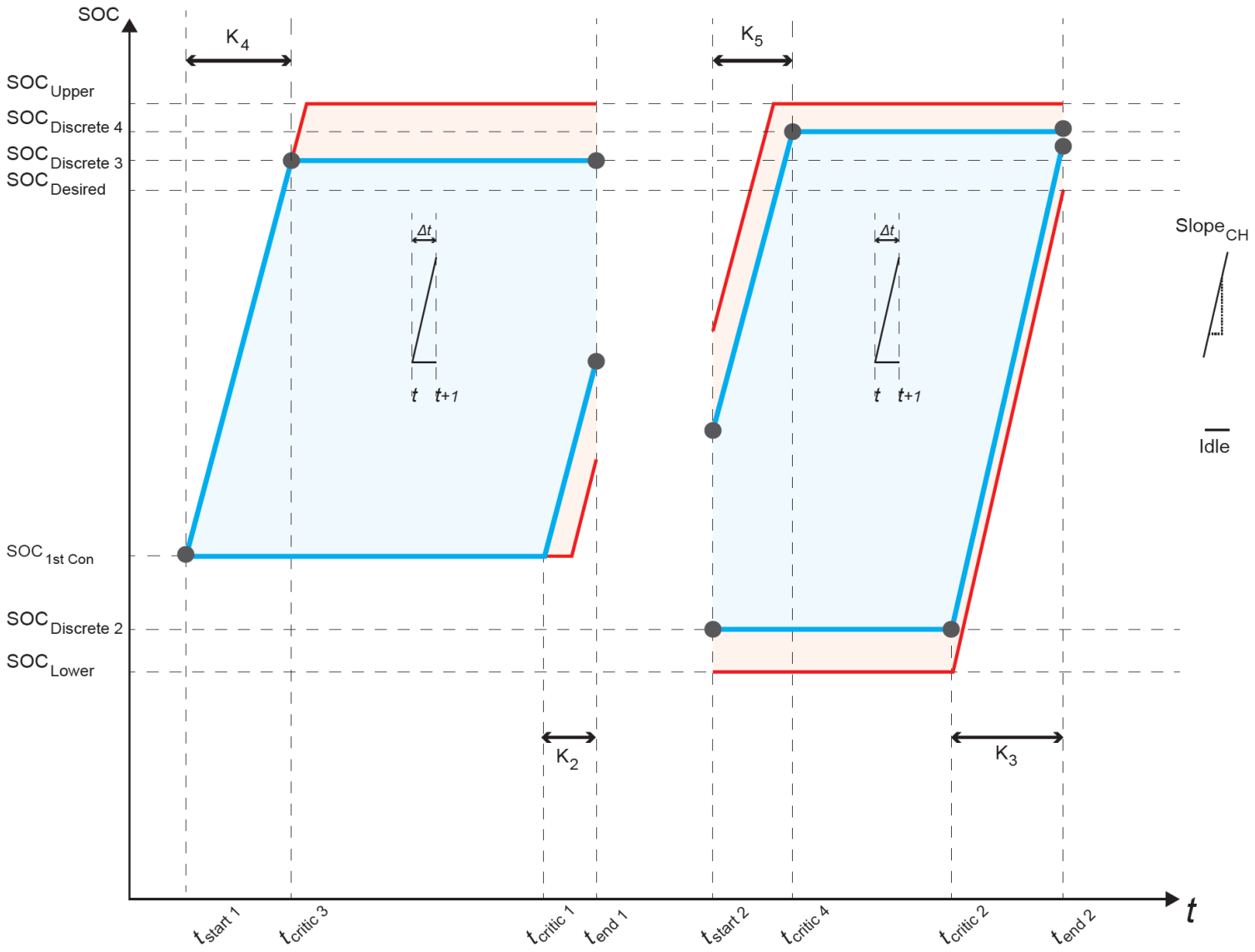

Figure 4.5 Minimum/maximum state of charge values during the charging process

equation 4.10 should be modified to:

$$\text{if } t_{critic\,1\,n}^{\ a} < t_{end\,1\,n}^{\ a}$$

$$E_{PEV\ n}^{\ a}(t)_{LOWER} = \begin{cases} 0, & t < t_{start\,1\,n}^{\ a} \\ 0, & t_{start\,1\,n}^{\ a} \le t < t_{critic\,1\,n}^{\ a} \\ \left(SOC_{n}^{\ a}(t) \mid Lower - SOC_{1st\,Con\ n}^{\ a}\right) \times Bat\ Cap_{n}^{\ a} \times (1/\eta_{CH}), & t_{critic\,1\,n}^{\ a} \le t < t_{end\,1\,n}^{\ a} \\ E_{PEV\ n}^{\ a}(t_{end\,1\,n}^{\ a} - 1)_{LOWER}, & t_{end\,1\,n}^{\ a} \le t < t_{start\,2\,n}^{\ a} \\ E_{PEV\ n}^{\ a}(t-1)_{LOWER}, & t_{start\,2\,n}^{\ a} \le t < t_{critic\,2\,n}^{\ a} \\ E_{PEV\ n}^{\ a}(t-1)_{LOWER} + \left(SOC_{n}^{\ a}(t) \mid Lower - SOC_{n}^{\ a}(t-1) \mid Lower\right) \times Bat\ Cap_{n}^{\ a} \times (1/\eta_{CH}), & t_{critic\,2\,n}^{\ a} \le t < t_{end\,2\,n}^{\ a} \\ E_{PEV\ n}^{\ a}(t_{end\,2\,n}^{\ a} - 1)_{LOWER}, & t_{end\,2\,n}^{\ a} \le t \end{cases} \quad (4.47)$$

$$\forall\, t \in [1,T], \forall\, n \in [1,N(a)], \forall\, a \in [1,A]$$

$$\text{if } t_{critic\,1\,n}^{\ a} = t_{end\,1\,n}^{\ a}$$

$$E_{PEV\ n}^{\ a}(t)_{LOWER} = \begin{cases} 0, & t < t_{start\,1\,n}^{\ a} \\ 0, & t_{start\,1\,n}^{\ a} \le t < t_{end\,1\,n}^{\ a} \\ 0, & t_{end\,1\,n}^{\ a} \le t < t_{start\,2\,n}^{\ a} \\ 0, & t_{start\,2\,n}^{\ a} \le t < t_{critic\,2\,n}^{\ a} \\ E_{PEV\ n}^{\ a}(t-1)_{LOWER} + \left(SOC_{n}^{\ a}(t) \mid Lower - SOC_{n}^{\ a}(t-1) \mid Lower\right) \times Bat\ Cap_{n}^{\ a} \times (1/\eta_{CH}), & t_{critic\,2\,n}^{\ a} \le t < t_{end\,2\,n}^{\ a} \\ E_{PEV\ n}^{\ a}(t_{end\,2\,n}^{\ a} - 1)_{LOWER}, & t_{end\,2\,n}^{\ a} \le t \end{cases} \quad (4.48)$$

$$\forall\, t \in [1,T], \forall\, n \in [1,N(a)], \forall\, a \in [1,A]$$

equation 4.11 should be adjusted to:

$$E_{PEV\ n}^{\ a}(t)_{UPPER} = \begin{cases} 0, & t < t_{start\ 1\ n}^{\ a} \\ \left(SOC_{n}^{\ a}(t)\,|\,Upper - SOC_{1st\ Con\ n}^{\ a}\right) \times Bat\ Cap_{n}^{\ a} \times (1/\eta_{CH}), & t_{start\ 1\ n}^{\ a} \le t < t_{critic\ 3\ n}^{\ a} \\ E_{PEV\ n}^{\ a}(t-1)_{UPPER}, & t_{critic\ 3\ n}^{\ a} \le t < t_{end\ 1\ n}^{\ a} \\ E_{PEV\ n}^{\ a}(t_{end\ 1\ n}^{\ a}-1)_{UPPER}, & t_{end\ 1\ n}^{\ a} \le t < t_{start\ 2\ n}^{\ a} \\ E_{PEV\ n}^{\ a}(t_{end\ 1\ n}^{\ a}-1)_{UPPER} + \left(SOC_{n}^{\ a}(t)\,|\,Upper - \left(SOC_{Discrete\ 3\ n}^{\ a} - Trip_{2\ n}^{\ a}\right)\right) \times Bat\ Cap_{n}^{\ a} \times (1/\eta_{CH}), & t_{start\ 2\ n}^{\ a} \le t < t_{critic\ 4\ n}^{\ a} \\ E_{PEV\ n}^{\ a}(t-1)_{UPPER}, & t_{critic\ 4\ n}^{\ a} \le t < t_{end\ 2\ n}^{\ a} \\ E_{PEV\ n}^{\ a}(t_{end\ 2\ n}^{\ a}-1)_{UPPER}, & t_{end\ 2\ n}^{\ a} \le t \end{cases} \quad (4.\ 49)$$

$$\forall\ t \in [1,T],\ \forall\ n \in [1,N(a)],\ \forall\ a \in [1,A]$$

and equation 4.12 corrected to:

$$SOC_{n}^{\ a}(t)\,|\,Lower = \begin{cases} \max\begin{cases} SOC_{1st\ Con\ n}^{\ a} \\ SOC_{1st\ Con\ n}^{\ a} + \dfrac{k_{2\ n}^{\ a} \times P_{Rate\ n}^{\ a} \times \Delta t}{Bat\ Cap_{n}^{\ a}} + \dfrac{P_{Rate\ n}^{\ a} \times \Delta t \times (t - (t_{end\ 1\ n}^{\ a} - 1))}{Bat\ Cap_{n}^{\ a}}, & t_{start\ 1\ n}^{\ a} \le t < t_{end\ 1\ n}^{\ a} \end{cases} \\ \max\begin{cases} SOC_{Discrete\ 2\ n}^{\ a} \\ SOC_{Discrete\ 2\ n}^{\ a} + \dfrac{k_{3\ n}^{\ a} \times P_{Rate\ n}^{\ a} \times \Delta t}{Bat\ Cap_{n}^{\ a}} + \dfrac{P_{Rate\ n}^{\ a} \times \Delta t \times (t - (t_{end\ 2\ n}^{\ a} - 1))}{Bat\ Cap_{n}^{\ a}}, & t_{start\ 2\ n}^{\ a} \le t < t_{end\ 2\ n}^{\ a} \end{cases} \end{cases} \quad (4.\ 50)$$

$$\forall\ t \in [t_{start\ 1\ n}^{\ a}, t_{end\ 1\ n}^{\ a} - 1], [t_{start\ 2\ n}^{\ a}, t_{end\ 2\ n}^{\ a} - 1],\ \forall\ n \in [1,N(a)],\ \forall\ a \in [1,A]$$

where:

$SOC_{Discrete\,2\,n}^{\,a}$ in equation 5.17 should be replaced by:

$$SOC_{Discrete\,2\,n}^{\,a} = SOC_{1st\,Con\,n}^{\,a} + \frac{k_{2\,n}^{\,a} \times P_{Rate\,n}^{\,a} \times \Delta t}{Bat\,Cap_{n}^{\,a}} - Trip_{2\,n}^{\,a}, \quad \forall\, n \in [1, N(a)], \forall\, a \in [1, A] \tag{4.51}$$

and $k_{2\,n}^{\,a}$ in equation 4.21 should be corrected to:

$$k_{2\,n}^{\,a} = \max \begin{cases} ceiling\left(\dfrac{SOC_{Lower\,n}^{\,a} + Trip_{2\,n}^{\,a} - SOC_{1st\,Con\,n}^{\,a}}{\dfrac{P_{Rate\,n}^{\,a} \times \Delta t}{Bat\,Cap_{n}^{\,a}}} \right), \\ 0 \end{cases} \quad \forall\, n \in [1, N(a)], \forall\, a \in [1, A] \tag{4.52}$$

The rest of the equations of the first optimization stage remain the same except for equations 4.14, 4.15, 4.16, 4.20, 4.29, and 4.30 that are removed.

4.7.2 Second Stage Modifications

The second stage modifications are mainly due to the $U_{DH\,n,t}^{\,a}$ term. No discharge implicates $U_{DH\,n,t}^{\,a} = 0$, therefore, all equations can disregard it. The first change comes up with the objective function term $P_{PEV\,t}^{\,a}$ of equation 4.34 that may be redefined as:

$$P_{PEV\,t}^{\,a} = \sum_{n=1}^{N(a)} \left(\frac{U_{CH\,n,t}^{\,a} \times P_{CH\,n}^{\,a}}{\eta_{CH}} \right), \quad \forall\, t \in [1, T], \forall\, a \in [1, A] \tag{4.53}$$

which as a consequence implies that the number of decision variables on the objective function is reduced from $2 \times N \times T$ to $N \times T$.

Additionally, the constraint of equation 4.36 becomes void, equation 4.37 is fixed to:

$$U_{CH\ n,t}^{\ a} \leq 1, \forall\ t \in [1,T], \forall\ n \in [1,N(a)], \forall\ a \in [1,A] \qquad (4.\ 54)$$

and equation 4.38 is reformulated as:

$$SOC(t)_{n}^{\ a} = \begin{cases} SOC_{1st\ Con\ n}^{\ a} + \sum_{t_{start\ 1\ n}^{\ a}}^{t} \left(\frac{U_{CH\ n,t}^{\ a} \times P_{CH\ n}^{\ a} \times \Delta t}{Bat\ Cap_{n}^{\ a}} \right), & t_{start\ 1\ n}^{\ a} \leq t < t_{end\ 1\ n}^{\ a} \\ SOC(t_{end\ 1\ n}^{\ a} - 1)_{n}^{\ a} - Trip_{2\ n}^{\ a} + \sum_{t_{start\ 2\ n}^{\ a}}^{t} \left(\frac{U_{CH\ n,t}^{\ a} \times P_{CH\ n}^{\ a} \times \Delta t}{Bat\ Cap_{n}^{\ a}} \right), & t_{start\ 2\ n}^{\ a} \leq t < t_{end\ 2\ n}^{\ a} \\ N\ /\ A \quad (Unknown), & otherwise \end{cases} \qquad (4.\ 55)$$

$$\forall\ t \in [1,T], \forall\ n \in [1,N(a)], \forall\ a \in [1,A]$$

With respect to the switching frequency constraints, they are no longer needed. Since discharging is not considered, the PEV operation cannot switch between one mode to the other, leaving equations 4.41 - 4.44 out of context. After all, the result of the second optimization stage has slightly changed in dimensions and equation 4.45 about the PEV status can be now showed as a vector of the form:

$$PEV_{Status\ n}^{\ a} = \begin{bmatrix} U_{CH\ n,1}^{\ a} \\ U_{CH\ n,2}^{\ a} \\ U_{CH\ n,3}^{\ a} \\ \vdots \\ U_{CH\ n,T}^{\ a} \end{bmatrix}, \forall\ n \in [1,N(a)], \forall\ a \in [1,A] \qquad (4.\ 56)$$

4.8 Summary

The proposed method to intelligently schedule the PEVs was mathematically formulated and explained in this chapter. The algorithm seeks to determine optimal charging and V2G operations so that the final net load curve has the least variation over an extended time horizon. To achieve the objective, a two-stage strategy was used in order to reduce the computational effort which may result from large scale PEV penetration. The first stage is a quadratic programming (QP) optimization problem whose decision variables depend only on the number of aggregators and the time slots, while the second stage is a mixed-integer quadratic programming (MIQP) optimization problem where the variables rely on the amount of PEVs allocated on each aggregator and the time slots. Under this formulation, this means that, once the first optimization stage is concluded, all aggregators can compute their PEV optimal schedules (second stage optimization) at the same time because they are independent of each other. This technique results in a time performance improvement of the overall algorithm if compared to other methods that schedule all their PEVs under the same aggregator. In general, the problem division provides an outstanding tool that enable V2G operators dispatch faster all their PEVs without affecting the quality of their schedules.

Interestingly, the possibility of considering continuous charging/discharging rates in the second optimization stage was evaluated. It was found, however, that it introduces a new level of complexity because the binary variables that determine the on/off status of the charge/discharge operations cannot be eliminated if efficiencies in the algorithm are to be considered. Therefore, the model is forced to use $4 \times N \times T$ variables on the second optimization stage, including a combination of continuos and binary variables.

Conversely, if the binary variables are not used, then a non-linear constraint must be employed to prevent the algorithm from allowing charge and discharge operations simultaneously in the same time interval. Hence, both of the alternatives make the quadratic programming optimization problem harder to solve.

From the perspective of this model, communication between PEVs, aggregators, master aggregator, and system operator is crucial. Principally, the master aggregator and all the aggregators, should have direct communication with the EVSE used to manage the charge/discharge operations of every PEV. A communication failure between an aggregator and its PEVs implies the loss of control of the charging and/or discharging process of every single PEV. Losing communication with a single PEV will be negligible to the system, but the charging process will not be completed, affecting PEV performance. However, if the master aggregator loses communication with an aggregator, all PEVs under the governance of that aggregator will fail to contribute to the grid. As a result, the overall load curve will be less flattened than expected as per optimal schedules. Therefore, a properly maintained communication system is one of the most critical aspects of effective integration of PEVs.

Chapter 5

5 Simulations and Case Studies

This chapter is dedicated to discussing and analyzing the numerical results of the simulations carried out using the proposed PEV integration algorithm described in Chapter 4. The usefulness of this study is proved through three different case studies considering multiple scenarios in each of the cases. Variations on specific parameters is performed in order to evaluate the impact they have in the proposed model results.

The first section provides a general overview on how the simulations are carried out and introduces the general simulation parameters including those related to the power system, the plug-in electric vehicles, and user behavior. The preceding sections consider several cases and scenarios to assess the performance of the two-stage optimization strategy on the load profile curve and evaluate the impact on the economic operation of the power system by means of the UC problem. Lastly, Section 5.5 shows some final remarks associated to all the simulation results obtained in this chapter.

5.1 Introduction

The control strategies developed to effectively manage the charge/discharge process of plug-in electric vehicles were conceptually tested by simulation frameworks. All of them were implemented under the mathematical software Matrix Laboratory (MATLAB 8.4

R2014b) on an Intel Core i5-6200U CPU @ 2.30 GHz with 8.00 GB of RAM. Also, an interface with MATLAB was created using GUROBI Optimization (simply mentioned as Gurobi) to solve the quadratic programming (QP) and the mixed-integer quadratic programming (MIQP) optimization problems that MATLAB on its own cannot handle (referring to the MIQP).

The Gurobi solver has the capability to manage both optimization problems defined in Chapter 4. In the first stage, which evaluates a continuous QP optimization problem, the model is solved to optimality subject to the default tolerances. This implies that an optimal solution is available. As the number of decision variables (aggregators *A* and time slots *T*) increases, the solver takes longer to achieve the solution, but overall, there is no inconvenient finding optimal solutions and providing the results in a reasonable time. However, for the second stage, which evaluates a mixed-integer QP (MIQP) optimization problem, the behavior was not the same. These problems are hard to solve, and as the dimension increases, the computational complexity grows significatively. As more PEVs were added in the simulation (*N*), more candidate solutions must be explored in the state space search. Therefore, for the dimensions considered in our simulations, some termination criteria parameters have been activated in order to obtain model solutions. If the algorithm reaches or exceeds any of these termination parameters, the solver interrupts and provides the best solution found up to that point. For this work, a time limit of 360 seconds and a node limit of 5,000 have been assumed for the branch and bound nodes. Whichever comes first, the solver will stop the optimization process, giving the best solution found up to that point as the problem solution.

Several cases have been studied based on typical islanded load profiles and the IEEE 10-unit system. On each of the cases, particular scenarios with different levels of PEVs have been implemented aiming to demonstrate the effectiveness of the integration algorithm and to evaluate the resulting load profiles with the addition of PEVs on the systems considered.

The simulations were modeled for uncoordinated charging, coordinated charging, and coordinated charging/discharging (V2G) cases for each of the load profiles considered. The base case simulation involves no PEV integration. That is, only a UC problem is evaluated in order to determine the original economic operation of the system when no PEVs are involved with the grid. Uncoordinated charging considers a possible scenario during upcoming years when PEVs become more attractive to vehicle owners and no restrictions are applied regarding their charging schedules. Particularly, this case simulates a scenario where all PEVs charge their batteries when they arrive home in the evening/night up to a full SOC. The coordinated charging case simulation includes just charging operations associated to the PEVs and the coordinated charging/discharging case comprises bidirectional power flow between the grid and the PEVs but in optimal ways as per the proposed algorithms in this work. For all the cases, the two-stage optimization algorithm, provides quantitative results in order to construct the new resulting load curve (except for the base case, where no integration algorithm is applied). Then, with the new obtained load profiles, UC problems were carried out to evaluate the impact on the economic operations of the system as a consequence of PEV addition.

The two-stage optimization method proposed in Chapter 4 is conducted for one-day cycles (24 hours). In our simulations, the cycle starts at 8:00 a.m. and concludes at 8:00

a.m. the next day. For better precision on the proposed models, the time slot is defined to be 0.25 hours ($\Delta t = 15\text{min}$) over the complete cycle; therefore, there are 96 time slots in a 24-hour period (cycle). Sections 5.1.1 – 5.1.3 provide the rest of the simulation parameter assumptions associated to the power system, the PEVs, and user behavior.

5.1.1 Power System Assumptions

Regarding the power system, the only input data needed to execute the two-stage optimization algorithm of the PEVs integration is the base load curve in watts (kW or MW). Usually, their values come from forecast algorithms or historical data recorded by the utilities. For the purpose of this work, the load curve is assumed to be known. Appendix B provides data for the IEEE 10-unit system and the typical islanded power system load profiles used for the simulations. Observe from some of the tables in Appendix B.1 and B.2 that they only have hourly values (i.e. data for 24 time slots over 24 hours). Therefore, due to the limited resolution in the data, the simulations (which require data for 96 time slots) will assume that the values for all the time slots of a specific hour will be the same as the corresponding hourly data. For example, from Table B.1.1 the hourly demand for 8:00 a.m. is 1300 MW. Thus, in the simulations, the 1300 MW will be applied from the first to the fourth time interval (8:00 a.m., 8:15 a.m., 8:30 a.m., and 8:45 a.m.). The same will occur with the 1400 MW at 9:00 a.m. which will be repeated over the 9:00 a.m., 9:15 a.m., 9:30 a.m., and 9:45 a.m. This way, we will obtain the complete load profile for the 96 time slots of the simulations.

To evaluate the economic operation of the power system, the UC problem should be carried out. This problem uses specific data of the generating units to execute its

mathematical procedures. Such information like minimum and maximum operating power of the units (operating range), cost coefficients, minimum up/down times, ramp rates, and hot/cold start-up costs are included in Appendix C. Tables C.1.1 and C.1.2 provide the generator parameters used for the UC problem of the IEEE 10-unit system.

The unit commitment problem will be solved on an hourly basis for a time horizon of 24 hours. However, the resultant load profile obtained from the proposed V2G and charging algorithms of Chapter 4 is in 15-minute time intervals. Hence, to match this difference, the load profile must be converted back from 96 to 24 time slots. The assumption will be to take the average of the four time slots on each hour. Consider time slots for the 8:00 a.m., 8:15 a.m., 8:30 a.m., and 8:45 a.m. Then, the average demand of all those time slots, will be used as the load data for the 8:00 a.m. time slot. In a similar way, this will be performed with the other time slots of each hour in the time horizon until the load profile data is reduced to 24 time slots. In addition, a match for the hours will be executed before performing the UC problem analysis. As previously mentioned, the simulation for the V2G and charging algorithms are performed starting at 8:00 a.m. for a period of 24 hours. However, the UC problem will be executed starting at 12:00 a.m. also for a 24-hour period. This causes a mismatch between both algorithms. Thus, a shifting in the load is executed to pair the hours and avoid losing synchronism among them.

5.1.2 Electric Vehicle Assumptions

Pure electric vehicles or battery electric vehicles are the only PEVs considered in this work. The electric vehicle model used in the simulations is the 2019 Nissan LEAF. It has a Lithium-ion battery pack with a storage capacity of 40 kWh, an onboard charger with maximum charging rate of 6.6 kW, and a driving consumption of 0.36 kWh/mi under the premise that the vehicle has a range of 112 MPGE (combined between city and highway). All this data have been obtained through the vehicle dealer web page [51]. Therefore, we have assumed these specifications as the vehicle's parameters for all case studies investigated in this work.

The charging and discharging behavior of the onboard batteries are modeled as linear, that is, the energy gained or released inside each battery is accounted as $\pm P_{Rate} \times \Delta t$ during any interval of the charging/discharging process. For simplicity, we have neglected any kind of internal battery inefficiency and self-discharge, and the losses associated to the power transfer to/from the grid are considered through the charging (η_{CH}) and discharging (η_{DH}) efficiencies in the algorithms. Both efficiencies involve the power loss in the AC-DC converter when doing charge or discharge operations with the battery. From the literature, it was found that some studies use a charging efficiency value of 92% [52], [53]. Similar studies that consider charge and discharge set both efficiencies to 90% [54], [55]. Other authors contemplate different charging (92%) and discharging (90%) efficiencies like [56]. Bai *et al.* in [57] employed diverse values for both efficiencies ranging from 87% to 95.24% in their simulation cases. However, all these studies do not base their efficiency parameters on any work that validates its value with certainty. Research from the point of view of chargers

demonstrates that charging efficiencies vary according to the output power, having their optimal values at almost rated value. Table 1 from [58] provides a list with the efficiency for various converters available in the literature at different values of rated power. Due to this variability, a value of 95% is set for the charging and discharging efficiencies in our work and is assumed to be constant for all case studies because the charging/discharging rates are fixed in our algorithms at their maximum value.

Finally, it is assumed that either the homes or charging stations (parking lots) are equipped with AC Level 2 connections to manage the V2G operations of the PEVs. For this level it means that PEVs can charge/discharge their batteries at higher rates with 240 V rather than traditional 120 V outlets. As previously mentioned in this section, a 6.6 kW fixed rate will be used which is the actual value for the 2019 Nissan LEAF.

5.1.3 User Behaviors Assumptions

It is assumed that most of the time, PEVs will be charged/discharged at home or at work. Thus, in this research work, we focus on two connection periods where the first one starts when you arrive at work and ends when departing from work, and the second period begins when you arrive back to home after work and concludes when leaving the house the next day again for work, as illustrated in Figure 4.2. PEV users make the first trip in the morning from home to work and the second trip in the evening/night from the work back to home. The daily distance travel associated to both trips is modeled with a normal distribution using a mean of 33 miles and a standard deviation of 5 miles. The assumption of the 33 miles is based on the average

12,000 miles per year used by most vehicle dealers to determine if a vehicle has been highly driven. The assumption is that the first trip takes between 40% to 50% of the total daily distance and the second trip takes the remaining of the total distance traveled (i.e. 100% of total distance less first trip).

The plug-in and un-plug times of the first and second connection periods are also assumed to follow normal distributions with mean and standard deviation. For each of the connection periods, their times are randomly generated according to the parameters shown in Table 5.1.

Times	Mean	Standard Deviation (h)	Lower Bound	Upper Bound
1st Connection	8:30 a.m.	0.5	8:00 a.m.	10:00 a.m.
1st Leave	5:00 p.m.	1.0	3:00 p.m.	8:00 p.m.
2nd Connection	-	-	3:30 p.m.	12:00 a.m.
2nd Leave	7:30 a.m.	0.5	5:00 a.m.	8:00 a.m.

Table 5.1 Mean, standard deviation, and bounds of plug-in/un-plug times

Observe from Table 5.1 that no mean and standard deviation are illustrated for the 2nd connection time. The reason is because you first need to know the 2nd trip duration in order to calculate the 2nd connection time. Under this assumption, the idea is to set the 2nd connection time equal to the 1st leave time plus 2nd trip duration and not to calculate it with a randomly hour. Hence, normal distribution is used instead to compute the 2nd trip duration, where the mean and standard deviation values are assumed to be 1 hour and 0.5 hour, respectively, for each trip. This 2nd trip duration

has no relation with the 2nd trip length, since users can do any other task during this time before arriving home, which is independent of the miles traveled. Also observe from Table 5.1 that each plug-in/un-plug time has a range defined by the lower and upper bounds. Any value generated that violates these bounds, is automatically adjusted to the corresponding bounded value.

Besides the daily distance traveled and the plug-in and un-plug times, it is also assumed that users will avoid deep discharges. This is critical in order to protect the battery from fast deterioration and is modeled in this work by setting the lower state of charge (SOC) to 50% of the battery capacity. PEVs must not drain their batteries below a 0.5 SOC value to support the grid. This means, that prior to leaving any connection period, each battery is guaranteed to be full enough to execute their next trip, and at the end have a SOC above the lower limit. Considering that batteries are one of the most expensive components of the vehicle, the SOC parameter is used quite conservative to extend the useful life. However, from the perspective of the power system, this is at the cost of having less energy available to provide services to the grid.

Other important parameters to complete the simulations are the SOC value prior to the first trip and the SOC value at the end of the second connection period. The former has been set to 95% and the latter equal or greater than 95%. This setting guarantees that PEVs charge their batteries to almost a full SOC for the next day before leaving home for work.

In this work, the user behavior was randomly generated according to the information of this section, specifically as per Table 5.1. Their values were fixed to be

used equally in all the scenarios of all study cases unless otherwise stated. Thus, throughout all the simulations, the same data have been adopted in order to do fair comparisons.

5.2 Case Study A

The main purpose of this case study is to examine the first and second stages of the coordinated charging and V2G algorithm methods proposed in Chapter 4. Particularly, it is focused on showing the operational behavior of both stages and how they interact when handling coordinated PEVs schedules. The usefulness of the results for each of the stages is shown, and the effectiveness of the optimization strategies on leveling a demand profile is demonstrated. Two scenarios are considered under case study A for typical islanded power system load profiles. Scenario 1 is based on a load profile for a distribution substation while scenario 2 is based on the load profile of a transmission transformer.

5.2.1 Case Study A: Scenario 1

Scenario 1 was carried out using the load demand curve for a traditional distribution substation. In the simulation, 15 aggregators with 75 battery electric vehicles under its domain were considered for a total of 1125 PEVs. All other parameters were used as previously explained in Section 5.1. The performance of the coordinated charging and V2G strategies is illustrated in Figure 5.1. It can be observed that both algorithms (charging and V2G) perform well on flattening the base load curve

with the integration of PEVs. For comparison purposes, the plot of 1125 uncoordinated vehicles and the base load curve (no PEVs added) have been included. Table 5.2 lists the minimum, maximum, and average power values of the load curves with their own standard deviation.

	Minimum (kW)	Maximum (kW)	Average (kW)	Standard Deviation (kW)
Base	20,600	27,780	24,977	2,433
Uncoordinated Charging	20,600	31,045	25,557	3,059
Coordinated Charging	23,636	27,780	25,599	1,575
Coordinated V2G	24,431	26,451	25,654	938

Table 5.2 Power values for load profiles on Figure 5.1

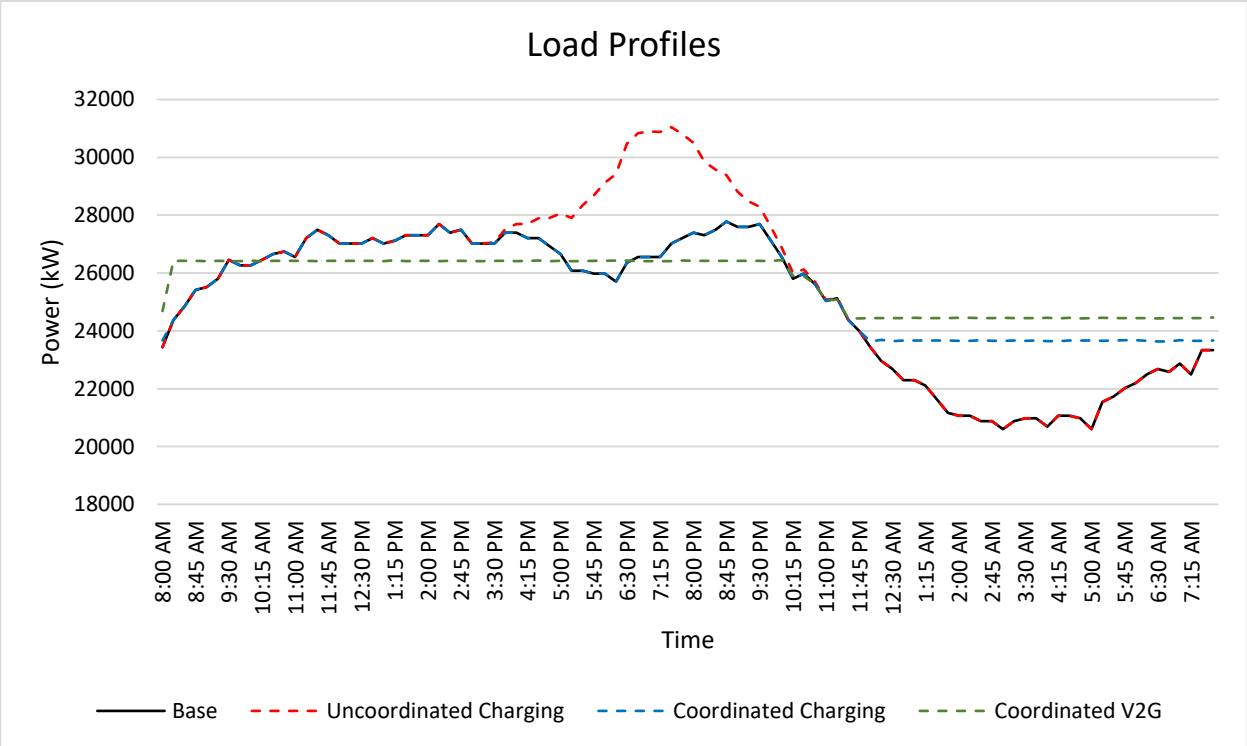

Figure 5.1 Load profiles before and after PEVs addition through different methods

The results of the first optimization stage, as explained in Chapter 4, provides the optimal curve that each aggregator must follow in the second optimization stage. Then, each aggregator, independently of the others, schedules its PEVs following the output results given by the master aggregator in the first stage. The results of the second stage are the schedules of every PEV under each aggregator. At this point, with the schedule of each PEV, the aggregator can submit the real power curve that can dispatch all their vehicles. Figures 5.2 and 5.3 depict the power curve that the aggregator must follow in the second stage (instructions or result from first stage) and the real power curve that is achieved with all their vehicle schedules (result of the second stage). Figure 5.2 is shown for aggregator 13 in the V2G model, while Figure 5.3 is for aggregator 13 in the charging model.

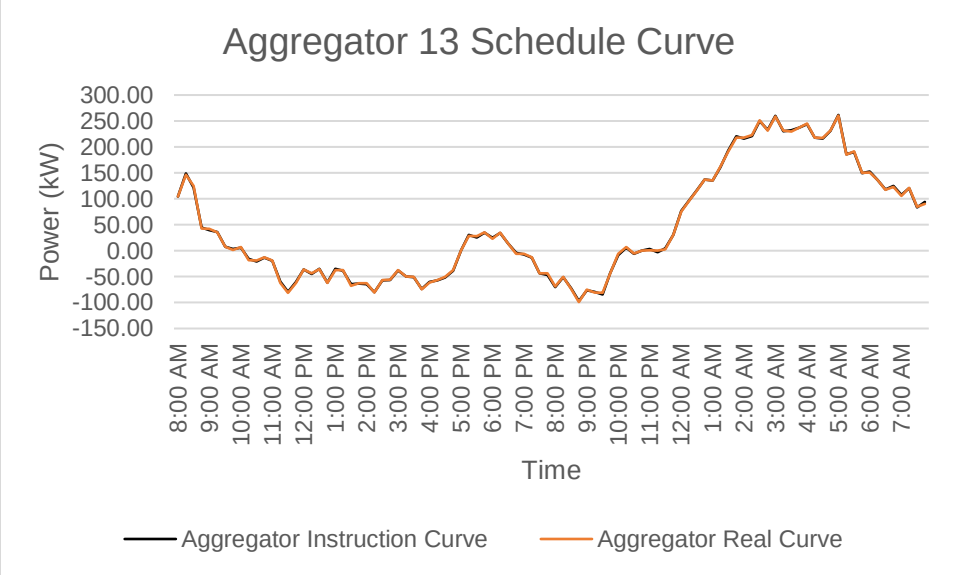

Figure 5.2 Aggregator 13 schedule curve in V2G algorithm

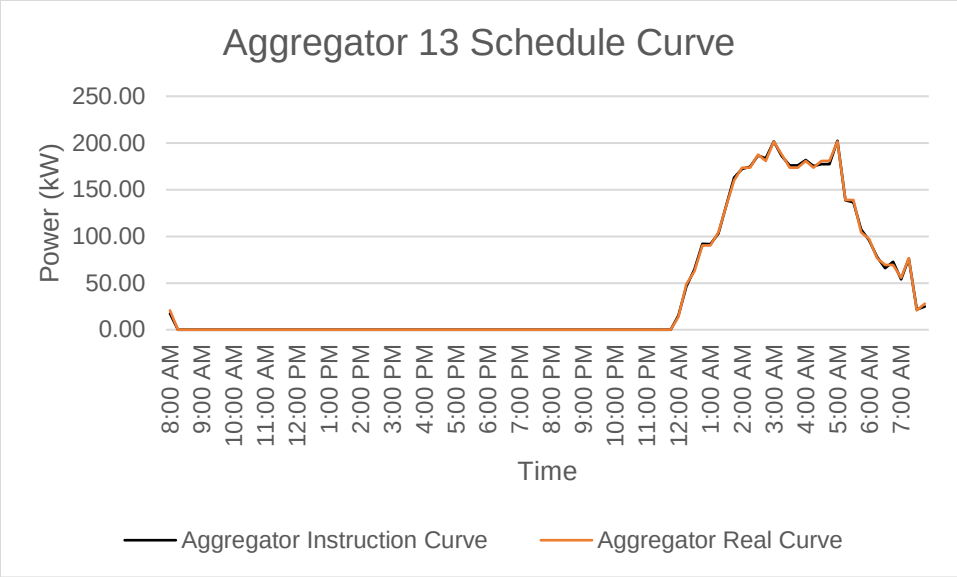

Figure 5.3 Aggregator 13 schedule curve in charging algorithm

From Figures 5.2 and 5.3, it can be identified that the real curve closely follows the instruction curve. As the algorithm of the second optimization stage finds a better solution, smaller differences will exist between these two curves. The errors for these plots are represented by the maximum, average and standard deviation of the difference between both curves which are listed in Table 5.3.

Aggregator	Methods	Maximum Difference (kW)	Average Difference (kW)	Standard Deviation (kW)
13	V2G	3.47	1.27	0.831
13	Charging	3.60	0.65	1.069

Table 5.3 Deviation between instruction and real curves of Figures 5.2 and 5.3

When all aggregators obtain the real load curve (created by the schedule of all their PEVs) of their fleet, they can submit it to the master aggregator. Once the master aggregator receives all of them, proceeds to construct the real load profile achieved in the system by the addition of all the coordinated PEVs. Therefore, the master aggregator real load curve is formed by all the individual aggregator real curves. In this scenario, the real load curve corresponds to the “Coordinated Charging” and “Coordinated V2G” plots in Figure 5.1 for the charging and V2G methods, respectively.

From the first optimization stage, it can be recognized that if we add all their results, the master aggregator optimal load curve is obtained. In other words, the optimal load curve is the sum of all the instructions given by the master aggregator to its individual aggregators. This means that if all the aggregators schedule their PEVs (in the second optimization stage) so that they exactly follow the instruction curve, the real load curve becomes the same as the optimal load curve. For both of the proposed methods, charging and V2G, it is observed that the real load curves are quite similar to the optimal load curves. Figures 5.4 and 5.5 depict this behavior on the scenario under study. Table 5.4 lists the average relative error and the maximum difference for the plots of Figures 5.4 and 5.5.

Method	Maximum Difference (kW)	Average Difference (kW)	Average Error (%)
V2G	32.81	6.54	0.026
Charging	30.00	3.16	0.013

Table 5.4 Deviations between optimal and real curves of Figures 5.4 and 5.5

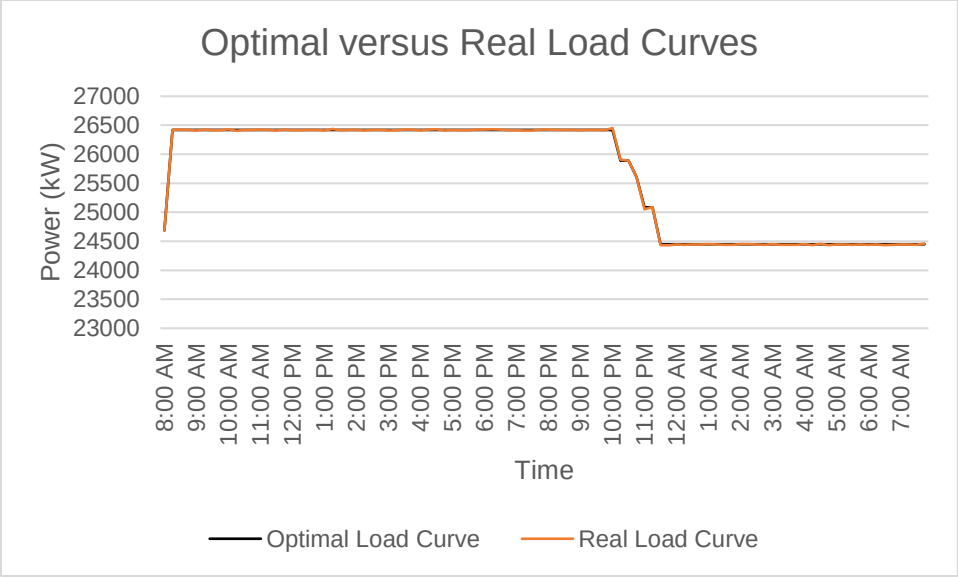

Figure 5.4 Optimal and real load curve of the V2G algorithm

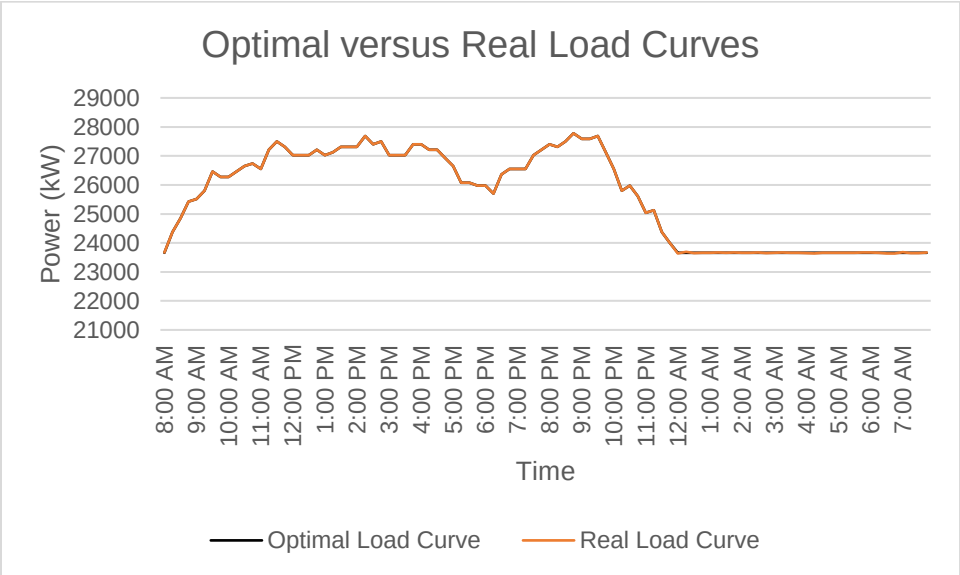

Figure 5.5 Optimal and real load curve of the charging algorithm

From the plots of Figures 5.4 and 5.5, due to the minimal difference between optimal and real load curves, it can be concluded that the optimal load curve obtained from the first optimization stage is a practical approach for analysis on load profiles. This approximation avoids having to perform second optimization stages, when the purpose of the study is just to evaluate the impact of the load profiles and it is not intended to schedule the charging/discharging process of every PEV. Note that with the increase in aggregators and the intensification in the deviation of the aggregator real curve from the aggregator instruction curve, the real load curve and the optimal load curve show a deviation from one another. Moreover, it should be understood that optimal and real load curves are not the same unless otherwise proved by performing the simulations for the second stage. However, for macro analysis from the point of view of system operation, this is a valid approach on assessing the behavior of peak shaving and valley filling on load profiles. Case study B and C of this chapter are developed under this assumption and use the optimal load curve of the first optimization stage to perform their analysis without the implementation of the second stage for all the aggregators.

Finally, Figures 5.6 and 5.7 illustrate an example of the optimal schedule of a PEV for the V2G and charging methods, respectively. The vertical bars represent the binary variable (1,0) of the status (charge and/or discharge). If no bar is present in a particular time slot, it is because the vehicle is idle or is not plugged in. The grey shadow at the background is the battery state of charge representation. The non-grey shadow background in the plots are those time slots where the PEV is not plugged in and its SOC is unknown. Figure 5.6 corresponds to the 10^{th} PEV of aggregator 1 of the V2G

algorithm, while Figure 5.7 corresponds to the same PEV, but for the charging algorithm.

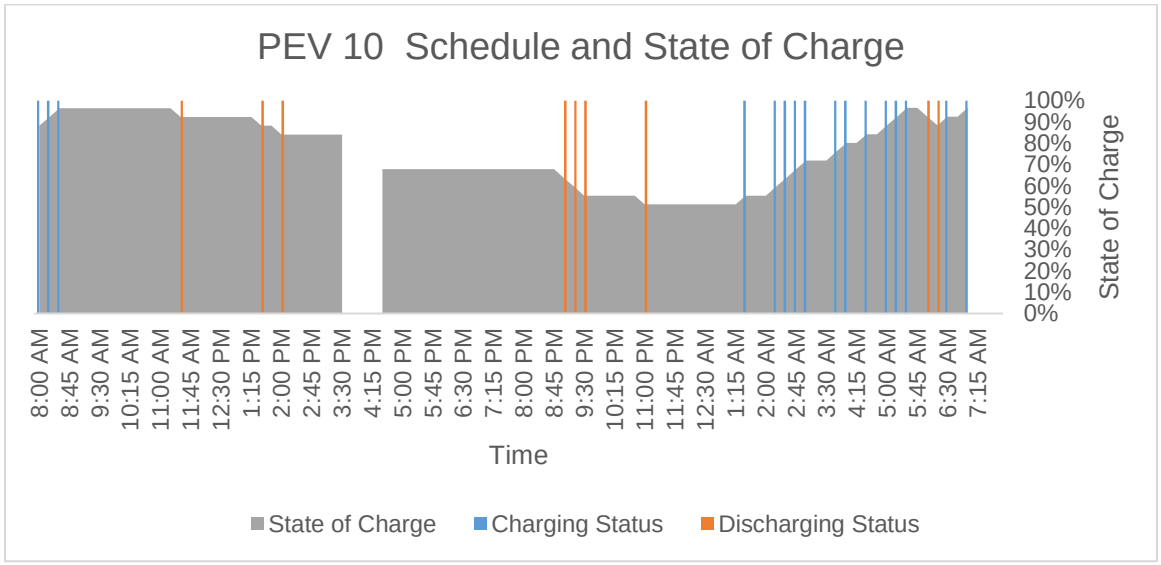

Figure 5.6 Optimal V2G schedule and SOC for PEV 10th of aggregator 1

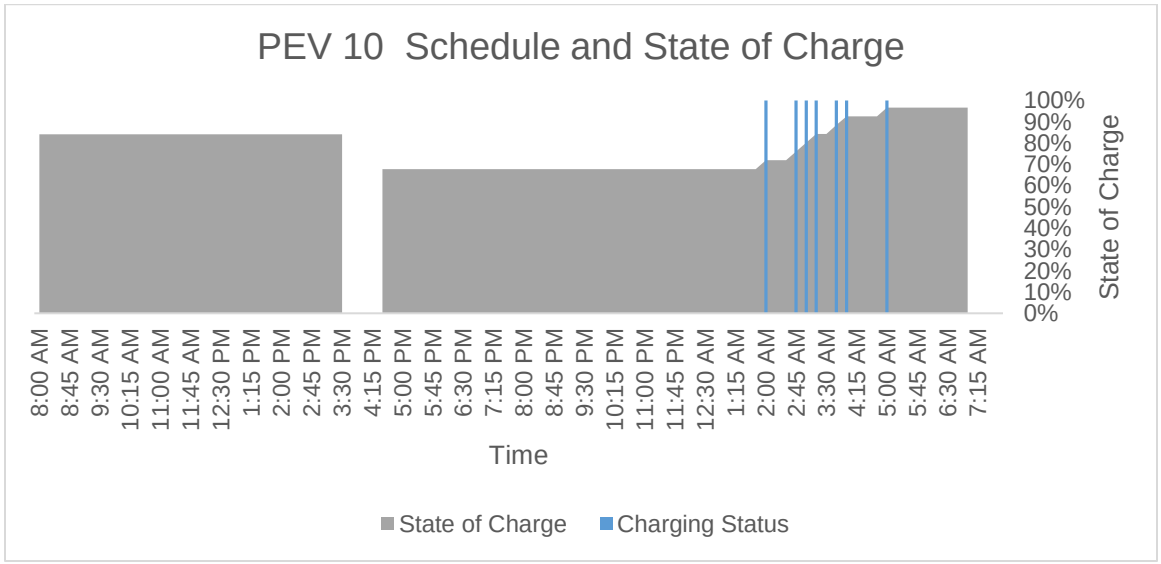

Figure 5.7 Optimal charging schedule and SOC for PEV 10th of aggregator 1

The simulation results of this scenario clearly show that the coordinated algorithms proposed in this work are effective for peak shaving and valley filling control strategies. Figure 5.1 confirms that both algorithms satisfy the objective of flattening the variance on the load curve, with the V2G method achieving better results due to its natural behavior of injecting power back to the grid. Interestingly, the V2G method can reduce peaks by 4.78%, while the uncontrolled charging can force a rise of 11.75%. Therefore, this is not about how coordinated methods can improve in the system, but about what they can avoid.

5.2.2 Case Study A: Scenario 2

This scenario is based on the load profile of a transmission transformer of a typical islanded power system. Simulation was performed with a total of 7,225 PEVs divided equally in 85 aggregators (each aggregator has 85 PEVs under its control). Results of the first optimization stage for the V2G and charging methods are illustrated in Figure 5.8. The base load curve and the uncoordinated charging are added for comparison purposes. Different than scenario 1, these plots show the master aggregator optimal load curve (results of the first optimization stage) and not the real load curve. The minimum, maximum, average and standard deviation values for the load curves are included in Table 5.5. In the same way as in the previous scenario, both methods reduce the overall variance of the load curve with the V2G method providing better results compared to coordinated charging. A larger peak, about 10.31% higher, could be obtained if no coordination methods are implemented.

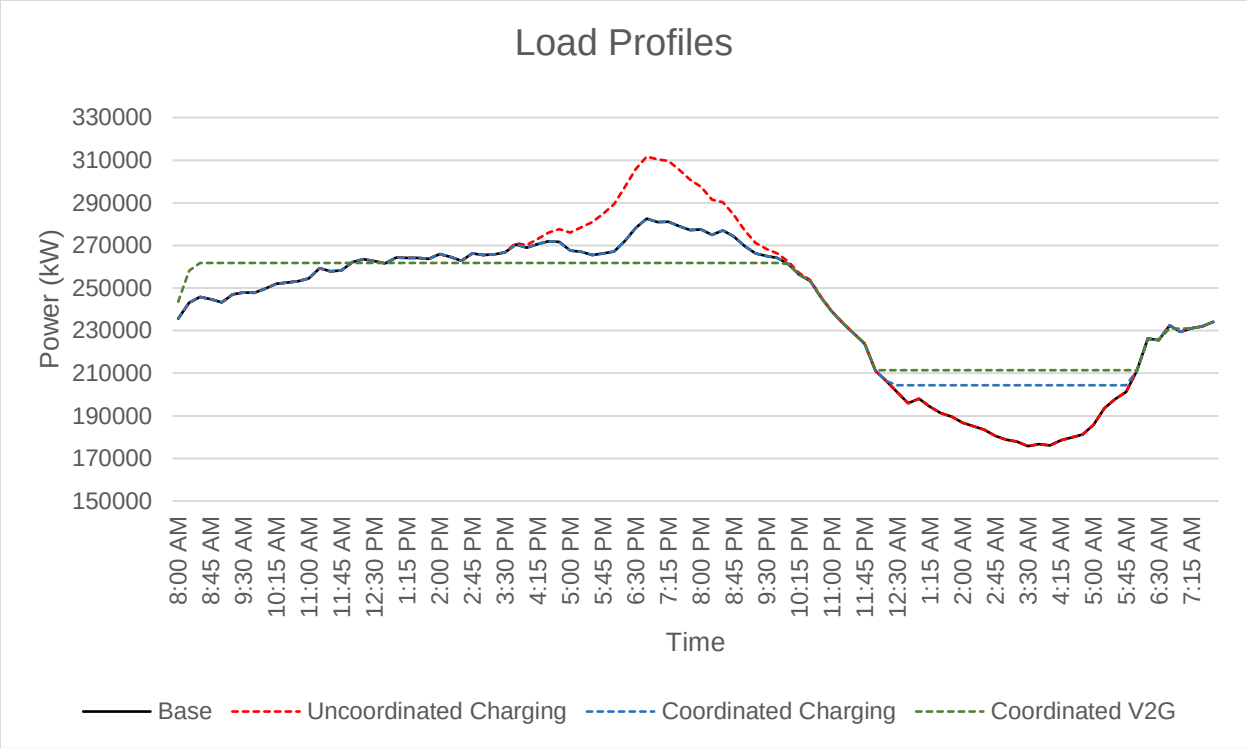

Figure 5.8 Load profiles for case study A scenario 2

	Minimum (MW)	Maximum (MW)	Average (MW)	Standard Deviation (MW)
Base	175.78	282.56	240.13	33.30
Uncoordinated Charging	175.78	311.69	243.90	37.88
Coordinated Charging	204.36	282.56	244.16	26.79
Coordinated V2G	211.41	261.77	244.53	22.01

Table 5.5 Power values for load profiles on Figure 5.8

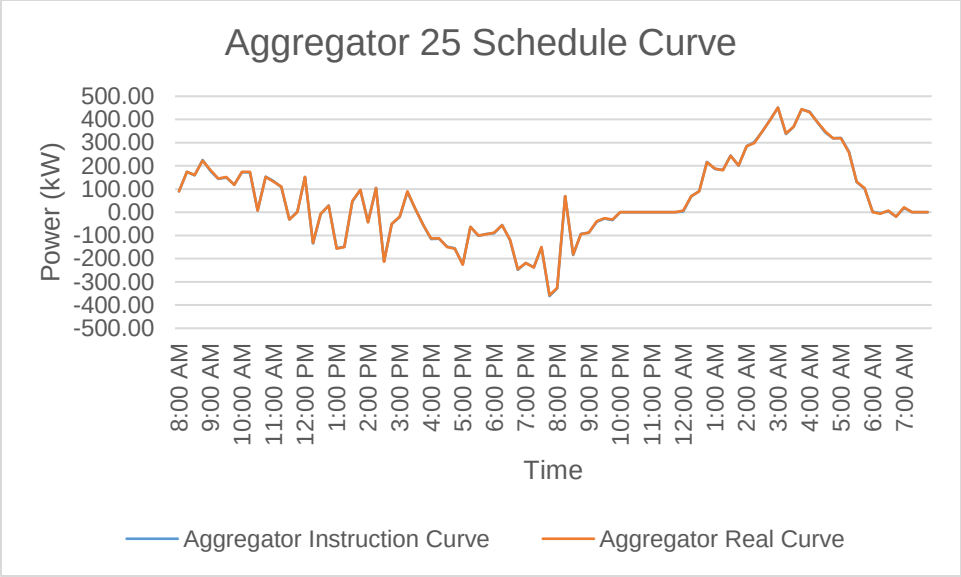

Figure 5.9 Aggregator 25 schedule curve in V2G algorithm

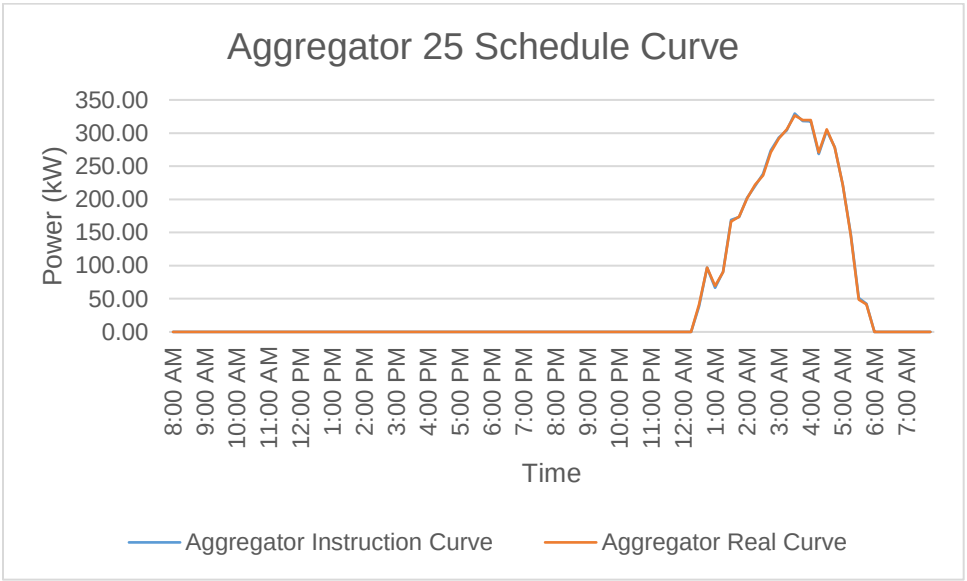

Figure 5.10 Aggregator 25 schedule curve in charging algorithm

Aggregator	Methods	Maximum Difference (kW)	Average Difference (kW)	Standard Deviation (kW)
25	V2G	4.07	1.47	1.070
25	Charging	2.93	0.39	0.837

Table 5.6 Deviation between instruction and real curves of Figure 5.9 and 5.10

Figures 5.9 and 5.10 plot the instruction and optimal curve of aggregator 25 for the V2G and charging methods, respectively. Although it seems that both curves follow each other pretty close, as expected, they have small variations that cannot be appreciated from the figures. They are analyzed in terms of the difference between both curves as listed in Table 5.6. Major differences in a time slot resulted in 4.07 kW. If this were to occur for all the aggregators at the same time slot, a total error of 345.95 kW is introduced in the master aggregator optimal curve for that specific time slot. However, master aggregator is in the order of MW, and this error (which is the worst case), may not be greater than 5% at peak values.

Figure 5.11 shows the load of all PEVs under each method. These are the master aggregator optimal values used to modify the base load curves. In other words, this is equivalent to the contribution that the master aggregator can submit to the grid. It is evident that the load for the charging method is positive during late night valley hours. In contrast, the V2G load alternates between positive and negative. When it is negative, it means that PEVs (as a whole) are injecting power back to the grid. Major injection comes at about 7:00 p.m. when highest load peak is present.

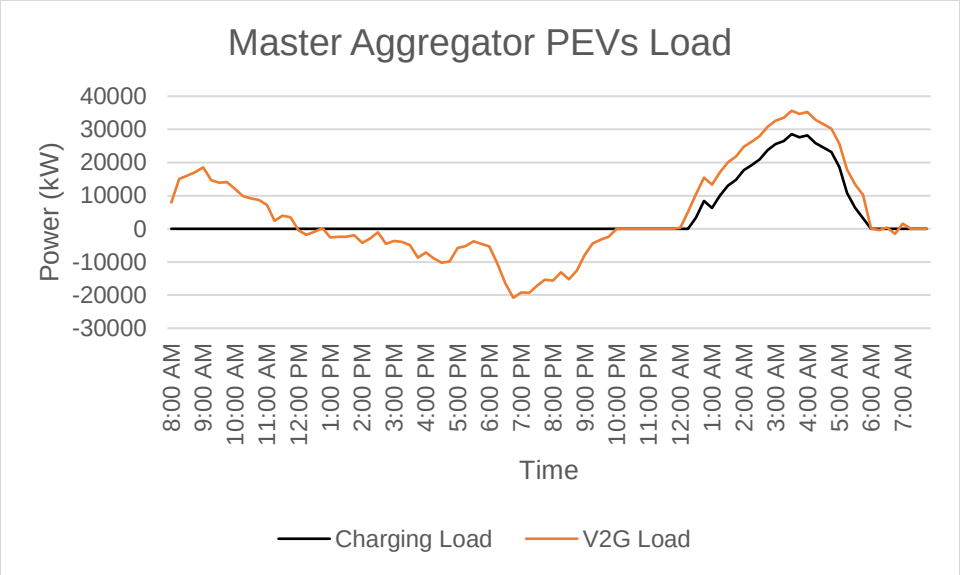

Figure 5.11 PEVs complete load for the V2G and charging methods

A representation of the optimal schedule for the PEV 50 of aggregator 25 is illustrated for the V2G and charging methods in Figures 5.12 and 5.13, respectively. Note that for the charging method, the PEV only perform charging operations during the night. In contrast, for the V2G method, the PEV charges at the beginning of the first connection period and increases its SOC to a higher value. Then, during peak hours, the PEV supports the grid discharging the energy accumulated in its battery. A charging process occurs again during the valley hours to complete the SOC for the next day.

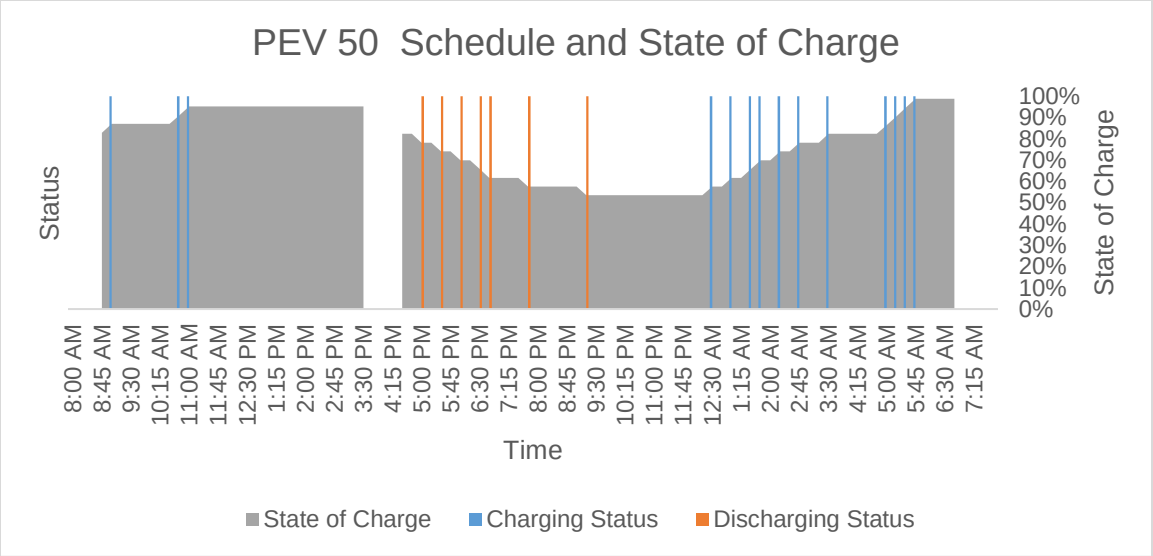

Figure 5.12 Optimal V2G schedule and SOC for PEV 50 of aggregator 25

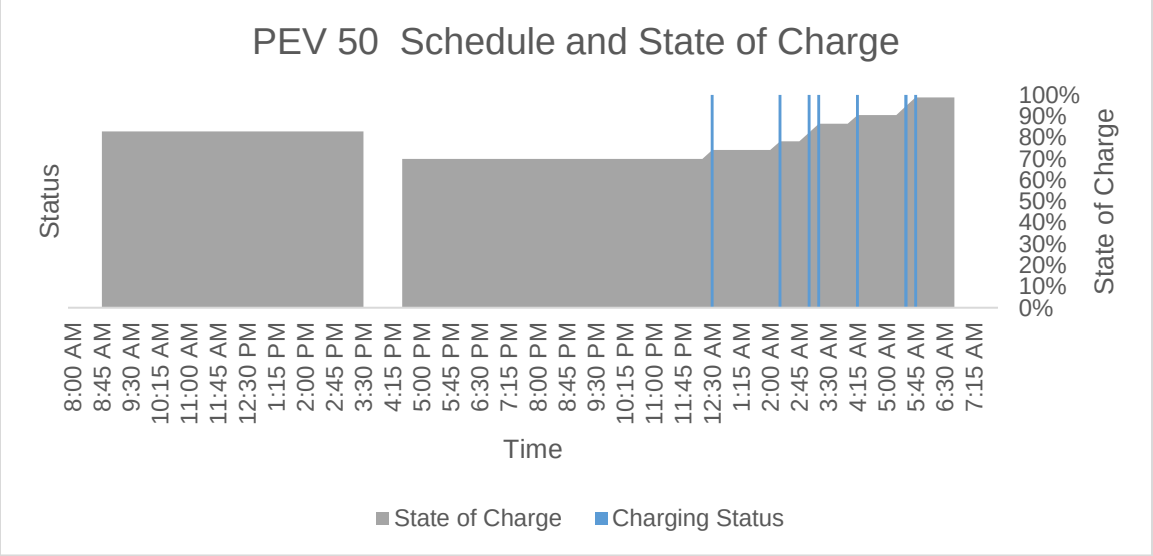

Figure 5.13 Optimal charging schedule and SOC for PEV 50 of aggregator 25

5.3 Case Study B

The objective of case study B goes beyond examining the effect on the new load curve resulting from the addition of PEVs by the algorithms proposed on Chapter 4. Particularly, it is focused on evaluating the economic operation of the system for the different load profiles obtained with and without the PEVs. This will be tested with a traditional unit commitment problem in order to determine how much will be the operating cost for the cycle been studied. Also, with the UC solution, we will study if the load changes in the demand curve resulting from the addition of PEVs will allow utilities to avoid turning on/off small expensive units as consequence of the peak shaving and valley filling technique achieved by the coordinated PEVs integration algorithm. Thus, a better insight on the viability of the PEVs interaction with the power grid can be obtained in the economic aspect.

Similar to case study A, the approaches that will be reviewed corresponds to: (1) the V2G and charging coordinated methods of PEVs and (2) uncoordinated charging of PEVs. For simplicity, in the V2G and charging approaches, the load profiles used are the optimal load curves obtained from the result of the first optimization stage. For macro analysis of this type, it is a good approximation, since the intention is not to obtain the exact load curve and neither to determine the PEV charging schedules, but remember that the optimal load curve obtained in the first optimization stage is not the same as the real load curve obtained from the result of all the aggregators in the second optimization stage. Uncoordinated approach is the resultant load curve formed when all PEVs charge their batteries to full SOC when they arrive back home.

This case study is based on the IEEE 10-unit system, which is a standard system that includes hourly demand load data and generating unit's data, as illustrated on Appendices B and C. Reserve requirements are assumed to be 10% of the demand on each hour. The data for this system have been taken from the literature on references [38], [59].

Case study B is composed of several scenarios considering different PEVs penetration levels. The scenarios contemplated in the simulations account for 15, 30, and 45 thousand PEVs, where each of them will be evaluated with the V2G and charging algorithm on the IEEE 10-unit load curve. In addition, some scenarios will be simulated varying specific parameters of the proposed methods to evaluate the impact they have. Table 5.7 break downs the scenarios that will be simulated. Sections 5.3.1 to 5.3.5 preview the numerical results for the base, uncoordinated charging, coordinated charging, and coordinated V2G approaches for the five scenarios considered. Scenario 2 is identified as the main scenario and is used by other scenarios to compare and contrast advantages and disadvantages between them.

Scenario	PEVs	Efficiency	SOC Lower Limit	Change
Scenario 1	A = 100, N = 150	$\eta_{CH} = \eta_{DH} = 0.95$	50%	PEVs
Scenario 2	A = 150, N = 200	$\eta_{CH} = \eta_{DH} = 0.95$	50%	N / A
Scenario 3	A = 150, N = 300	$\eta_{CH} = \eta_{DH} = 0.95$	50%	PEVs
Scenario 4	A = 150, N =200	$\eta_{CH} = \eta_{DH} = 1.00$	50%	Efficiency
Scenario 5	A = 100, N = 150 A = 150, N = 200	$\eta_{CH} = \eta_{DH} = 0.95$	40%, 30%	SOC

Table 5.7 Scenarios to be simulated in case study B

5.3.1 Case Study B: Scenario 1

Simulation runs for the first optimization stage of the V2G and charging algorithms were carried out in this scenario for 15,000 PEVs. The optimal load curves obtained by the results of the first optimization stage were used to compute the total generating costs by means of the UC problem in the IEEE 10-unit system. For comparison purposes, the UC of the base load curve and the uncoordinated charging were added. Figure 5.14 shows the load profiles under evaluation for the UC problems. The minimum, maximum, average, and standard deviation values for the load profiles are listed in Table 5.8 and total cost are given in Table 5.9.

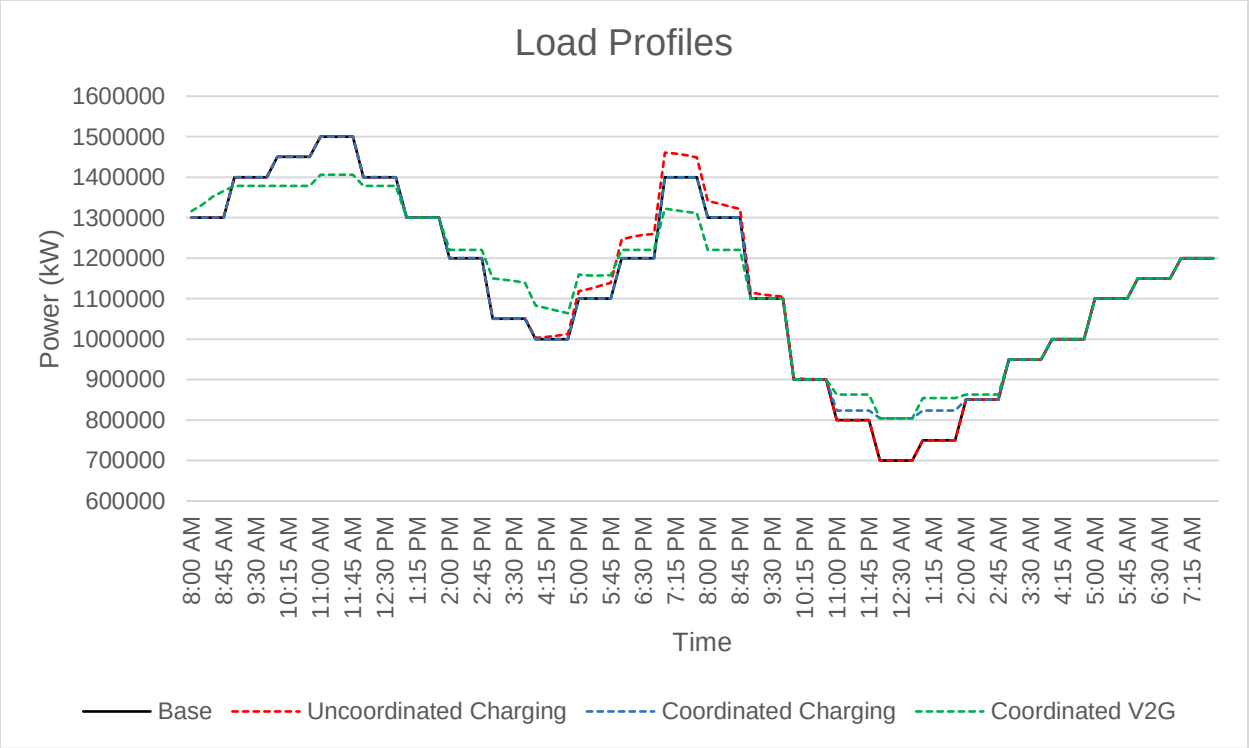

Figure 5.14 Load profiles for case study B scenario 1

	Minimum (MW)	Maximum (MW)	Average (MW)	Standard Deviation (MW)
Base	700.00	1,500.00	1,129.17	224.03
Uncoordinated Charging	700.00	1,500.00	1,136.98	228.65
Coordinated Charging	804.21	1,500.00	1,137.52	210.11
Coordinated V2G	804.21	1,405.95	1,138.28	186.06

Table 5.8 Power values for load profiles of case study B scenario 1

	Total Cost ($)
Base	$ 566,485.60
Uncoordinated Charging	$ 572,713.90
Coordinated Charging	$ 569,984.90
Coordinated V2G	$ 565,017.50

Table 5.9 Total cost for load profiles of case study B scenario 1

Results from this scenario illustrate that the best alternative is the coordinated V2G method. It reduces the peak value by 6.27% and costs even when carrying the load of the PEVs. The uncoordinated charging method does not reach the actual maximum value but increases the second peak of the day and therefore the operation costs. Although coordinated charging performs well on reducing the standard deviation, an increase in the costs is present as expected for the addition of the PEVs load. An important fact is that generating units 9 and 10 were not turned on for the V2G load profile, while for the other approaches, all units were used.

5.3.2 Case Study B: Scenario 2

An exact copy of case study B scenario 1 was reproduced in scenario 2 with the only difference that 30,000 PEVs were considered. Figure 5.15 illustrates the load profiles for this scenario. Table 5.10 provides the minimum, maximum, average, and standard deviation values for the load profiles and the total costs are listed in Table 5.11.

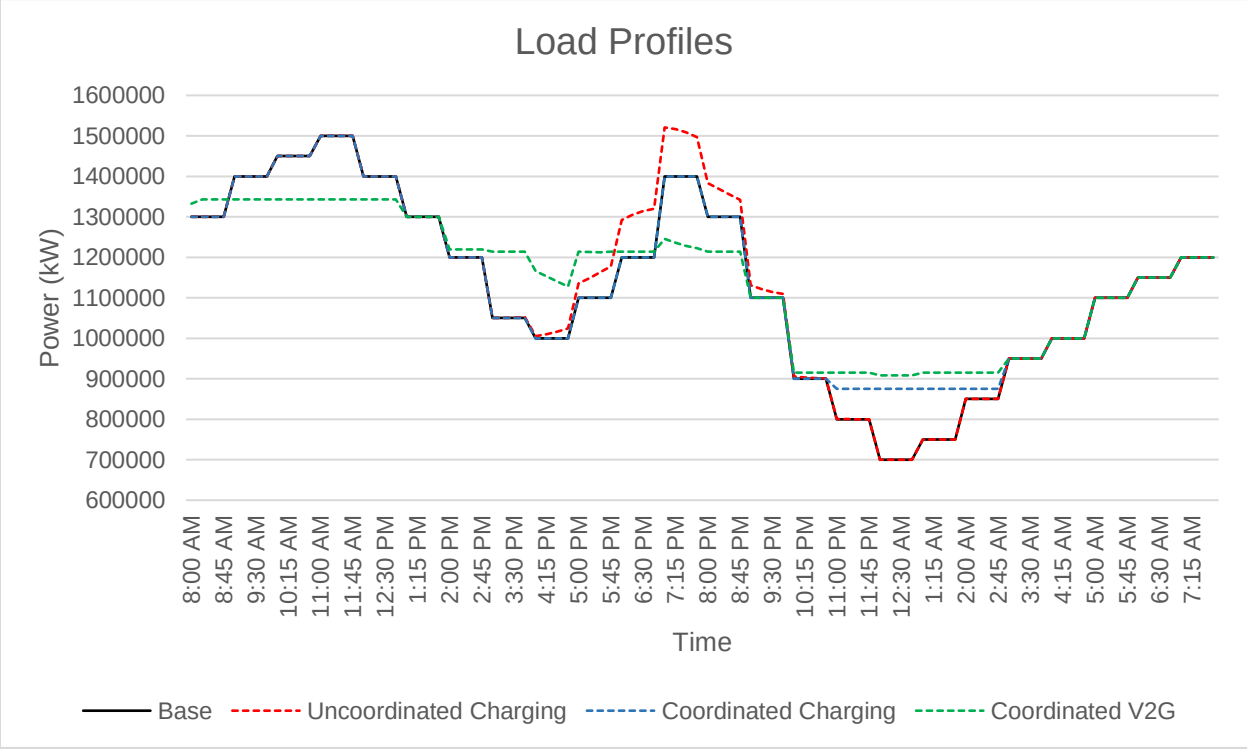

Figure 5.15 Load profiles for case study B scenario 2

	Minimum (MW)	Maximum (MW)	Average (MW)	Standard Deviation (MW)
Base	700.00	1,500.00	1,129.17	224.03
Uncoordinated Charging	700.00	1,520.82	1,144.79	234.37
Coordinated Charging	875.17	1,500.00	1,145.86	198.09
Coordinated V2G	908.42	1,343.09	1,147.38	156.22

Table 5.10 Power values for load profiles of case study B scenario 2

	Total Cost ($)
Base	$ 566,485.60
Uncoordinated Charging	-
Coordinated Charging	$ 574,971.20
Coordinated V2G	$ 566,080.40

Table 5.11 Total cost for load profiles of case study B scenario 2

Similar to the previous scenario, coordinated V2G achieves the best results. Peak is reduced by 10.46% while generating costs remain below base case serving 30 thousand PEVs. An additional unit turned out to be decommitted (unit 8), using only 7 units to supply the load. Coordinated charging cost increases due to the addition of load with the new 15,000 PEVs, but still improves the standard deviation.

However, with this PEVs penetration degree, it is recognized that the second peak elevates to 1520.82 MW which is higher than actual first peak (1500 MW) if no coordination exists. Unit commitment results for the uncoordinated charging could not be obtained because no feasible states were found specifically at hour 20, where the

load plus 10% reserve requirement cannot be satisfied by the capacity of the generating units available. This confirms that if coordinated methods are not implemented, limited systems may confront problems filling the demand in the peaks. Interestingly, analysis was made including the addition of another unit to the system equal to generation unit 10. The generation costs obtained with the 11 units were $576,371.70, but at the cost of having invested on a new unit.

5.3.3 Case Study B: Scenario 3

Another replica of case study B scenario 1 was repeated in scenario 3 adding more PEVs. A total of 45,000 have been considered in this scenario. The rest of the parameters remain the same. Figure 5.16 illustrates the load profiles for scenario 3 and Table 5.12 gives the minimum, maximum, average and standard deviation values for those load profiles. The total operating cost is shown in Table 5.13.

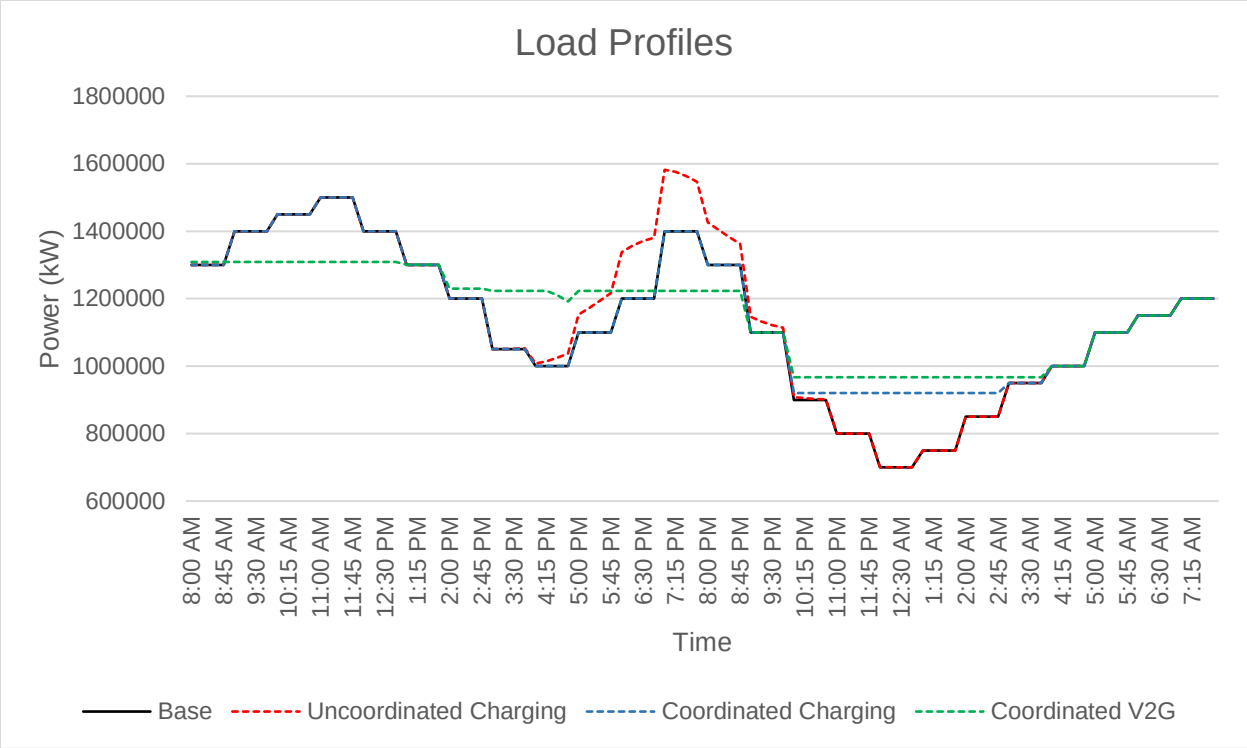

Figure 5.16 Load profiles for case study B scenario 3

	Minimum (MW)	Maximum (MW)	Average (MW)	Standard Deviation (MW)
Base	700.00	1,500.00	1,129.17	224.03
Uncoordinated Charging	700.00	1,581.93	1,152.59	241.14
Coordinated Charging	920.23	1,500.00	1,154.22	187.20
Coordinated V2G	967.06	1,308.84	1,156.49	131.65

Table 5.12 Power values for load profiles of case study B scenario 3

	Total Cost ($)
Base	$ 566,485.60
Uncoordinated Charging	-
Coordinated Charging	$ 578,562.00
Coordinated V2G	$ 569,225.80

Table 5.13 Total cost for load profiles of case study B scenario 3

Again, the coordinated V2G resulting load profile performed best. The standard deviation and peak are significantly reduced in 41.24% and 12.74%, respectively. Unlike the previous scenarios, for this amount of PEVs, the V2G generating costs begin to increase compared to base case. Also, coordinated charging costs increased compared to their counterparts (scenario 1 and 2) as expected, given the PEVs increase. Uncoordinated charging still boosts the second peak by 13% from the original curve and 5.46% of the actual peak. No results were computed for the uncoordinated charging since the load is out of the system limits.

5.3.4 Case Study B: Scenario 4

Scenario 4 of this case study is expected to assess the changes on the load profile by neglecting the efficiency parameter in the proposed V2G and charging algorithm considering the economic impact they have. To carry out this scenario, the data of scenario 2 have been adopted, but setting the charging and discharging efficiency values to 1 (ignoring the losses between the batteries and the grid). As scenarios 1 to 3, simulations were carried out and the resultant load curves were analyzed by means of UC. Figure 5.17 shows the load profiles under evaluation for this scenario. The

minimum, maximum, average, and standard deviation values for the load profiles and the total costs are illustrated in Tables 5.14 and 5.15, respectively.

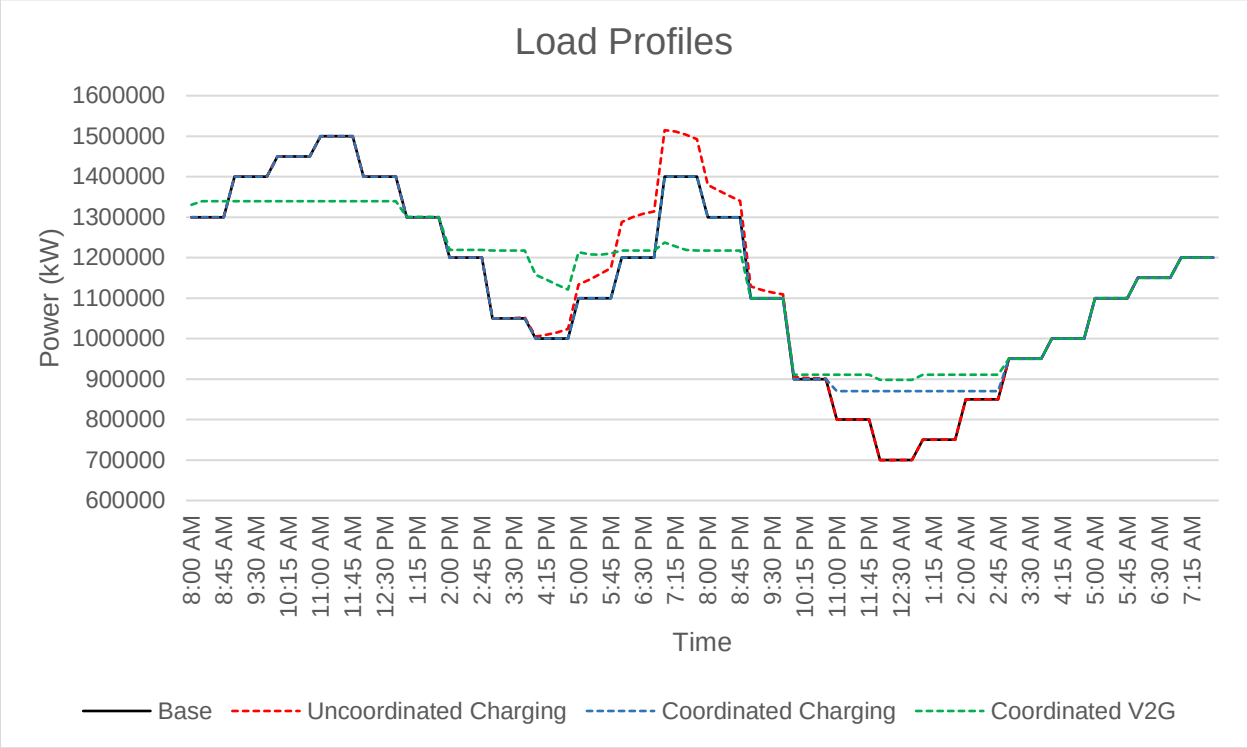

Figure 5.17 Load profiles for case study B scenario 4

	Minimum (MW)	Maximum (MW)	Average (MW)	Standard Deviation (MW)
Base	700.00	1,500.00	1,129.17	224.03
Uncoordinated Charging	700.00	1,514.78	1,144.00	233.75
Coordinated Charging	870.16	1,500.00	1,145.03	199.23
Coordinated V2G	898.00	1,339.44	1,145.03	157.01

Table 5.14 Power values for load profiles of case study B scenario 4

	Total Cost ($)
Base	$ 566,485.60
Uncoordinated Charging	-
Coordinated Charging	$ 574,620.60
Coordinated V2G	$ 564,644.60

Table 5.15 Total cost for load profiles of case study B scenario 4

This scenario compares directly with scenario 2, both assuming 30,000 PEVs. The only difference between the scenarios is the efficiency. It is observed that average and standard deviation values do not change significantly, when compared to their counterparts. Relatively small differences can be seen in the minimum and maximum values which are obviously less than scenario 2 due to neglecting the power losses. Even though generation costs for the charging method reflects a small change, the V2G method produces definitely higher variations indicating that depending on the depth of the analysis performed, the efficiency should be accounted.

5.3.5 Case Study B: Scenario 5

Scenario 5 is dedicated to investigating the effect load profiles may have by discharging PEV batteries to a deeper state of charges. Simulation runs of the first optimization stage were performed setting the state of charge lower limit of PEVs to 40 and 30 percent. The resulting optimal load curves were evaluated with the UC problem and analyzed. Scenario 5 was implemented with the data of scenarios 1 (15,000 PEVs) and 2 (30,000 PEVs), only changing the SOC parameter. In this scenario, only the V2G approach was evaluated. Figure 5.18 and Figure 5.19 illustrate

the V2G load profiles for the different SOC lower limit values assumed with 15 thousand PEVs and 30,000 PEVs, respectively. In both graphs, the corresponding V2G load profile of scenario 1 and 2 was included for comparison purposes because they were executed with a SOC lower limit of 50%. Tables 5.16 and 5.17 show the relevant power values (minimum, maximum, average, and standard deviation) of the load curves, while the generating costs are illustrated in Table 5.18. These three tables include the corresponding power values and generating costs from scenario 1 and 2 for a SOC lower limit of 50% to compare between SOC lower limits of 50%, 40%, and 30%.

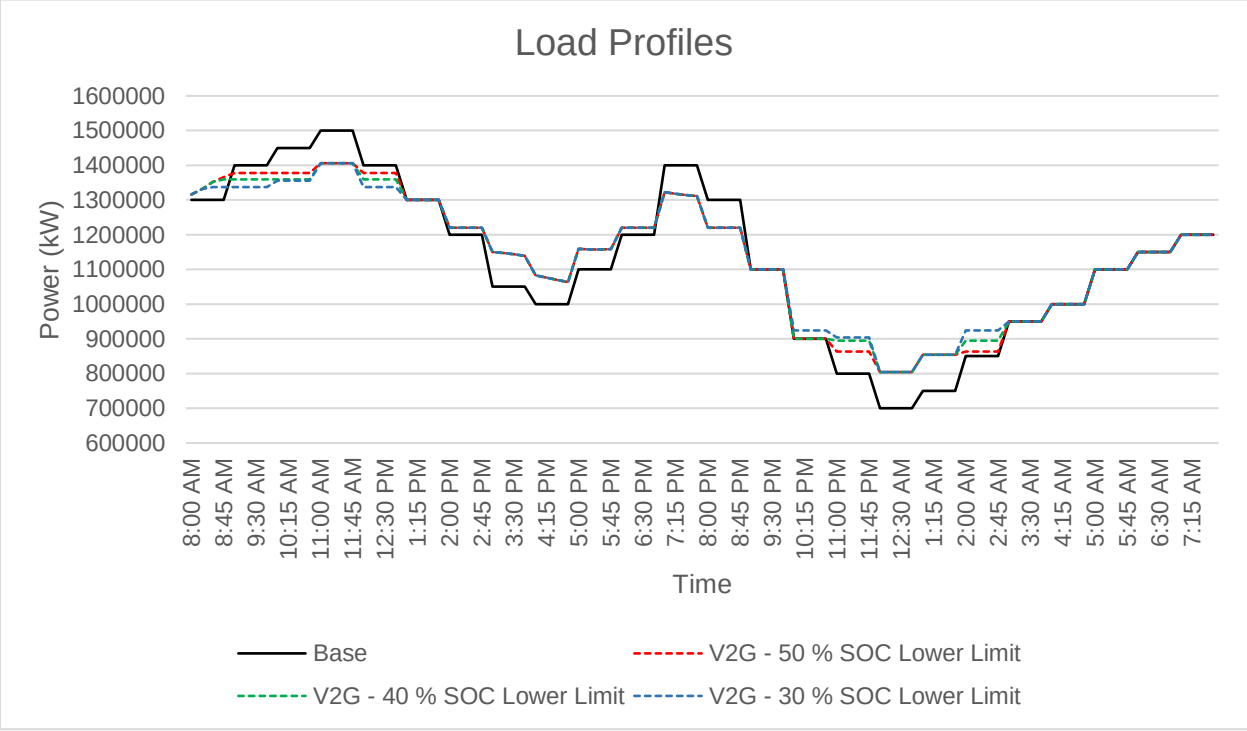

Figure 5.18 Load profiles for case study B scenario 5 with 15,000 PEVs

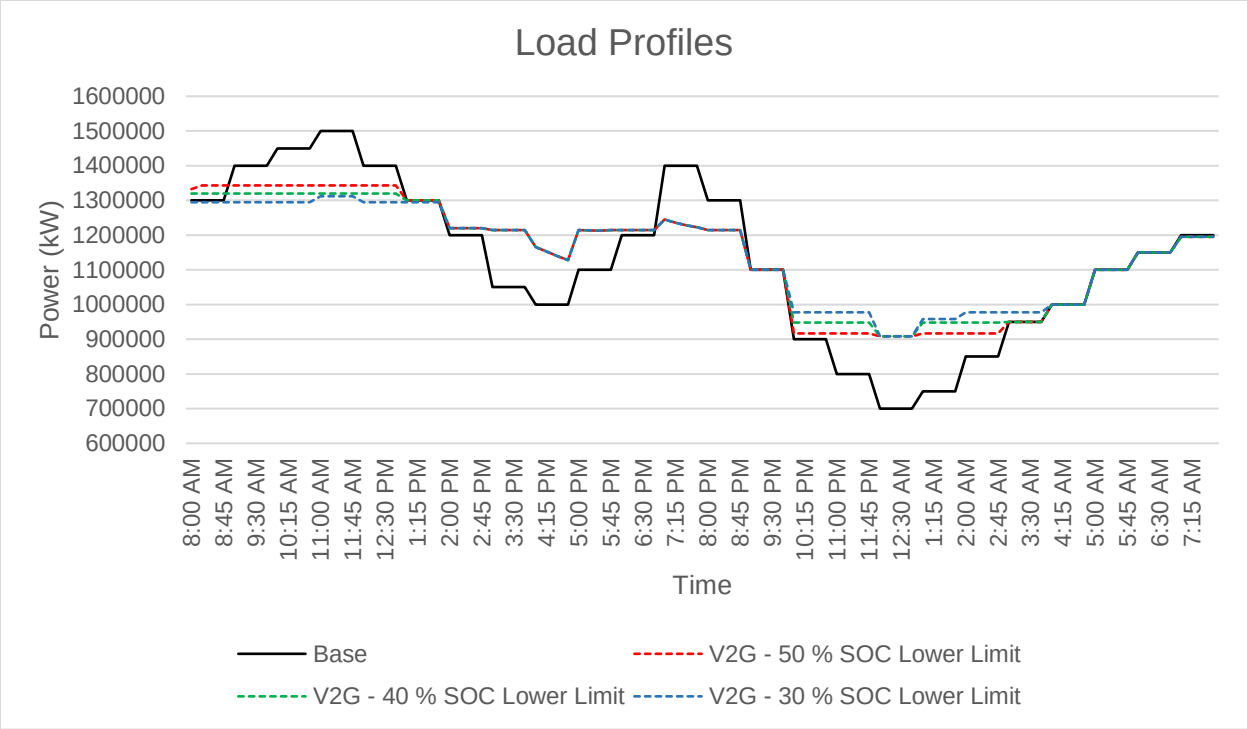

Figure 5.19 Load profiles for case study B scenario 5 with 30,000 PEVs

	SOC Lower Limit	Minimum (MW)	Maximum (MW)	Average (MW)	Standard Deviation (MW)
Base	N / A	700.00	1,500.00	1,129.17	224.03
Coordinated V2G	50%	804.21	1,405.95	1,138.28	186.06
Coordinated V2G	40%	804.21	1,405.95	1,138.54	179.32
Coordinated V2G	30%	804.21	1,405.95	1,138.79	173.06

Table 5.16 Power values for load profiles of case study B scenario 5 with 15,000 PEVs

	SOC Lower Limit	Minimum (MW)	Maximum (MW)	Average (MW)	Standard Deviation (MW)
Base	N / A	700.00	1,500.00	1,129.17	224.03
Coordinated V2G	50%	908.42	1,343.09	1,147.38	156.22
Coordinated V2G	40%	908.42	1,319.74	1,147.89	142.37
Coordinated V2G	30%	908.42	1,311.90	1,148.41	129.61

Table 5.17 Power values for load profiles of case study B scenario 5 with 30,000 PEVs

	SOC Lower Limit	Total Cost ($) for 15,000 PEVs	Total Cost ($) for 30,000 PEVs
Base	N /A	$ 566,485.60	$ 566,485.60
Coordinated V2G	50%	$ 565,017.50	$ 566,080.40
Coordinated V2G	40%	$ 562,789.30	$ 565,551.20
Coordinated V2G	30%	$ 562,765.40	$ 566,820.10

Table 5.18 Total cost for load profiles of case study B scenario 5

From the results obtained in this scenario, variations on the load profiles can be achieved with higher depth of discharge on the batteries of PEVs. Minimum and maximum values do not change for 15,000 PEVs while for 30,000 PEVs only the maximum value changes (refer to the graphs to observe the behavior on the plots). When the SOC lower limit value is 30%, a reduction in the standard deviation of 13 MW and 26.61 MW can be obtained for 15 and 30 thousand PEVS, respectively. The greatest impact is seen on the generating costs which are reduced as batteries receive deeper and longer discharges. This is the case for 15,000 PEVs. In contrast, observe

that the generating costs for 30,000 PEVs decrease when using a SOC lower limit of 40% but increase above the SOC lower limit of 50% when a 30% SOC lower limit was considered. Overall, using deeper discharges from vehicle batteries can improve system operations, but it should be carefully studied to avoid scenarios like the SOC lower limit of 30% with 30 thousand vehicles. However, in real life, this is not a practical approach because customers will suffer an accelerated battery degradation.

5.4 Case Study C

The goal of case study C is to evaluate the behavior of several load profiles with high peak conditions and different seasons of the year with the integration of plug-in electric vehicles by the V2G and charging algorithms. This case is based on load demand curves of typical islanded power systems. A reasonable number of PEVs that achieve an almost flattened load curve and a minimized load variance have been used to complete the simulation runs.

To carry out this study, only the first stage of the proposed V2G optimization algorithm was performed. The second stage is not necessary, since the main objective of this stage is not to obtain the exact load curve and neither to determine the PEV charging schedules. With the optimal load curve obtained from the first optimization stage, the performance of reducing the overall load variance can be figured out in the load profiles of the system under consideration. Advantages and disadvantages of the resulting new profiles based on the peak shaving and valley filling strategies were highlighted. Refer to Table 5.19 for a complete summary of the load profiles tested in this case study.

Load Profile	Reason
1	Peak
2	Summer
3	Winter

Table 5.19 Load profiles evaluated on case study C

5.4.1 Case Study C: Scenario 1

The scenario 1 of case study C is based on a load profile for a typical islanded power system. For this scenario, it is assumed that the highest peak of demand was recorded. Simulation runs of the V2G and charging algorithms with this load profile were implemented considering 160 aggregators with 250 PEVs under its domain, creating a fleet of 40,000 PEVs interacting with the grid. Results of the new flattened curves are displayed at Figure 5.20 and their relevant power values are showed in Table 5.20. Base load curve and the uncoordinated charging resulting curve have been added for comparison purposes.

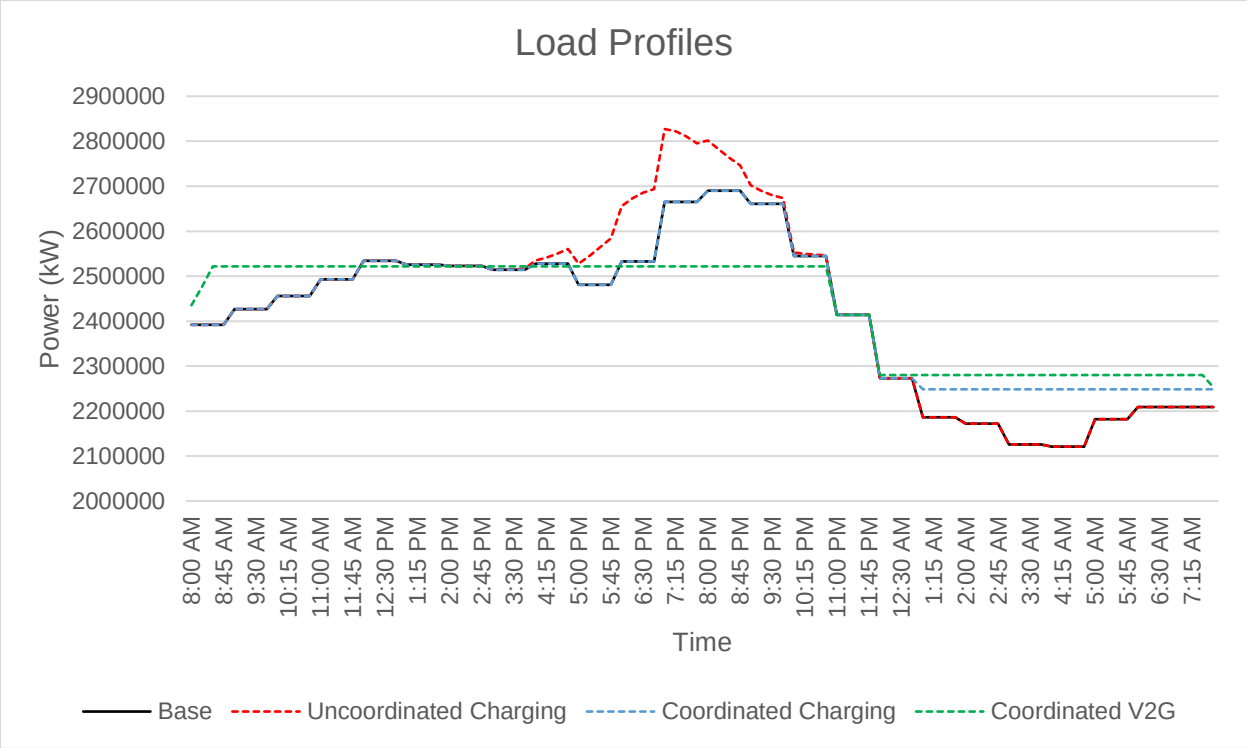

Figure 5.20 Load profiles for case study C scenario 1

	Minimum (MW)	Maximum (MW)	Average (MW)	Standard Deviation (MW)
Base	2,121.00	2,690.00	2,410.83	175.99
Uncoordinated Charging	2,121.00	2,827.07	2,431.66	201.76
Coordinated Charging	2,248.49	2,690.00	2,433.10	145.68
Coordinated V2G	2,253.19	2,521.73	2,435.13	112.49

Table 5.20 Power values for load profiles of case study C scenario 1

The simulation results, as expected, show that the coordinated methods can suppress critical system conditions compared to uncoordinated. The highest peak of

2,807.07 MW using uncoordinated charging brings a considerable increment of 137.07 MW above the already highest peak. This is equivalent to a 5.1% increase. In contrast, the V2G method can avoid that critical condition by almost eliminating the peak and flattening the curve to 2,521.73 MW. A peak reduction of 6.26% was achieved. A difference of 305.34 MW between both peaks can be suppressed if the coordinated schemes are implemented versus if they are not. Definitely, this scenario illustrates that the highest possible peak can be reduced almost entirely with 40,000 PEVs engaging in V2G transactions with the power grid.

5.4.2 Case Study C: Scenario 2

This scenario is intended to review the load profiles over different seasons of the year under the presence of PEVs. A summer load curve and a winter load curve for a typical islanded power system, displayed in Figure 5.21, will be investigated. Both profiles appear to behave likewise with an upward shift in load. However, the inconsistency on the difference between maximum and minimum values on each profile, makes them different as far as PEVs integration are concerned. In other words, curves with greater variance are more likely used to receive the benefits of PEVs coordinated methods. Simulations will examine which integration method is suitable over different seasons of the year for this particular system.

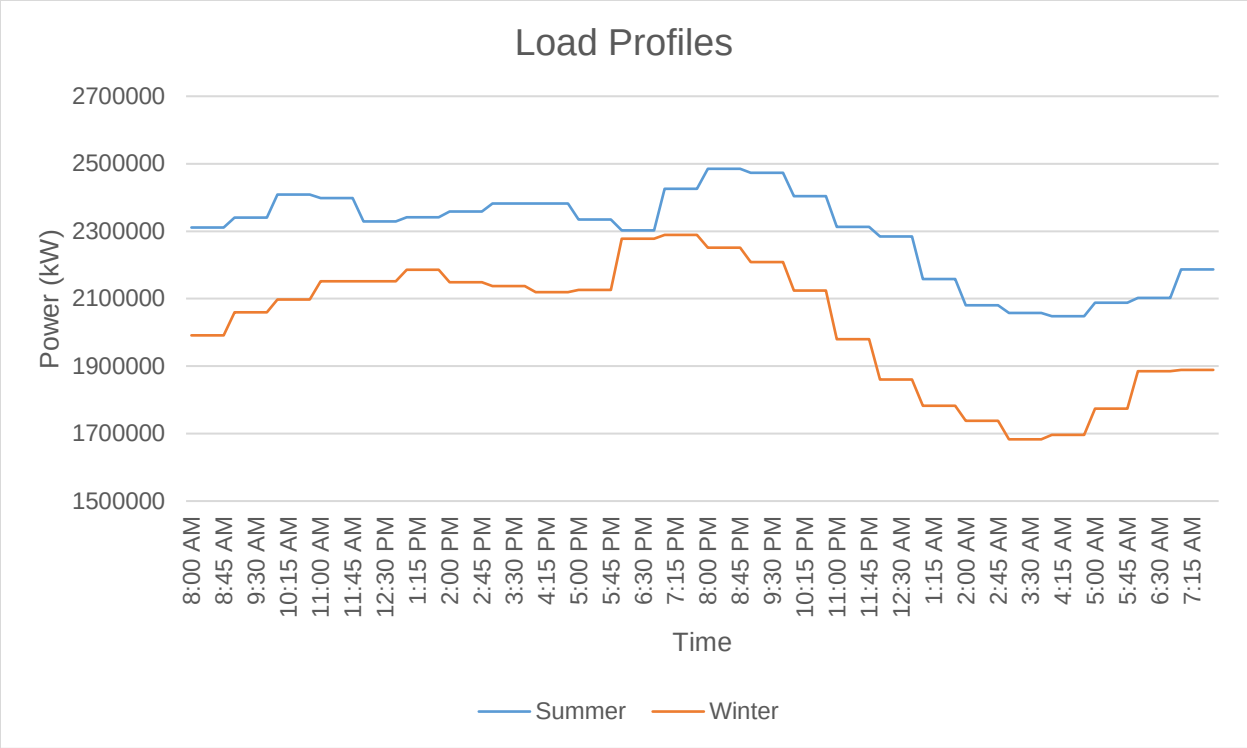

Figure 5.21 Base load curves on summer and winter for a typical islanded power system

Similar to the previous scenario, 40 thousand PEVs are integrated to the grid using the first optimization stage of the V2G and charging algorithms proposed in this work. Simulations were performed for summer and winter profiles. Results of load profiles and power values for the summer and winter are shown in Figures 5.22 and 5.23 and Tables 5.21 and 5.22, respectively.

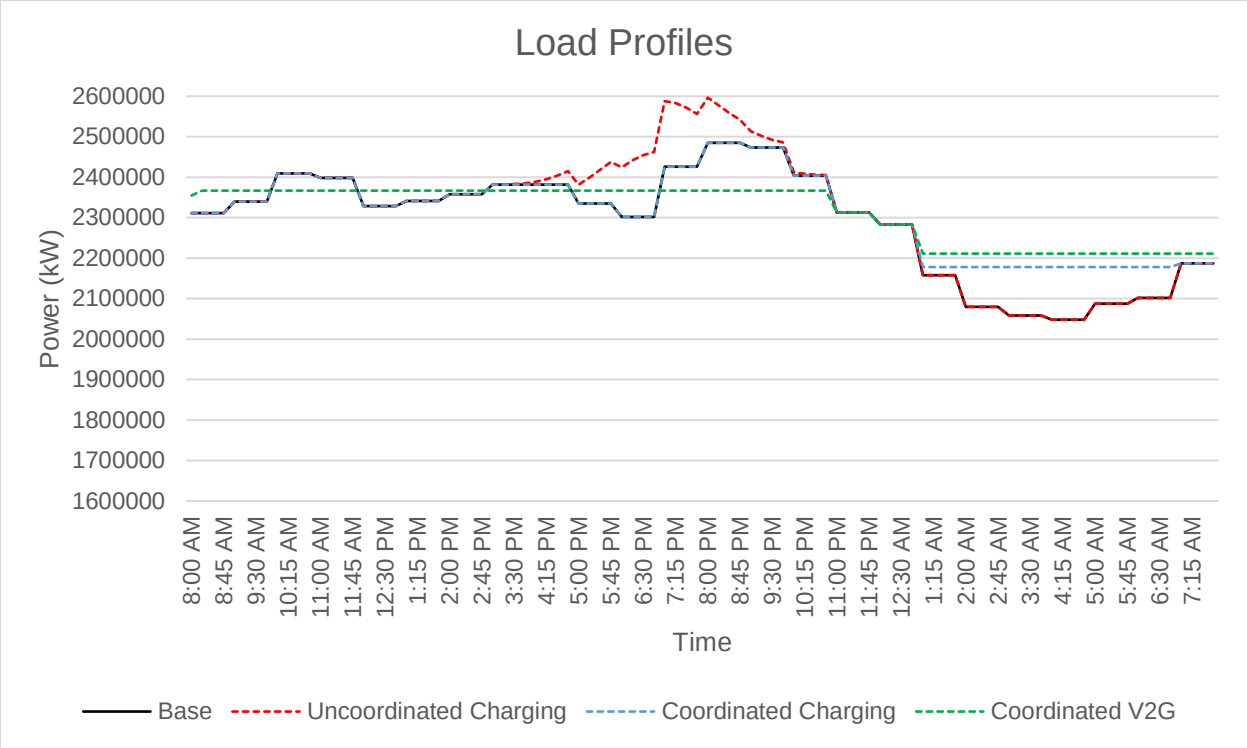

Figure 5.22 Summer load profiles for case study C scenario 2

	Minimum (MW)	Maximum (MW)	Average (MW)	Standard Deviation (MW)
Base	2,048.00	2,485.00	2,291.38	132.41
Uncoordinated Charging	2,048.00	2,596.80	2,312.21	153.28
Coordinated Charging	2,178.07	2,485.00	2,313.64	98.43
Coordinated V2G	2,211.24	2,366.89	2,315.68	69.65

Table 5.21 Power values for summer load profiles of case study C scenario 2

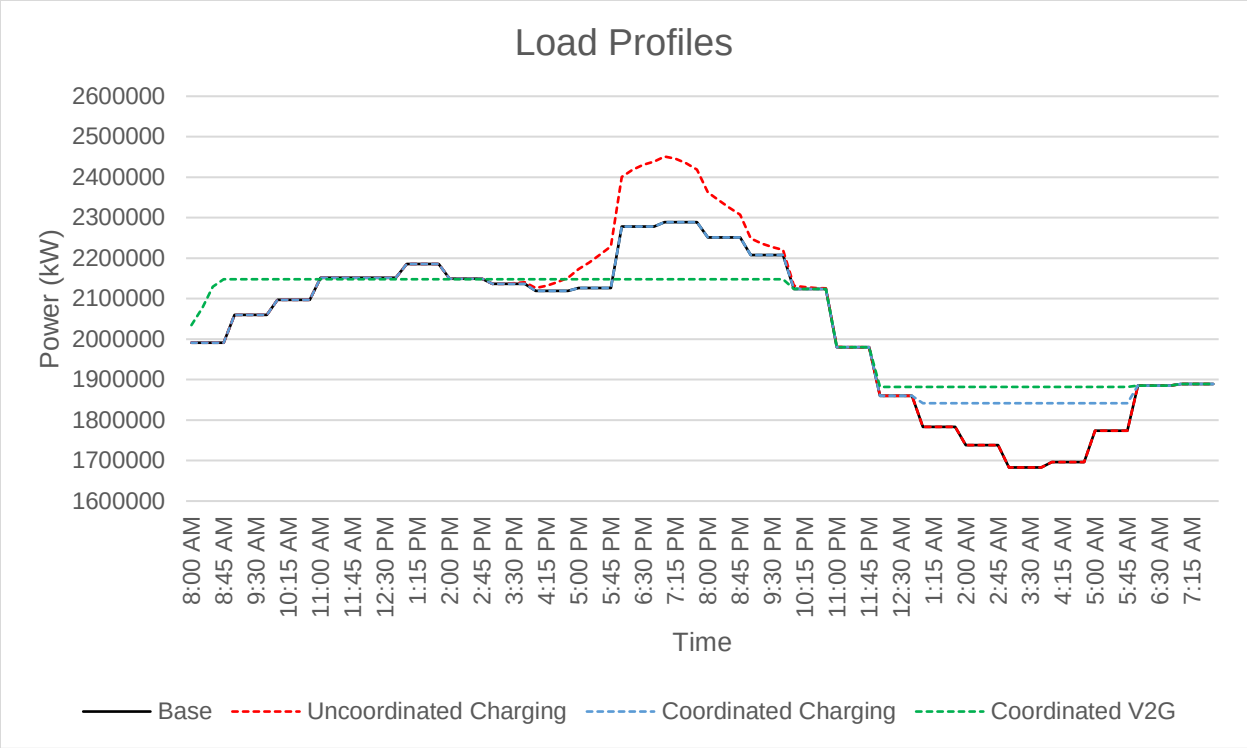

Figure 5.23 Winter load profiles for case study C scenario 2

	Minimum (MW)	Maximum (MW)	Average (MW)	Standard Deviation (MW)
Base	1,683.00	2,289.00	2,025.92	186.78
Uncoordinated Charging	1,683.00	2,451.07	2,046.12	214.31
Coordinated Charging	1,841.69	2,289.00	2,047.56	153.29
Coordinated V2G	1,881.95	2,147.94	2,049.58	122.80

Table 5.22 Power values for winter load profiles of case study C scenario 2

Standard deviation for the summer base load curve is much smaller than in winter.

In addition, the difference between minimum and maximum power values are 437 MW

for summer and 606 MW for winter. This fact, in theory, simplifies the profile issues in summer compared to winter, but care should be taken with the uncoordinated charging because it always aggravates the problem. Two main conclusions support this scenario. First, during summer, fewer PEVs are needed to achieve the same results of winter because fluctuations between minimum and maximum values is much smaller than winter. In other words, variance in the summer load curve is slighter compared to winter and fewer kWh are needed to flatten the overall load curve. Second, just performing coordinated charging operations during the summer valley hours create a meaningful impact on the load profile even without doing V2G operations. A promising alternative should be using the charging method during the summer and considering V2G transactions only during the winter periods, which evidently produce greater impacts. This way, PEV batteries degradation can be delayed while power system still benefits from PEVs addition to the grid.

5.5 Final Remarks

Through the three case studies of this chapter, the coordinated V2G and charging algorithms aiming to support the peak shaving and valley filling strategies were put under investigation. Simulation results were reported for the different case studies and scenarios, indicating that the V2G and charging operations can help flatten the overall load curves. Coordinated charging strategies merely postpone the PEVs load until late at night alleviating the stress of the system. In contrast, coordinated V2G algorithm, besides successfully allocating the PEVs load to the valley hours, demonstrates that it can greatly suppress the peak periods of the profiles.

Case study A validates the algorithm methods of the first and second optimization stages to appropriately schedule the PEVs. The operational costs fluctuations as a consequence of PEV integration was proved in case study B. In addition, it was confirmed that peaking units can be delayed or avoided to supply the peak periods if load curves are modified as per the proposed strategies. This was the case for generating units 9 and 10 in scenario 1 and 8,9, and 10 for scenario 2 of the coordinated V2G approach. In case study C, the viability of the proposed methods was investigated on the critical day where the largest peak was documented and for two different seasons of the year.

From all the simulations it can be concluded that the proposed methods bring positive results to the grid. Although V2G methods, which greatly alleviate negative impacts, were not implemented, charging methods are still promising alternatives because in some way, there is a real control of the new load and power system utilization can be maximized during nights. Now, huge penetrations of PEVs charging their batteries without any control cannot be allowed because system operations can be threatened.

Chapter 6

6 Conclusions and Future Works

This chapter discusses the conclusions accomplished through this work and points out some recommendations for future developments. Section 6.1 provides the concluding statements and section 6.2 offers guidelines that may result on the improvement of this work.

6.1 Conclusion

In this work, a modeling approach technique to effectively manage the integration of plug-in electric vehicles with the power system was developed and evaluated through simulations frameworks. The proposed PEV schedule model solution is based on a two-stage optimization process that aims to reduce the overall load variance considering a discrete charge/discharge rate. The first stage is a quadratic programming (QP) optimization problem whose decision variables depend on the number of aggregators and the time slots, while the second stage is a mixed-integer quadratic programming (MIQP) optimization problem where the variables rely on the amount of PEVs allocated on each aggregator and the time slots. The algorithm was successful in finding optimal solutions on the first optimization stage. However, in the second optimization stage, whose decision variables are discrete (i.e. binary), as the number of PEVs grow, the problem becomes

harder to solve making the convergence time to drastically increase and the optimality of the solution to decrease. In this work, the second optimization stage results were the best feasible solutions found, up to the point where a forced termination criterion of time was applied. Even though no proof of optimal solution exists in our second stage, the results obtained demonstrate that the algorithm performed well on scheduling the charge and/or discharge status of PEVs. If optimal solutions had been obtained in the second optimization stage, the difference would be a smaller gap between real load curves and optimal load curves.

In this work, two centralized approaches were presented to schedule PEVs, corresponding to coordinated V2G and coordinated charging methods. Several case studies, focusing on minimizing the overall load variance, were tested with both methods showing great performance. Simulation results evidenced that V2G operations can achieve the best results on flattening the overall load profiles and coordinated charging to bring positive effects by strategically filling the valleys. Although V2G is preferred from the power system perspective, charging methods are promising alternatives to reduce the load variance when compared to uncoordinated charging, which may result in complications to the grid.

The case studies evaluated demonstrate that generating costs can be reduced when PEVs are scheduled in coordination. Unit commitment solutions show that start up and shut down of peaking units can be avoided by intelligent PEV integration, since large swings on the daily demand curve are reduced. It was proved that underutilized capacity of the system during nights can be used (maximized) to supply the new PEV load instead of force peaking units to being committed during rush hours. In contrast, results illustrate

that under some uncoordinated charging schemes (specifically with highly PEV adoption rates), the system can encounter scenarios where available units cannot supply the demand. This impact may vary between different utilities, so proper studies should be evaluated within each specific system.

Overall, intelligent scheduling introduces great opportunity for evolving a sustainable electric vehicle integration to the grid. Measures of the impact on the resulting load curve should be performed on the system with and without electric vehicles. This is the case for the obtained results of the first optimization stage on this work, since it provides the necessary tools to assess good approximations concerning PEVs integration at a macro level without performing the schedule of each electric vehicle through the second stage. This can lead utilities to make accurate planning assessments since it can provide a good insight into implementation.

Up to this date, V2G and charging techniques are under development at their conceptual stages. However, it is clear that they have great potential to effectively manage large scale of PEVs in a centralized manner. As electric vehicles gain wider acceptance and as major drawbacks in computational complexity advance in technology, it is expected that better scheduling strategies will be developed.

6.2 Future Work

This work presented a coordinated method to effectively integrate electric vehicles to the power system grid. It was modeled mathematically by a two-stage optimization problem. The second stage, which consists of a mixed integer quadratic programming

problem, cannot be solved to optimality. Solutions obtained were the best solutions found up to a specified time termination criterion forced by a manual parameter. Thus, a better solver, specialized for this type of MIQP, should be considered to improve the execution time of the aforementioned problem.

Simulations considering high number of PEVs was another of the limitations of the second optimization stage. When large penetration under each aggregator were used (i.e. $N > 85$ in the second stage), the computational complexity arising from the dimension of the decision variables became tremendously high, making the solver unavailable to run due to lack of memory. Therefore, machines with higher memory capacities could allow simulations considering more PEVs.

It is evident, that from the coordinated methods proposed, parallel computing is a natural model between aggregators. Therefore, the implementation of a parallel computing technique within every aggregator will further simplify the computational complexity of the second optimization stage, allowing for improvements in the executing time and convergence to an optimal solution.

Overall, in order to improve the above-mentioned limitations, it is suggested that future works investigate the viability to find optimal solutions by avoiding all the obstacles so far experimented in this work. It is important to recognize that second optimization results correspond to the optimal schedules of every single EVs.

Optimal scheduling of the electric vehicles was formulated and solved by means of traditional optimization problems. Hence, further research efforts can be focused on evaluating non-traditional techniques to investigates if the performance of the proposed

method can be improved. One interesting possibility can be incorporate heuristic methods that can handle large penetration of PEVs and all the constraints involved in the model.

This work can be further extended by modifying the objective function of the optimization problem to consider other PEV parameters. This can be implemented through a multi-objective optimization problem considering, for example, the signal cost in the second term of the objective function. However, this feature will increase the complexity and may result in greater difficulty in finding optimal solutions due to the large amount of decision variables involved.

It is well known that optimal schedules of electric vehicles require greater understanding of driving patterns, daily distance traveled, parked times, and owner behavior. The certainty of the results depends entirely on the accuracy of the information corresponding to each EV. In a similar way, precise load forecast curves regarding power system are needed to achieve real solutions. Moreover, specific data of generator units is necessary to carry out unit commitment problems to evaluate the feasibility of PEVs in terms of generating costs. In this work, all transportation data was assumed as per everyday life (no statistical data) and power system data corresponds to a traditional islanded power system and the standard IEEE10-unit system. Therefore, obtaining real transportation and power system data, will result in one of the most critical steps on improving the contribution of this work.

Recent studies are looking to incorporate renewable energy with storage capacity technologies. However, the coordinated V2G and charging methods proposed do not provide any features to integrate them to the transportation system. Wind or solar integration can be considered separately by means of the base load curve. Thus, an

extension of the V2G concept can be implemented to consider different levels of wind or solar integration in order to incorporate both clean energy transitions.

Several questions should be addresses in the near future concerning V2G implementation. Although this work provides a general background of the V2G concept, a more comprehensive study is required to advance the understanding of real implementation drawbacks. Besides the technical challenges concerning V2G, additional social, cultural, economic, and political issues should be explored. To this end, optimal schedules to effectively manage PEV integration can be implemented, but as far as the practical issues mentioned above were not attended, electric and transportation systems cannot be combined.

Reference List

[1] W. Kempton and J. Tomić, “Vehicle-to-grid power fundamentals: calculating capacity and net revenue,” *J. Power Sources*, vol. 144, no. 1, pp. 268–279, Jun. 2005.

[2] A. G. Boulanger, A. C. Chu, S. Maxx, and D. L. Waltz, “Vehicle electrification: status and issues,” *Proc. IEEE*, vol. 99, no. 6, pp. 1116–1138, 2011.

[3] D. B. Richardson, “Encouraging vehicle-to-grid (V2G) participation through premium tariff rates,” *J. Power Sources*, vol. 243, pp. 219–224, Dec. 2013.

[4] W. Kempton, V. Udo, K. Huber, K. Komara, S. Letendre, S. Baker, D. Brunner, and N. Pearre, “A test of vehicle-to-grid (V2G) for energy storage and frequency regulation in the PJM system,” 2009.

[5] J. Tomić and W. Kempton, “Using fleets of electric-drive vehicles for grid support,” *J. Power Sources*, vol. 168, no. 2, pp. 459–468, Jun. 2007.

[6] W. Kempton and J. Tomić, “Vehicle-to-grid power implementation: from stabilizing the grid to supporting large-scale renewable energy,” *J. Power Sources*, vol. 144, no. 1, pp. 280–294, Jun. 2005.

[7] L. Jian, X. Zhu, Z. Shao, S. Niu, and C. C. Chan, “A scenario of vehicle-to-grid implementation and its double-layer optimal charging strategy for minimizing load variance within regional smart grids,” *Energy Convers. Manag.*, vol. 78, pp. 508–517, Feb. 2014.

[8] H. Morais, T. Sousa, Z. Vale, and P. Faria, “Evaluation of the electric vehicle impact in the power demand curve in a smart grid environment,” *Energy Convers. Manag.*, vol. 82, pp. 268–282, Jun. 2014.

[9] Maigha and M. L. Crow, “Electric vehicle scheduling considering co-optimized customer and system objectives,” *IEEE Trans. Sustain. Energy*, vol. 9, no. 1, pp. 410–419, 2018.

[10] W. Kempton, J. Tomic, S. Letendre, A. Brooks, and T. Lipman, “Vehicle-to-grid power: battery, hybrid, and fuel cell vehicles as resources for distributed electric power in California,” 2001.

[11] B. Kramer, S. Chakraborty, and B. Kroposki, “A review of plug-in vehicles and vehicle-to-grid capability,” *Proc. - 34th Annu. Conf. IEEE Ind. Electron. Soc. IECON 2008*, pp. 2278–2283, 2008.

[12] P. Grahn and L. Söder, “The customer perspective of the electric vehicles role on the electricity market,” *2011 8th Int. Conf. Eur. Energy Mark. EEM 11*, pp. 141–148, 2011.

[13] M. Ehsani, Y. Gao, and A. Emadi, *Modern electric, hybrid electric and fuel cell vehicles*. 2010.

[14] S. Shao, “An approach to demand response for alleviating power system stress conditions due to electric vehicle penetration,” Virginia Polytechnic Institute and State University, 2011.

[15] S. E. Letendre and W. Kempton, “The V2G concept: a new model for power?,” *Public Util. Fornightly*, vol. 140, no. 4, pp. 16 – 26, 2002.

[16] X. Luo, J. Wang, M. Dooner, and J. Clarke, “Overview of current development in electrical energy storage technologies and the application potential in power system operation,” *Appl. Energy*, vol. 137, pp. 511–536, Oct. 2015.

[17] R. Carnegie, D. Gotham, D. Nderitu, and P. V Preckel, “Utility scale energy storage systems: benefits, applications, and technologies,” 2013.

[18] K. C. Divya and J. Østergaard, “Battery energy storage technology for power systems - an overview,” *Electr. Power Syst. Res.*, vol. 79, no. 4, pp. 511–520, Apr. 2009.

[19] D. O. Akinyele and R. K. Rayudu, “Review of energy storage technologies for sustainable power networks,” *Sustain. Energy Technol. Assessments*, vol. 8, pp. 74–91, 2014.

[20] M. A. Hannan, M. M. Hoque, A. Hussain, Y. Yusof, and P. J. Ker, “State-of-the-Art

and Energy Management System of Lithium-Ion Batteries in Electric Vehicle Applications: Issues and Recommendations," *IEEE Access*, vol. 6, pp. 19362–19378, 2018.

[21] S. L. Huat, Y. Yonghuang, and A. A. O. Tay, "Integration issues of lithium-ion battery into electric vehicles battery pack," *J. Clean. Prod.*, vol. 113, pp. 1032–1045, 2015.

[22] J. Jaguemont, L. Boulon, and Y. Dubé, "A comprehensive review of lithium-ion batteries used in hybrid and electric vehicles at cold temperatures," *Appl. Energy*, vol. 164, pp. 99–114, 2016.

[23] A. Fotouhi, D. J. Auger, K. Propp, S. Longo, and M. Wild, "A review on electric vehicle battery modelling: from lithium-ion toward lithium–sulphur," *Renew. Sustain. Energy Rev.*, vol. 56, pp. 1008–1021, 2016.

[24] A. Chen and P. K. Sen, "Advancement in battery technology: A state-of-the-art review," *IEEE Ind. Appl. Soc. 52nd Annu. Meet. IAS 2016*, pp. 1–10, 2016.

[25] C. Guille and G. Gross, "A conceptual framework for the vehicle-to-grid (V2G) implementation," *Energy Policy*, vol. 37, no. 11, pp. 4379–4390, Nov. 2009.

[26] A. Hoke, A. Brissette, K. Smith, A. Pratt, and D. Maksimovic, "Accounting for lithium-ion battery degradation in electric vehicle charging optimization," *IEEE J. Emerg. Sel. Top. Power Electron.*, vol. 2, no. 3, pp. 691–700, 2014.

[27] J. Mullan, D. Harries, T. Bräunl, and S. Whitely, "The technical, economic and commercial viability of the vehicle-to-grid concept," *Energy Policy*, vol. 48, pp. 394–406, Sep. 2012.

[28] S. Kamboj, W. Kempton, and K. S. Decker, "Deploying power grid-integrated electric vehicles as a multi-agent system," *Information Sciences*. pp. 13–20, 2011.

[29] P. Denholm and W. Short, "An evaluation of utility system impacts and benefits of optimally dispatched plug-in hybrid electric vehicles," 2006.

[30] I. Hiskens and D. Callaway, "Achieving controllability of plug-in electric vehicles," *5th IEEE Veh. Power Propuls. Conf. VPPC '09*, pp. 1215–1220, 2009.

[31] C. Guille Diplome, “A conceptual framework for the vehicle-to-grid (V2G) implementation,” University of Illinois at Urbana-Champaign, 2007.

[32] H. Zhang, Z. Hu, Z. Xu, and Y. Song, “Optimal Planning of PEV Charging Station with Single Output Multiple Cables Charging Spots,” *IEEE Trans. Smart Grid*, vol. 8, no. 5, pp. 2119–2128, 2017.

[33] P. K. Roy and R. Sarkar, “Solution of unit commitment problem using quasi-oppositional teaching learning based algorithm,” *Int. J. Electr. Power Energy Syst.*, vol. 60, pp. 96–106, 2014.

[34] A. Y. Saber, G. K. Venayagamoorthy, and S. Member, “Unit commitment with vehicle-to-grid using particle swarm optimization,” *2009 IEEE Bucharest PowerTech*, pp. 1–8, 2009.

[35] R. Pérez Guerrero, “Differential evolution based power dispatch algorithms,” University of Puerto Rico, Mayagüez Campus, 2004.

[36] A. J. Wood and B. F. Wollenberg, *Power generation, operation, and control*, Second Edi. A Wiley-Interscience Publication, 1996.

[37] J. J. Grainger and W. D. Stevenson, *Power system analysis*. Mc Graw Hill, 1994.

[38] M. Govardhan and R. Roy, “Economic analysis of unit commitment with distributed energy resources,” *Int. J. Electr. Power Energy Syst.*, vol. 71, pp. 1–14, 2015.

[39] Z. Wang and S. Wang, “Grid power peak shaving and valley filling using vehicle-to-grid systems,” *IEEE Trans. Power Deliv.*, vol. 28, no. 3, pp. 1822–1829, 2013.

[40] P. Shinde and K. S. Swarup, “Optimal Electric Vehicle charging schedule for demand side management,” *2016 1st Int. Conf. Sustain. Green Build. Communities, SGBC 2016*, pp. 1–6, 2017.

[41] H. K. Nguyen and J. Bin Song, “Optimal charging and discharging for multiple PHEVs with demand side management in vehicle-to-building,” *J. Commun. Networks*, vol. 14, no. 6, pp. 662–671, 2012.

[42] K. N. Genikomsakis, B. Bocquier, S. Lopez, and C. S. Ioakimidis, “Utilizing Plug-in

Electric Vehicles for Peak Shaving and Valley Filling in Non-residential Buildings with Solar Photovoltaic Systems," *2016 5th Int. Conf. Smart Cities Green ICT Syst.*, pp. 179–188, 2016.

[43] L. Jian, H. Xue, G. Xu, X. Zhu, D. Zhao, and Z. Y. Shao, "Regulated charging of plug-in hybrid electric vehicles for minimizing load variance in household smart microgrid," *IEEE Trans. Ind. Electron.*, vol. 60, no. 8, pp. 3218–3226, 2013.

[44] K. Mets, R. D'Hulst, and C. Develder, "Comparison of intelligent charging algorithms for electric vehicles to reduce peak load and demand variability in a distribution grid," *J. Commun. Networks*, vol. 14, no. 6, pp. 672–681, 2012.

[45] J. García-Villalobos, I. Zamora, J. I. San Martín, F. J. Asensio, and V. Aperribay, "Plug-in electric vehicles in electric distribution networks: a review of smart charging approaches," *Renew. Sustain. Energy Rev.*, vol. 38, pp. 717–731, Oct. 2014.

[46] L. Zhang, F. Jabbari, T. Brown, and S. Samuelsen, "Coordinating plug-in electric vehicle charging with electric grid: valley filling and target load following," *J. Power Sources*, vol. 267, pp. 584–597, Dec. 2014.

[47] H. Farzin, M. Fotuhi-Firuzabad, and M. Moeini-Aghtaie, "Charging/discharging management of electric vehicles: Technical viewpoint," *2016 Smart Grids Conf. SGC 2016*, pp. 1–6, 2016.

[48] B. Sun, Z. Huang, X. Tan, and D. H. K. Tsang, "Optimal scheduling for electric vehicle charging with discrete charging levels in distribution grid," *IEEE Trans. Smart Grid*, vol. 9, no. 2, pp. 624–634, 2018.

[49] C. Le Floch, "Methods for Optimal Charging of Large Fleets of Electric Vehicles," University of Calofornia,Berkeley, 2017.

[50] S. Habib, M. M. Khan, J. Huawei, K. Hashmi, M. T. Faiz, and H. Tang, "A study of implemented international standards and infrastructural system for electric vehicles," *Proc. IEEE Int. Conf. Ind. Technol.*, vol. 2018-Febru, pp. 1783–1788, 2018.

[51] "Nissan USA." [Online]. Available: https://www.nissanusa.com/vehicles/electric-

cars/leaf.html. [Accessed: 09-Mar-2018].

[52] Z. Xu, W. Su, Z. Hu, Y. Song, and H. Zhang, “A hierarchical framework for coordinated charging of plug-in electric vehicles in China,” *IEEE Trans. Smart Grid*, vol. 7, no. 1, pp. 428–438, 2016.

[53] H. Chen, Z. Hu, H. Zhang, and H. Luo, “Coordinated charging and discharging strategies for plug-in electric bus fast charging station with energy storage system,” *IET Gener. Transm. Distrib.*, vol. 12, no. 9, pp. 2019–2028, 2018.

[54] M. Gulin, M. Vasak, and M. Baotic, “Analysis of microgrid power flow optimization with consideration of residual storages state,” *2015 Eur. Control Conf. ECC 2015*, pp. 3126–3131, 2015.

[55] D. T. Nguyen and L. B. Le, “Joint optimization of electric vehicle and home energy scheduling considering user comfort preference,” *IEEE Trans. Smart Grid*, vol. 5, no. 1, pp. 188–199, 2014.

[56] Maigha and M. L. Crow, “Multi-objective electric vehicle scheduling considering customer and system objectives,” *2017 IEEE Manchester PowerTech, Powertech 2017*, pp. 1–6, 2017.

[57] X. Bai, W. Qiao, H. Wei, F. Huang, and Y. Chen, “Bidirectional coordinating dispatch of large-scale V2G in a future smart grid using complementarity optimization,” *Int. J. Electr. Power Energy Syst.*, vol. 68, pp. 269–277, 2015.

[58] K. N. Kumar and K. J. Tseng, “Efficiency evaluation of coordinated charging methods used for charging electric vehicles,” *IEEE PES Innov. Smart Grid Technol. Conf. Eur.*, pp. 270–275, 2016.

[59] E. Talebizadeh, M. Rashidinejad, and A. Abdollahi, “Evaluation of plug-in electric vehicles impact on cost-based unit commitment,” *J. Power Sources*, vol. 248, pp. 545–552, 2014.

Appendix

Appendix A: Numerical Examples for Lower/Upper State of Charge Limits

A.1 V2G Example

Appendix A.1 illustrates a graphical representation of the lower and upper state of charge bound values of a single PEV during a complete V2G operation cycle. These values are then used to construct the minimum and maximum limits for the accumulated energy constraint equation of the first optimization stage. Assume that the charge/discharge rate (inside the battery) is ± 3 kW, the time interval $\Delta t = 1h$, and the data presented in Table A.1.1 correspond to the user behaviors and the parameters used to carry out the example. Therefore, with these data, the slope of all changes associated to the energy in the battery are $\frac{(\pm 3kW)\times(1h)}{(24kWh)} = \pm 0.125$. If operation is idle, the value is zero. Figure A.1.1 shows the SOC paths with their corresponding values.

Battery Capacity	24 kWh
Driving Demand	0.29 kWh/mi
Total Travel Distance	33.104 mi
Trip 1 Length (45% of Total)	14.897 mi
Trip 2 Length (55% of Total)	18.207 mi
SOC decrease from Trip 1	0.18
SOC decrease from Trip 2	0.22
Departure SOC before Trip 1	0.95
Minimum Desired SOC at 2nd Leave Time	0.85
Lower SOC Allowed	0.40
Upper SOC Allowed	0.99
1st Connection Time / $t_{Start\,1}$	8:17 a.m. / 9:00 a.m.
1st Leave Time / $t_{End\,1}$	5:05 p.m. / 5:00 p.m.
2nd Connection Time / $t_{Start\,2}$	6:10 p.m. / 7:00 p.m.
2nd Leave Time / $t_{End\,2}$	7:40 a.m. / 7:00 a.m.

Table A.1.1 User behaviors and parameters data for V2G example

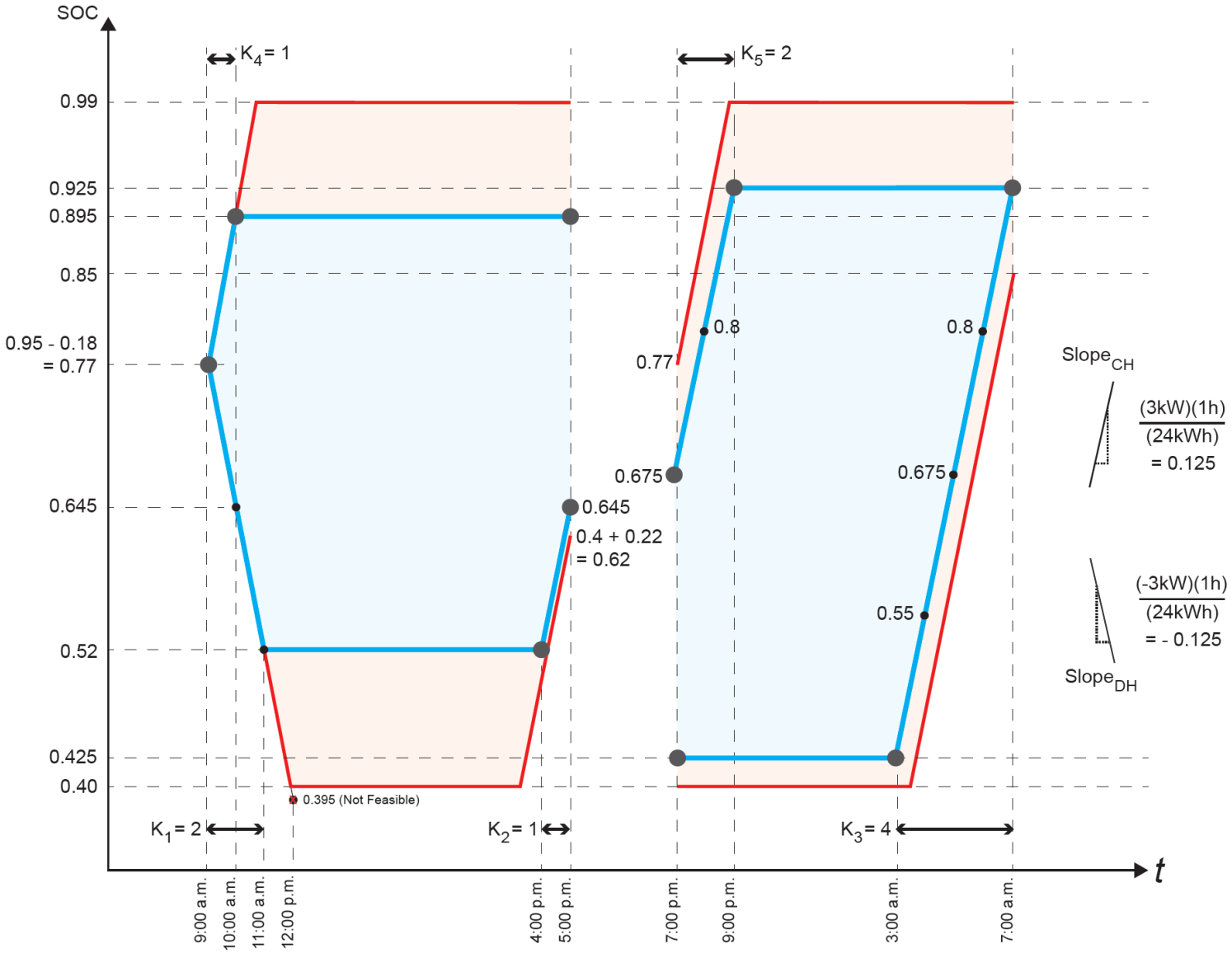

Figure A.1.1 Minimum/maximum state of charge values for the V2G example

A.2 Charging Example

Appendix A.2 is very similar to the example presented in Appendix A.1 with the only difference that just considers charging process. Like the previous example, assume also that the charge rate (inside the battery) is 3 kW, the time interval $\Delta t = 1h$, and the data presented in Table A.2.1 correspond to the user behaviors and the parameters used to carry out the example. In this case, the slope is modified to $\frac{(3kW)\times(1h)}{(24kWh)} = 0.125$, and like the V2G example, if it is idle a zero value is assigned. Figure A.2.1 illustrates the SOC paths with their corresponding values.

Battery Capacity	24 kWh
Driving Demand	0.29 kWh/mi
Total Travel Distance	31.723 mi
Trip 1 Length (40% of Total)	12.689 mi
Trip 2 Length (60% of Total)	19.034 mi
SOC decrease from Trip 1	0.153
SOC decrease from Trip 2	0.230
Departure SOC before Trip 1	0.84
Minimum Desired SOC at 2nd Leave Time	0.85
Lower SOC Allowed	0.50
Upper SOC Allowed	0.99
1st Connection Time / $t_{Start\,1}$	7:55 a.m. / 8:00 a.m.
1st Leave Time / $t_{End\,1}$	4:15 p.m. / 4:00 p.m.
2nd Connection Time / $t_{Start\,2}$	5:32 p.m. / 6:00 p.m.
2nd Leave Time / $t_{End\,2}$	7:20 a.m. / 7:00 a.m.

Table A.2.1 User *behaviors and parameters data for charging example*

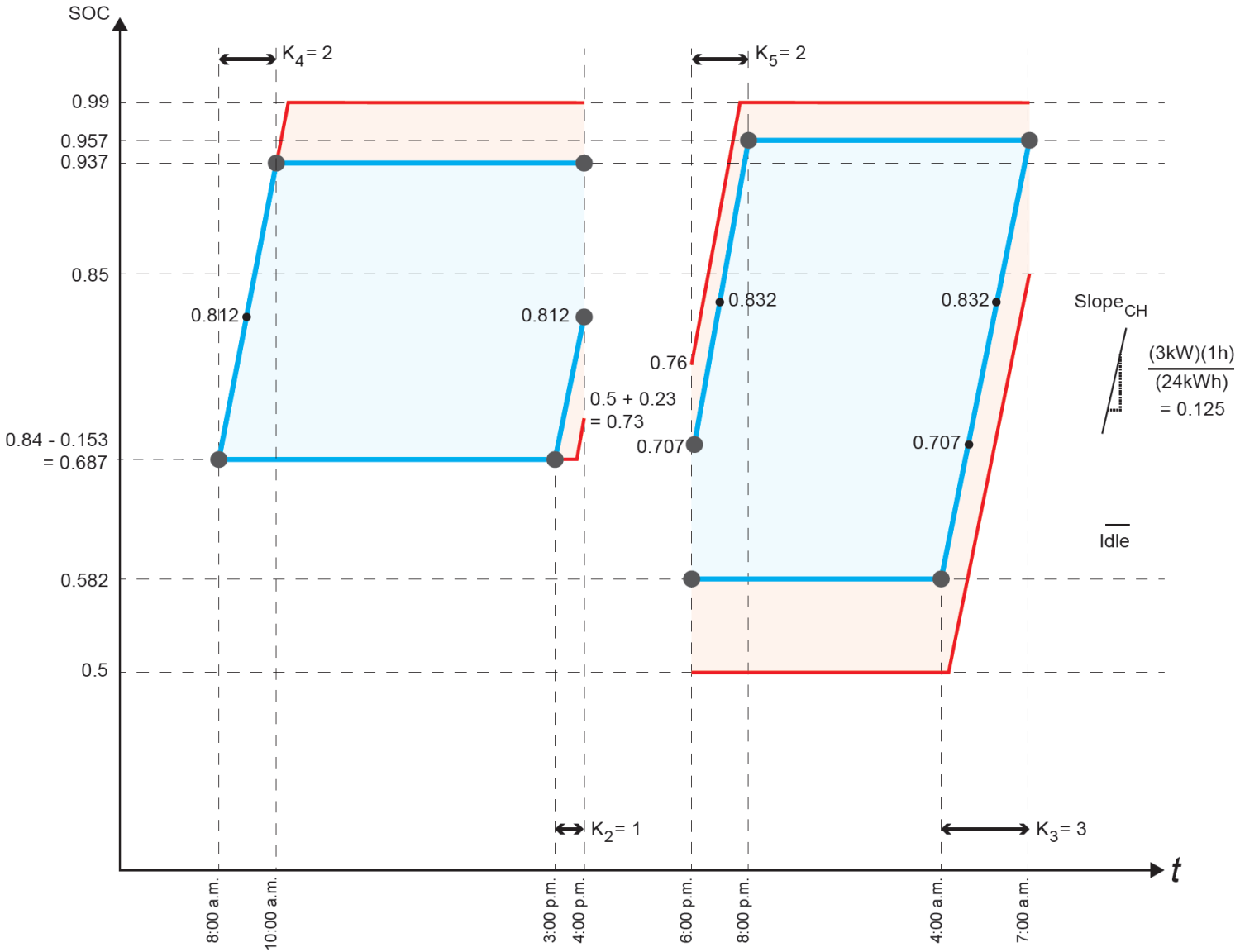

Figure A.2.1 Minimum/maximum state of charge values for the charging example

Appendix B: Load Curves Data

B.1 IEEE 10-Unit System Load Curve

Time Slot Hour	1 12:00 a.m.	2 1:00 a.m.	3 2:00 a.m.	4 3:00 a.m.	5 4:00 a.m.	6 5:00 a.m.
Demand (MW)	700	750	850	950	1000	1100
Time Slot Hour	7 6:00 a.m.	8 7:00 a.m.	9 8:00 a.m.	10 9:00 a.m.	11 10:00 a.m.	12 11:00 a.m.
Demand (MW)	1150	1200	1300	1400	1450	1500
Time Slot Hour	13 12:00 p.m.	14 1:00 p.m.	15 2:00 p.m.	16 3:00 p.m.	17 4:00 p.m.	18 5:00 p.m.
Demand (MW)	1400	1300	1200	1050	1000	1100
Time Slot Hour	19 6:00 p.m.	20 7:00 p.m.	21 8:00 p.m.	22 9:00 p.m.	23 10:00 p.m.	24 11:00 p.m.
Demand (MW)	1200	1400	1300	1100	900	800

Table B.1.1 Hourly load demand of IEEE 10-unit system

B.2 Typical Islanded Power System Load Curves

Time Slot Hour	1 12:00 a.m.	2 12:15 a.m.	3 12:30 a.m.	4 12:45 a.m.	5 1:00 a.m.	6 1:15 a.m.
Demand (MW)	23.43	22.96	22.68	22.30	22.30	22.11
Time Slot Hour	7 1:30 a.m.	8 1:45 a.m.	9 2:00 a.m.	10 2:15 a.m.	11 2:30 a.m.	12 2:45 a.m.
Demand (MW)	21.64	21.17	21.07	21.07	20.88	20.88
Time Slot Hour	13 3:00 a.m.	14 3:15 a.m.	15 3:30 a.m.	16 3:45 a.m.	17 4:00 a.m.	18 4:15 a.m.
Demand (MW)	20.60	20.88	20.98	20.98	20.69	21.07
Time Slot Hour	19 4:30 a.m.	20 4:45 a.m.	21 5:00 a.m.	22 5:15 a.m.	23 5:30 a.m.	24 5:45 a.m.
Demand (MW)	21.07	20.98	20.60	21.54	21.73	22.02
Time Slot Hour	25 6:00 a.m.	26 6:15 a.m.	27 6:30 a.m.	28 6:45 a.m.	29 7:00 a.m.	30 7:15 a.m.
Demand (MW)	22.2	22.49	22.68	22.58	22.87	22.49
Time Slot Hour	31 7:30 a.m.	32 7:45 a.m.	33 8:00 a.m.	34 8:15 a.m.	35 8:30 a.m.	36 8:45 a.m.
Demand (MW)	23.34	23.34	23.43	24.38	24.85	25.42
Time Slot Hour	37 9:00 a.m.	38 9:15 a.m.	39 9:30 a.m.	40 9:45 a.m.	41 10:00 a.m.	42 10:15 a.m.
Demand (MW)	25.51	25.80	26.46	26.27	26.27	26.46
Time Slot Hour	43 10:30 a.m.	44 10:45 a.m.	45 11:00 a.m.	46 11:15 a.m.	47 11:30 a.m.	48 11:45 a.m.
Demand (MW)	26.65	26.74	26.55	27.21	27.50	27.31
Time Slot Hour	49 12:00 p.m.	50 12:15 p.m.	51 12:30 p.m.	52 12:45 p.m.	53 1:00 p.m.	54 1:15 p.m.
Demand (MW)	27.02	27.02	27.02	27.21	27.02	27.12
Time Slot Hour	55 1:30 p.m.	56 1:45 p.m.	57 2:00 p.m.	58 2:15 p.m.	59 2:30 p.m.	60 2:45 p.m.
Demand (MW)	27.31	27.31	27.31	27.69	27.40	27.50

Time Slot Hour	61 3:00 p.m.	62 3:15 p.m.	63 3:30 p.m.	64 3:45 p.m.	65 4:00 p.m.	66 4:15 p.m.
Demand (MW)	27.02	27.02	27.02	27.40	27.40	27.21
Time Slot Hour	67 4:30 p.m.	68 4:45 p.m.	69 5:00 p.m.	70 5:15 p.m.	71 5:30 p.m.	72 5:45 p.m.
Demand (MW)	27.21	26.93	26.65	26.08	26.08	25.98
Time Slot Hour	73 6:00 p.m.	74 6:15 p.m.	75 6:30 p.m.	76 6:45 p.m.	77 7:00 p.m.	78 7:15 p.m.
Demand (MW)	25.98	25.70	26.36	26.55	26.55	26.55
Time Slot Hour	79 7:30 p.m.	80 7:45 p.m.	81 8:00 p.m.	82 8:15 p.m.	83 8:30 p.m.	84 8:45 p.m.
Demand (MW)	27.02	27.21	27.40	27.31	27.50	27.78
Time Slot Hour	85 9:00 p.m.	86 9:15 p.m.	87 9:30 p.m.	88 9:45 p.m.	89 10:00 p.m.	90 10:15 p.m.
Demand (MW)	27.59	27.59	27.69	27.12	26.55	25.80
Time Slot Hour	91 10:30 p.m.	92 10:45 p.m.	93 11:00 p.m.	94 11:15 p.m.	95 11:30 p.m.	96 11:45 p.m.
Demand (MW)	25.98	25.61	25.04	25.13	24.38	24.00

Table B.2.1 Traditional load profile for a distribution substation on a typical islanded power system

Time Slot Hour	1 12:00 a.m.	2 12:15 a.m.	3 12:30 a.m.	4 12:45 a.m.	5 1:00 a.m.	6 1:15 a.m.
Demand (MW)	211.10	206.25	201.00	195.98	198.11	194.27
Time Slot Hour	7 1:30 a.m.	8 1:45 a.m.	9 2:00 a.m.	10 2:15 a.m.	11 2:30 a.m.	12 2:45 a.m.
Demand (MW)	191.32	189.57	186.73	185.10	183.43	180.64
Time Slot Hour	13 3:00 a.m.	14 3:15 a.m.	15 3:30 a.m.	16 3:45 a.m.	17 4:00 a.m.	18 4:15 a.m.
Demand (MW)	178.75	177.94	175.78	176.71	176.17	178.45
Time Slot Hour	19 4:30 a.m.	20 4:45 a.m.	21 5:00 a.m.	22 5:15 a.m.	23 5:30 a.m.	24 5:45 a.m.
Demand (MW)	179.79	181.18	185.72	193.56	197.95	201.19
Time Slot Hour	25 6:00 a.m.	26 6:15 a.m.	27 6:30 a.m.	28 6:45 a.m.	29 7:00 a.m.	30 7:15 a.m.
Demand (MW)	211.26	226.22	225.48	232.45	229.38	231.09
Time Slot Hour	31 7:30 a.m.	32 7:45 a.m.	33 8:00 a.m.	34 8:15 a.m.	35 8:30 a.m.	36 8:45 a.m.
Demand (MW)	232.04	234.03	235.62	243.11	245.75	244.71
Time Slot Hour	37 9:00 a.m.	38 9:15 a.m.	39 9:30 a.m.	40 9:45 a.m.	41 10:00 a.m.	42 10:15 a.m.
Demand (MW)	243.19	247.07	247.89	247.68	249.70	251.90
Time Slot Hour	43 10:30 a.m.	44 10:45 a.m.	45 11:00 a.m.	46 11:15 a.m.	47 11:30 a.m.	48 11:45 a.m.
Demand (MW)	252.55	253.10	254.53	259.35	257.76	258.31
Time Slot Hour	49 12:00 p.m.	50 12:15 p.m.	51 12:30 p.m.	52 12:45 p.m.	53 1:00 p.m.	54 1:15 p.m.
Demand (MW)	262.21	263.58	262.59	261.60	264.35	264.19
Time Slot Hour	55 1:30 p.m.	56 1:45 p.m.	57 2:00 p.m.	58 2:15 p.m.	59 2:30 p.m.	60 2:45 p.m.
Demand (MW)	264.19	263.65	265.98	264.62	262.83	266.28
Time Slot Hour	61 3:00 p.m.	62 3:15 p.m.	63 3:30 p.m.	64 3:45 p.m.	65 4:00 p.m.	66 4:15 p.m.
Demand (MW)	265.43	265.75	266.64	270.43	268.90	270.59

Time Slot Hour	67 4:30 p.m.	68 4:45 p.m.	69 5:00 p.m.	70 5:15 p.m.	71 5:30 p.m.	72 5:45 p.m.
Demand (MW)	271.98	271.64	267.53	266.92	265.55	266.26
Time Slot Hour	73 6:00 p.m.	74 6:15 p.m.	75 6:30 p.m.	76 6:45 p.m.	77 7:00 p.m.	78 7:15 p.m.
Demand (MW)	267.10	272.16	278.21	282.56	280.97	281.06
Time Slot Hour	79 7:30 p.m.	80 7:45 p.m.	81 8:00 p.m.	82 8:15 p.m.	83 8:30 p.m.	84 8:45 p.m.
Demand (MW)	278.92	277.14	277.42	274.90	277.05	274.26
Time Slot Hour	85 9:00 p.m.	86 9:15 p.m.	87 9:30 p.m.	88 9:45 p.m.	89 10:00 p.m.	90 10:15 p.m.
Demand (MW)	269.68	266.18	265.07	264.14	261.27	256.30
Time Slot Hour	91 10:30 p.m.	92 10:45 p.m.	93 11:00 p.m.	94 11:15 p.m.	95 11:30 p.m.	96 11:45 p.m.
Demand (MW)	253.32	245.54	238.92	233.54	228.61	223.83

Table B.2.2 Traditional load profile for a transmission transformer on typical islanded power system

Time Slot Hour	1 12:00 a.m.	2 1:00 a.m.	3 2:00 a.m.	4 3:00 a.m.	5 4:00 a.m.	6 5:00 a.m.
Demand (MW)	2273	2186	2172	2126	2121	2182
Time Slot Hour	7 6:00 a.m.	8 7:00 a.m.	9 8:00 a.m.	10 9:00 a.m.	11 10:00 a.m.	12 11:00 a.m.
Demand (MW)	2209	2209	2392	2427	2456	2493
Time Slot Hour	13 12:00 p.m.	14 1:00 p.m.	15 2:00 p.m.	16 3:00 p.m.	17 4:00 p.m.	18 5:00 p.m.
Demand (MW)	2534	2526	2523	2514	2528	2481
Time Slot Hour	19 6:00 p.m.	20 7:00 p.m.	21 8:00 p.m.	22 9:00 p.m.	23 10:00 p.m.	24 11:00 p.m.
Demand (MW)	2533	2665	2690	2661	2545	2414

Table B.2.3 Traditional peak load curve for a typical islanded power system

Time Slot Hour	1 12:00 a.m.	2 1:00 a.m.	3 2:00 a.m.	4 3:00 a.m.	5 4:00 a.m.	6 5:00 a.m.
Demand (MW)	2284	2158	2080	2058	2048	2088
Time Slot Hour	7 6:00 a.m.	8 7:00 a.m.	9 8:00 a.m.	10 9:00 a.m.	11 10:00 a.m.	12 11:00 a.m.
Demand (MW)	2102	2187	2311	2340	2409	2398
Time Slot Hour	13 12:00 p.m.	14 1:00 p.m.	15 2:00 p.m.	16 3:00 p.m.	17 4:00 p.m.	18 5:00 p.m.
Demand (MW)	2329	2341	2358	2382	2382	2335
Time Slot Hour	19 6:00 p.m.	20 7:00 p.m.	21 8:00 p.m.	22 9:00 p.m.	23 10:00 p.m.	24 11:00 p.m.
Demand (MW)	2302	2426	2485	2473	2404	2313

Table B.2.4 Traditional summer load curve for a typical islanded power system

Time Slot Hour	1 12:00 a.m.	2 1:00 a.m.	3 2:00 a.m.	4 3:00 a.m.	5 4:00 a.m.	6 5:00 a.m.
Demand (MW)	1860	1783	1738	1683	1696	1774
Time Slot Hour	7 6:00 a.m.	8 7:00 a.m.	9 8:00 a.m.	10 9:00 a.m.	11 10:00 a.m.	12 11:00 a.m.
Demand (MW)	1885	1889	1991	2060	2097	2152
Time Slot Hour	13 12:00 p.m.	14 1:00 p.m.	15 2:00 p.m.	16 3:00 p.m.	17 4:00 p.m.	18 5:00 p.m.
Demand (MW)	2152	2186	2149	2137	2119	2126
Time Slot Hour	19 6:00 p.m.	20 7:00 p.m.	21 8:00 p.m.	22 9:00 p.m.	23 10:00 p.m.	24 11:00 p.m.
Demand (MW)	2278	2289	2251	2208	2124	1980

Table B.2.5 Traditional winter load curve for a typical islanded power system

Appendix C: Generator Data

C.1 IEEE 10-Unit System Generator Data

Unit	P_{Min}	P_{Max}	a ($\$/MWh^2$)	b ($\$/MWh$)	c ($)
1	150	455	0.00048	16.19	1000
2	150	455	0.00031	17.26	970
3	20	130	0.00200	16.60	700
4	20	130	0.00211	16.50	680
5	25	162	0.00398	19.70	450
6	20	80	0.00712	22.26	370
7	25	85	0.00079	27.74	480
8	10	55	0.00413	25.92	660
9	10	55	0.00222	27.27	665
10	10	55	0.00173	27.79	670

Table C.1.1 Generator data for the IEEE 10-unit system

Unit	Min Up (h)	Min Down (h)	Ramp Up (MW)	Ramp Down (MW)	Hot Start Cost ($)	Cold Start Cost ($)	Status (h)
1	8	8	152.5	152.5	4500	9000	8
2	8	8	152.5	152.5	5000	10000	8
3	5	5	55.0	55.0	550	1100	-5
4	5	5	55.0	55.0	560	1120	-5
5	6	6	68.5	68.5	900	1800	-6
6	3	3	30.0	30.0	170	340	-3
7	3	3	30.0	30.0	260	520	-3
8	1	1	22.5	22.5	30	60	-1
9	1	1	22.5	22.5	30	60	-1
10	1	1	22.5	22.5	30	60	-1

Table C.1.2 Generator data for the IEEE 10-unit system